Aus der Medizinische Klinik und Poliklinik III
Klinikum der Ludwig-Maximilians-Universität München

Dissertation

zum Erwerb des Doctor of Philosophy (Ph.D.)

an der Medizinischen Fakultät der

Ludwig-Maximilians-Universität München

Multifunctional antibody constructs for cancer immunotherapy: combining CD47 checkpoint blockade with tumor targeting for enhanced efficacy

vorgelegt von:

Alexandra Lena Leutbecher

aus:

München

Jahr:

2025

Mit Genehmigung der Medizinischen Fakultät der
Ludwig-Maximilians-Universität München

Erstes Gutachten von: Prof. Dr. Marion Subklewe

Zweites Gutachten von: Prof. Dr. Elfriede Nößner

Drittes Gutachten von: Prof. Dr. Iris Helfrich

Viertes Gutachten von: Prof. Dr. Christian Kellner

Dekan: **Prof. Dr. med. Thomas Gudermann**

Datum der Verteidigung:

05.09.2025

Affidavit

LMU | LUDWIG-MAXIMILIANS-UNIVERSITÄT MÜNCHEN | Promotionsbüro Medizinische Fakultät | MMRS

Affidavit

Leutbecher, Alexandra

Surname, first name

Feodor-Lynen-Str. 25

Street

81377, Munich, Germany

Zip code, town, country

I hereby declare that the submitted thesis entitled:

Multifunctional antibody constructs for cancer immunotherapy: combining CD47 checkpoint blockade with tumor targeting for enhanced efficacy

is my own work. I have only used the sources indicated and have not made unauthorized use of the services of a third party. Where the work of others has been quoted or reproduced, the source is always given.
I further declare that the dissertation presented here has not been submitted in the same or similar form to any other institution for the purpose of obtaining an academic degree.

Munich, 08.09.2025 Alexandra Leutbecher

place, date Signature doctoral candidate

Confirmation of congruency

LMU LUDWIG-MAXIMILIANS-UNIVERSITÄT MÜNCHEN

Promotionsbüro Medizinische Fakultät

MMRS

Confirmation of congruency between printed and electronic version of the doctoral thesis

Leutbecher, Alexandra

Surname, first name

Feodor-Lynen-Str. 25

Street

81377, Munich, Germany

Zip code, town, country

I hereby declare that the submitted thesis entitled:

Multifunctional antibody constructs for cancer immunotherapy: combining CD47 checkpoint blockade with tumor targeting for enhanced efficacy

is congruent with the printed version both in content and format.

Munich, 08.09.2025 Alexandra Leutbecher

place, date Signature doctoral candidate

Table of Contents

List of abbreviations

ACT	Adoptive cell transfer
ADC	Antibody-drug conjugate
ADCC	Antibody-dependent cellular cytotoxicity
ADCP	Antibody-dependent cellular phagocytosis
AML	Acute myeloid leukemia
APCs	Antigen-presenting cells
BiTE	Bispecific T-cell engager
bsAbs	Bispecific antibodies
CA-125	Cancer antigen 125
CAR	Chimeric antigen receptor
CDC	Complement-dependent cytotoxicity
CDRs	Complementarity-determining regions
CiTE	Checkpoint inhibitory T-cell engager
C_L and C_H	Constant light and heavy domain
CTLA-4	Cytotoxic T-lymphocyte antigen 4
DART	Dual-affinity retargeting
DCs	Dendritic cells
DNMT3A	DNA methyltransferase 3 α
ECD	Extracellular domain
EGFR	Epidermal growth factor receptor
EMA	European Medicines Agency
EOC	Epithelial ovarian cancer
Fab	Antigen-binding fragment
Fc	Fragment crystallizable
FcγR	Fcγ receptor
FcRn	Neonatal Fc receptor
FDA	Food and Drug Administration
FLT3	Fms-related tyrosine kinase 3
FolRα	Folate receptor α
GPC3	Glypican-3
GPI	Glycosylphosphatidylinositol
HER2	Human epidermal growth factor receptor 2
HGSOC	High-grade serous ovarian carcinoma
HRD	Homologous recombination deficiency
HSCT	Hematopoietic stem cell transplantation
IAP	Integrin-associated protein
IDH1	Isocitrate dehydrogenase 1
Igs	Immunoglobulins
IL	Interleukin
IL-3R	Interleukin-3 receptor
irAEs	Immune-related adverse events
ITIM	Immunoreceptor tyrosine inhibitory motif

KiH	Knob-into-hole
LAG-3	Lymphocyte-activation gene 3
LicMAb	Local inhibitory checkpoint monoclonal antibody
LSCs	Leukemic stem cells
mAb	Monoclonal antibody
MDS	Myelodysplastic syndromes
MDSCs	Myeloid-derived suppressor cells
MHC	Major histocompatibility complex
MPF	Megakaryocyte potentiating factor
MRD	Measurable residual disease
MSLN	Mesothelin
NHL	Non-Hodgkin's lymphoma
NK	Natural killer
NPM1	Nucleophosmin 1
OS	Overall survival
pAML	Primary AML
PARPi	Poly ADP ribose polymerase inhibitors
PD-1	Programmed cell death protein 1
PD-L1	Programmed cell death protein 1 ligand
PDAC	Pancreatic ductal adenocarcinoma
pDCs	Plasmacytoid DCs
PDX	Patient-derived xenografts
r/r	Relapsed/refractory
RBCs	Red blood cells
scFv	Single-chain variable fragment
sdAb	Single-domain antibody
SHP	Src-homology 2 tyrosine phosphatase
SIRPα	Signal regulatory protein α
STING	Stimulator of interferon genes
TAA	Tumor-associated antigen
TCR-T	Transgenic T-cell receptor T cells
TILs	Tumor-infiltrating lymphocytes
TME	Tumor microenvironment
Treg	Regulatory T cell
TriKE	Trispecific killer engager
TriTAC	Trispecific T-cell activating construct
VEGF	Vascular endothelial growth factor
V_L and V_H	Variable light and heavy domain
WT1	Wilm's tumor 1

List of publications

This thesis includes two publications that have been accepted for publication in peer-reviewed journals. My contribution to each paper is stated in the chapter of the respective summary (2.1 and 2.2).

"**Targeted CD47 checkpoint blockade using a mesothelin-directed antibody construct for enhanced solid tumor-specific immunotherapy**"

Anna Reischer*, **Alexandra Leutbecher***, Björn Hiller, Enrico Perini, Kieron White, Alejandra Hernández Cáceres, Alexandra Schele, Benjamin Tast, Lisa Rohrbacher, Lis Winter, Bastian Czogalla, Sven Mahner, Heinrich Flaswinkel, Heinrich Leonhardt, Lorenza Wyder, Christian Wichmann, Denis Maenner, Fabian Trillsch, Mirjana Kessler, Karl-Peter Hopfner, Nadja Fenn*, Marion Subklewe*

* contributed equally

Cancer Immunology Immunotherapy (2025) 74:214; https://doi.org/10.1007/s00262-025-04032-0

"**SIRPα-αCD123 fusion antibodies targeting CD123 in conjunction with CD47 blockade enhance the clearance of AML-initiating cells**"

Siret Tahk, Binje Vick, Björn Hiller, Saskia Schmitt, Anetta Marcinek, Enrico D. Perini, **Alexandra Leutbecher**, Christian Augsberger, Anna Reischer, Benjamin Tast, Andreas Humpe, Irmela Jeremias, Marion Subklewe, Nadja C. Fenn, Karl-Peter Hopfner
Journal of Hematology & Oncology (2021) 14:155; https://doi.org/10.1186/s13045-021-01163-6

Additionally, I have contributed to the following publications, which have been accepted for publication in peer-reviewed journals but are not included in this thesis.

"**Combining venetoclax and azacytidine with T-cell bispecific antibodies for treatment of acute myeloid leukemia: a preclinical assessment**"
G. Hänel, A. Schönle, A-S. Neumann, D. Nixdorf, N. Philipp, M. Sponheimer, **A. Leutbecher**, A-J. Emhardt, G. Magno, V. Bücklein, J. Eckmann, D. Dunshee, V. Kramar, K. Korfi, S. Colombetti, P. Umaña, C. Klein, M. Subklewe
Leukemia (2024) 38: 398–402. https://doi.org/10.1038/s41375-023-02127-0

"**Characterization and prognostic impact of ACTBL2-positive tumor-infiltrating leukocytes in epithelial ovarian cancer**"
N. E. Topalov, D. Mayr, C. Kuhn, **A. Leutbecher**, C. Scherer, F. B. T. Kraus, C. V. Tauber, S. Beyer, S. Meister, A. Hester, T. Kolben, A. Burges, S. Mahner, F. Trillsch, M. Kessler, U. Jeschke, B. Czogalla
Scientific Reports (2023) 13: 22620. https://doi.org/10.1038/s41598-023-49286-9

"**Accumulation of mutations in antibody and CD8 T cell epitopes in a B cell depleted lymphoma patient with chronic SARS-CoV-2 infection**"
E: Khatamzas, M. Antwerpen, A. Rehn, A. Graf, J. Hellmuth, A. Hollaus, A-W. Mohr, E. Gaitzsch, T. Weiglein, E. Georgi, C. Scherer, S-S. Stecher, S. Gruetzner, H. Blum, S. Krebs, A. Reischer, **A. Leutbecher**, M. Subklewe, A. Dick, S. Zange, P. Girl, K. Müller, O. Weigert, K-P. Hopfner, H-J. Stemmler, M. von Bergwelt-Baildon, O. Keppler, R. Wölfel, M. Muenchhoff, A. Moosmann

Nature Communications (2022) 13: 5586; https://doi.org/10.1038/s41467-022-32772-5
"**T-cell exhaustion induced by continuous bispecific molecule exposure is ameliorated by treatment-free intervals**"
N. Philipp, M. Kazerani, A. Nicholls, B. Vick, J. Wulf, T. Straub, M. Scheurer, A. Muth, G. Hänel, D. Nixdorf, M. Sponheimer, M. Ohlmeyer, S. M. Lacher, B. Brauchle, A. Marcinek, L. Rohrbacher, **A. Leutbecher**, K. Rejeski, O. Weigert, M. von Bergwelt-Baildon, S. Theurich, R. Kischel, I. Jeremias, V. Bücklein, M. Subklewe
Blood (2022) 140 (10): 1104–1118; https://doi.org/10.1182/blood.2022015956

"**Impaired function and delayed regeneration of dendritic cells in COVID-19**"
E. Winheim, L. Rinke, K. Lutz, A. Reischer, **A. Leutbecher**, L. Wolfram, L. Rausch, J. Kranich, P. R. Wratil, J. E. Huber, D. Baumjohann, S. Rothenfusser, B. Schubert, A. Hilgendorff, J. C. Hellmuth, C. Scherer, M. Muenchhoff, M. von Bergwelt-Baildon, K. Stark, T. Straub, T. Brocker, O. T. Keppler, M. Subklewe, A. B. Krug
PLOS Pathogens (2021) 17(10): e1009742. https://doi.org/10.1371/journal.ppat.1009742

"**COVID-19 in Patients Receiving CD20-depleting Immunochemotherapy for B-cell Lymphoma**"
E. Gaitzsch, V. Passerini, E. Khatamzas, C. Strobl, M. Muenchhoff, C. Scherer, A. Osterman, M. Heide, A. Reischer, M. Subklewe, **A. Leutbecher**, B. Tast, A. Ruhle, T. Weiglein, S.S. Stecher, H. Stemmler, M. Dreyling, P. Girl, E. Georgi, R. Wölfel, L. Mateyka, E. D'Ippolito, K. Schober, D. Busch, J. Kager, C. Spinner, M. Treiber, S. Rasch, T. Lahmer, R. Iakoubov, J. Schneider, U. Protzer, C. Winter, J. Ruland, M. Quante, O. Keppler, M. von Bergwelt-Baildon, J. Hellmuth, O. Weigert
HemaSphere (2021) 5(7): e603. DOI: 10.1097/HS9.0000000000000603

In addition, I worked extensively on a project characterizing the tumor microenvironment of primary ovarian cancer with a particular focus on T-cell exhaustion of tumor-infiltrating T-cells. A manuscript preliminary entitled "**The exhausted and immunosuppressive tumor microenvironment of epithelial ovarian cancer can be restored in combinatorial approaches**" is currently in preparation. This project is not part of the presented doctoral thesis.
A. Leutbecher, M. Petry, S. Geweniger, K. White, L. Rohrbacher, G. Hänel, N. Philipp, A-S. Neumann, A. Reischer, B. Czogalla, A. Burges, F. Trillsch, M. Subklewe
Manuscript in preparation

1. Introductory summary

1.1 Immunotherapy has revolutionized cancer treatment

Cancer is emerging as a leading global cause of mortality, with approximately 18 million new cases diagnosed annually, resulting in nearly 10 million deaths [1,2]. Despite advancements in cancer prevention and early diagnosis, both incidence and mortality rates continue to rise. For a long time, cancer treatment was based on three pillars: surgery, radiotherapy, and chemotherapy, with limited durable responses, particularly for patients with advanced diseases. However, in the last 30 years, cancer immunotherapy has remarkably improved patients' survival and quality of life. It is now firmly established as the fourth pillar of cancer treatment in various entities [3].

Cellular aberrations develop continuously through several mechanisms, including infections, DNA and cellular damage, and aging. Internal control mechanisms or immune surveillance usually destroy and eliminate these mutated cells. The immune system comprises the innate and adaptive arms. The innate immune system is characterized by a rapid, non-specific response of myeloid and lymphoid cells, such as macrophages and natural killer (NK) cells, while the adaptive immune system induces an antigen-specific response of lymphocytes. Upon antigen exposure, T cells and B cells proliferate, differentiate for effector functions, and ensure long-term memory in a tightly regulated homeostatic balance [4,5].

Normally, endogenous immune responses alone are highly efficient in recognizing and destroying infected and mutated cells. However, cancerous cells develop various mechanisms to escape the immune system's surveillance, such as antigen loss or downregulation of the major histocompatibility complex (MHC) I and II pathways and inhibitory receptor expression, like programmed cell death protein 1 (PD-1) ligand (PD-L1), for promoting anergy and tolerance. Furthermore, a dysfunctional immune system and immunosuppressive tumor microenvironment (TME), including regulatory T cells (Tregs), "M2"-like polarized macrophages, and myeloid-derived suppressor cells (MDSCs), support tumor development, progression, and recurrence [6,7].

Hence, immunotherapies aim to counteract these mechanisms by modifying and activating immune cells to eliminate tumor cells, boosting the endogenous immune response, and establishing long-term, cancer-specific immunity [8]. The goal is the sustained clearance of residual cancer cells to prevent tumor relapse. Cancer immunotherapy generally involves several strategies leveraging distinct mechanisms to enhance anti-tumor immunity. These include monoclonal antibodies (mAbs), checkpoint inhibition, immunomodulators, adoptive cell transfer (ACT), oncolytic viruses, and vaccination (Figure 1) [8,9].

Conventional or modified mAbs represented a milestone in cancer treatment, as they enhance tumor-specific targeting and induce immune-mediated tumor elimination [10]. Furthermore, antibody-based immune checkpoint inhibition led to a new wave in cancer immunotherapy by restoring the endogenous immune-cell activity against cancer cells. Small molecules are also currently investigated as checkpoint inhibitors overcoming antibody-based limitations, such as suboptimal tumor penetration and potential immunogenicity [11,12]. These antibody-based strategies will be discussed in the following chapters. Other concepts, such as ACT, include the reinfusion of *ex vivo* expanded tumor-infiltrating lymphocytes (TILs) [13], genetically engineered tumor-reactive transgenic T-cell receptor T cells (TCR-T) [14], and chimeric antigen receptor (CAR) T cells [15] into patients. Immunomodulators, such as cytokines [16], and small molecules, such as toll-like receptor agonists [17], stimulate immune responses to enhance tumor recognition. In addition, either naturally occurring or genetically modified, oncolytic viruses infect and lyse tumor cells while stimulating an anti-tumor immune response [18]. Lastly, cancer vaccines, for instance, administered as peptide cocktails or peptide-pulsed dendritic cells (DCs), prime the immune system to recognize tumor antigens and promote long-term immune surveillance [19,20].

Overall, these immunotherapy strategies have remarkably improved cancer treatment, offering effective and durable responses and new therapeutic possibilities. However, only a subset of patients benefit from immunotherapy, and immune evasion mechanisms, primary and acquired resistance, and immune-related adverse events (irAEs) are critical limitations [15,21]. Therefore, novel strategies are urgently needed.

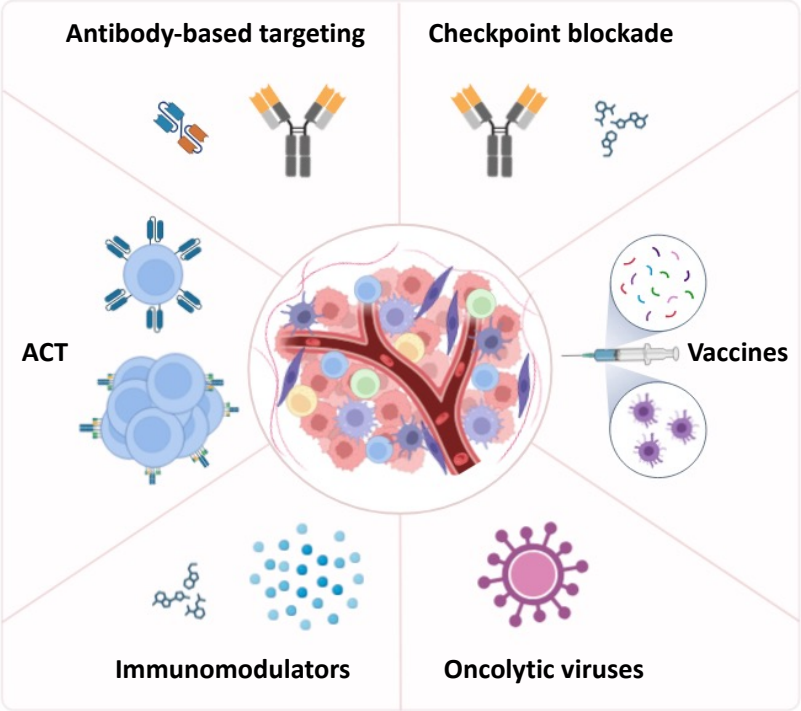

Figure 1 Strategies of cancer immunotherapy [8,9]**.** Different immunotherapeutic approaches are currently used and further evaluated for cancer treatment. These include tumor targeting by monospecific and bispecific mAbs, blockade of immune checkpoints by mAbs or drugs, adoptive cell transfer (ACT) of engineered CAR-T cells or *ex vivo* expanded TILs, vaccination by administration of tumor-specific peptides or pulsed DCs, immunomodulators to activate immune cells or the TME, and oncolytic viruses to infect and lyse cancer cells. This scheme was created with BioRender.com.

1.2 Antibody-based immunotherapy enables a broad therapeutic window

Immunotherapeutic mAbs can target cancer cells specifically and with high affinity to induce tumor-restricted endogenous immune reactions, a major benefit to conventional treatments, such as chemotherapy and radiation therapy.

1.2.1 Monoclonal antibodies have evolved from research tools to powerful therapeutics

Key technologies have enabled the therapeutic use of antibodies. One milestone was the development of the hybridoma technique by Köhler and Milstein in 1975, which facilitated the robust and efficient production of highly specific mouse mAbs against human antigens [22]. However, mouse mAbs can be cleared due to a human anti-mouse immune response after infusion [23]. Subsequently, grafting human antibody constant regions onto mouse antibody variable regions led to the creation of chimeric antibodies with improved therapeutic efficacy and reduced side effects. In 1997, the U.S. Food and Drug Administration (FDA) approved rituximab, the first chimeric therapeutic anti-CD20 mAb, which led to remarkable results and is now the standard of care for treating patients with B-cell lymphomas [24]. To further minimize antibody-based immune responses, the human content of mouse mAbs was increased through "humanization", a process that involves grafting the mouse antibody's complementarity-determining regions (CDRs) onto a human antibody framework. Trastuzumab was one of the first humanized mAbs directed against human epidermal growth factor receptor 2 (HER2) [25], followed by several others, including pembrolizumab and atezolizumab targeting PD-1 and PD-L1, respectively. In the 1990s, advancements such as transgenic mouse models [26] and phage display systems [27] enabled the generation of fully human antibodies for targeting cancer. These innovations have driven a rapid expansion of antibody-based therapeutics over the past 25 years, resulting in more than fifty FDA- and European Medicines Agency (EMA)-approvals for treating hematologic and solid tumors today [28].

However, an obstacle to mAb targeting is the risk of irAEs, including anaphylaxis, autoimmunity, and cytokine release syndrome [29], which was most prominently detected by the dramatic and life-threatening cytokine storm seen after infusing TGN1412, an anti-CD28 mAb [30].

1.2.2 A variety of antibody formats have been developed

Antibodies are characterized by a symmetric Y-shaped structure consisting of two identical light and heavy chains connected by disulfide bonds. Both comprise a variable (V_L and V_H) and a constant (C_L and C_H) domain (Figure 2a). The variable region mediates antigen binding, whereas the constant domain enables the effector function. The antibody can be split into two identical antigen-binding fragments (Fab) and a fragment crystallizable (Fc) domain [31].
Natural antibody formats consist of full-length immunoglobulins (Igs) that bind monospecifically to one target antigen. They are bivalent due to one binding site (paratope) per Fab arm. Igs exist in five distinct isotype forms: IgA, IgD, IgE, IgG, and IgM. For immunotherapy, the IgG isotype is commonly used due to its long half-life (approximately 21 days), tissue penetration capability, and optimal interaction with activating Fcγ receptors (FcγRs) while diminishing binding to inhibitory FcγRs. IgG antibodies are divided into four subclasses (IgG1, IgG2, IgG3, and IgG4), with most therapeutic antibodies focusing on the IgG1 subclass to mediate effector functions [32]. Modifications of the Fc domain, such as glycosylation and key residue amino acid substitution, can increase effector binding and activation [33] but also induce Fc-silencing to reduce immune reactions [34]. In addition, the selection of IgG2 or IgG4 isotypes can initiate weakened Fc activation due to reduced binding to FcγRs [35].
Based on their structure and function, therapeutic antibody formats can be categorized into monospecific**,** bispecific, multispecific, fusion, and payload-conjugated mAbs **(Figure 2).**

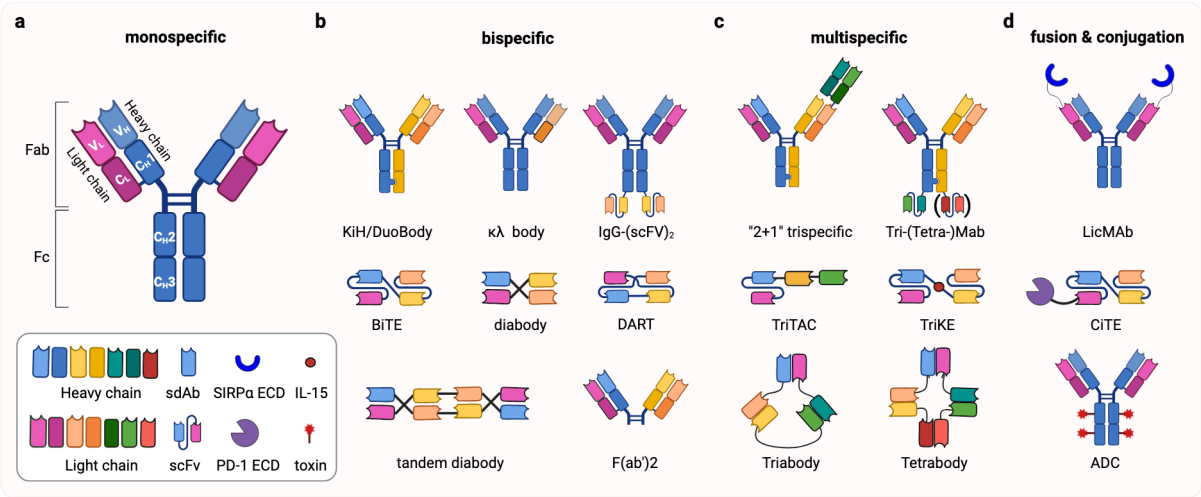

Figure 2 Monoclonal antibodies are developed in various formats [31,36,37]. (**a**) The structure of a monospecific naturally occurring antibody and fragment-based monospecific constructs. Representative examples of artificially engineered bispecific (**b**) and multispecific (**c**), and fusion and conjugation (**d**) mAb constructs based on IgG (upper row) and fragments (middle and lower rows). V_L and V_H: variable light and heavy domain; C_L and C_H: constant light and heavy domain; Fab: antigen-binding fragments; Fc: fragment crystallizable; sdAb: single-domain antibody; scFv: single-chain variable fragment; KiH: Knob-into-hole; IgG: immunoglobulin G; LicMAb: local inhibitory checkpoint monoclonal antibody; BiTE: bispecific T-cell engager; TriTAC: trispecific T-cell activating construct; DART: dual-affinity retargeting; TriKE: trispecific killer engager; CiTE: checkpoint inhibitory T-cell engager; ADC: antibody-drug conjugate; SIRPα: signal regulatory protein α; ECD: extracellular domain. This scheme was created with BioRender.com.

Monospecific IgG antibodies include conventional IgG mAbs and non-IgG fragment-based antibodies, such as engineered single-chain variable fragments (scFv), generated by directly linked V_L and V_H chains [38] and Fab subunits [39] (Figure 2a).

Bispecific antibodies (bsAbs) include the IgG-based formats that can be engineered by heterodimerization of the heavy or light chains, such as knob-into-hole (KiH) [40] and DuoBody [41], or κλ body [42], respectively, and the homodimeric IgG-scFv [43]. In addition, fragment-based bsAbs are developed, for instance, tandem scFv bsAbs, such as bispecific T-cell engager (BiTE) [44], (tandem) diabody [45], dual-affinity retargeting (DART) [46], and F(ab')2 constructs [47] (Figure 2b). Particularly, blinatumomab, the first-in-class CD19xCD3 BiTE, shows remarkable success in patients with relapsed/refractory (r/r), precursor B cell acute lymphoid leukemia [44].
Multispecific constructs are specific to more than two targets, such as the "2+1" trispecific [48], tri- or tetraMab IgG formats [49,50], fragment-based trispecific T-cell activating construct (TriTAC) [51], cross-linking interleukin (IL)-15 TriKE (trispecific killer engager) [52], Triabody, and Tetrabody molecules [53] (Figure 2c).
Furthermore, there are plenty of fusion constructs that can enhance the antibodies' specificity. For instance, the signal regulatory protein α (SIRPα) extracellular domain (ECD) can be fused to a full-length IgG mAb, generating a so-called LicMAb (**Publication I: Reischer* & Leutbecher* et al.**), or the PD-1 ECD can be fused to a BiTE format, generating a so-called CiTE (checkpoint inhibitory T-cell–engager) [54]. Moreover, antibody-drug conjugates (ADC) are developed by conjugating a toxin to IgG- and fragment-based mAbs [55,56] (Figure 2d).
In general, conventional IgG-based mAbs have longer half-lives due to neonatal Fc receptor (FcRn)-mediated recycling, higher solubility, and thermostability than fragment-based antibodies. However, these are beneficial for large-scale production in microbial systems and enhanced tissue penetration [57].

1.2.3 Antibody-based immunotherapy can mediate several modes of action

Most mAbs target tumor-associated antigens (TAAs) and induce cancer cell killing through several mechanisms, including innate immune cell activation, drug delivery, and bispecific immune cell engagement, particularly involving T cells. They can also block inhibitory immune checkpoints and pro-tumoral signaling pathways regarding survival, proliferation, and angiogenesis [58] (Figure 3). Of note, mAbs can combine more than one strategy per molecule.
One major mode of action is the Fc-dependent activation of innate immune cells. Particularly, IgG1 has a strong affinity to the activating FcγRI (CD64), FcγRIIa (CD32a), FcγRIIIa (CD16a), and FcγRIIIb (CD16b), expressed by NK cells, macrophages, and neutrophils [32]. Binding to FcγR induces activating signal cascades, which mediate antibody-dependent cellular cytotoxicity (ADCC) and antibody-dependent cellular phagocytosis (ADCP). Moreover, the C1 complex binds opsonized tumor cells and initiates the complement cascade, inducing complement-dependent cytotoxicity (CDC) [32].
In contrast to directly targeting tumor cells, immune checkpoint-blocking mAbs bind regulatory receptors or their ligands to disrupt inhibitory signaling cascades. T-cell responses are mostly regulated by immune checkpoints, such as PD-1 and cytotoxic T-lymphocyte antigen 4 (CTLA-4). Their expression is induced after T-cell stimulation to limit further T-cell activation by interacting with their respective ligands [59]. More precisely, CTLA-4 competes with the co-stimulatory receptor CD28 for binding to B7-1 (CD80) and B7-2 (CD86) expressed on antigen-presenting cells (APCs), predominantly DCs [60]. PD-1 binds to its ligands PD-L1 and PD-L2, expressed on several cells, like APCs, and particularly tumor cells [59], resulting in an inhibitory signal suppressing T-cell activation and proliferation [61,62]. In that regard, checkpoint blockade provides a powerful therapeutic option leading to enhanced T-cell activation by lowering the activation threshold [63], reinvigorating exhausted T cells [64], and recruiting new T-cells into tumors [65]. Blocking the innate CD47-SIRPα axis, predominantly present between tumor cells and macrophages, inhibits the anti-phagocytic signal in phagocytes and thus triggers ADCP [66].
Additionally, due to their specificity and high affinity, mAbs can be used for targeted drug delivery of agents, such as immunotoxins and radiopharmaceuticals. The binding and internalization of ADCs lead to toxin accumulation in the cytoplasm, such as immunotoxins derived from bacteria or plant proteins, which promote cellular apoptosis and death by harming DNA or microtubules [55].

An important mechanism is the direct blockade of pro-tumoral signals, including survival, proliferation, and angiogenesis. Targeting epidermal growth factor family receptors, such as HER2 and epidermal growth factor receptor (EGFR) expressed in solid tumors, blocks receptor dimerization, resulting in cell cycle arrest and apoptosis [58]. Targeting CD52 was shown to induce caspase-independent cell death in leukemia [67]. Binding to vascular endothelial growth factor (VEGF) ligands and receptors impedes their interaction, disrupting the tumor blood supply [68].

Bispecific or bifunctional mAbs target two distinct antigens or epitopes. Depending on the structure or format of the bsAb and the addressed target, they can engage multiple mechanisms. For instance, immune cells, particularly T cells, can be recruited to tumors. Various signaling pathways, such as tumor-restricted checkpoint blockade and co-stimulation, can be addressed. Additionally, target specificity can be enhanced [69]. These targeting and activation strategies can be amplified using multispecific and multifunctional antibodies [70].

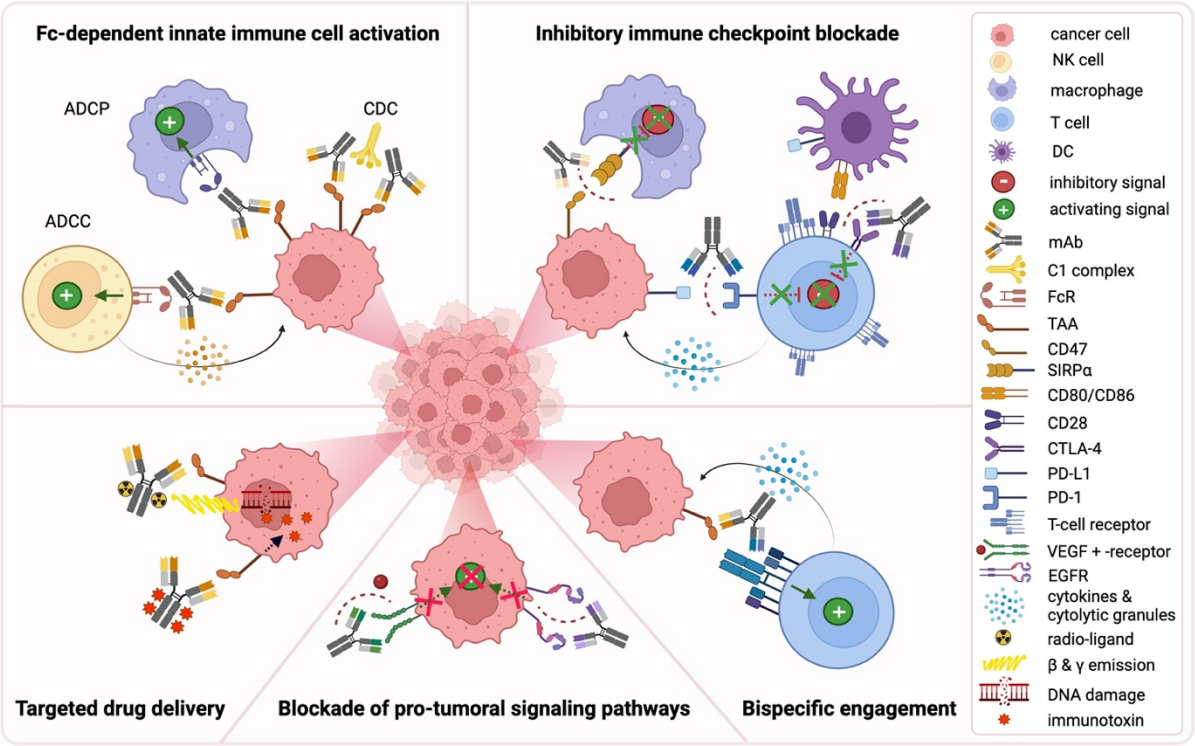

Figure 3 Mode of action of antibody-based immunotherapy [58,66]. Monoclonal antibodies can induce activation of innate immune cells by interaction of the mAb's fragment crystallizable (Fc) domain with the Fc receptor (FcR) on FcR-expressing innate cells, such as NK cells and macrophages, thereby inducing antibody-dependent cellular cytotoxicity (ADCC) and phagocytosis (ADCP), respectively. The complement C1 complex can bind opsonizing mAbs, initiating complement-dependent cytotoxicity (CDC). Another mode of action is the blockade of inhibitory immune checkpoints. Thus, the innate CD47-SIRPα axis involving phagocytic cells, such as macrophages, and the adaptive PD-1/PD-L1 axis involving T cells and tumor cells, as well as the CTLA-4-CD80/CD86 axis, involving T cells and DCs, can be blocked. Moreover, mAbs conjugated with immunotoxins (ADCs) or radio-ligands can mediate cancer cell death by internalizing cytotoxic agents and tumor-directed radioactive emissions, inducing DNA and microtubule damage. The blockade of pro-tumoral signaling pathways regarding survival, proliferation, and angiogenesis represents an additional approach. Bispecific engagement of immune cells comprises various mechanisms, such as tumor-directed target-cell recruitment, activation, and inhibition. For simplicity, a schematic IgG1 mAb is shown here. This scheme was created with BioRender.com.

1.2.4 Tumor-associated antigens are favorable targets

The ideal target antigens of antibodies are tumor-specific cell-surface proteins, which are overexpressed on malignant cells and absent in healthy cells [71]. Rituximab was the first FDA-approved mAb, followed by several FDA-and EMA-approved mAbs targeting TAAs, including HER2 and EGFR for treating solid tumors and CD19 and CD52 for hematologic cancers. In addition, various novel TAA-targeting mAbs are developed and clinically evaluated [28].

1.2.4.1 Mesothelin is a promising solid tumor antigen

Mesothelin (MSLN) was initially described as the target of the mAb K1 in ovarian cancer [72]. However, it is expressed as a 71 kDa glycosylphosphatidylinositol (GPI)-anchored cell surface precursor protein. It is cleaved enzymatically into soluble 31 kDa megakaryocyte potentiating factor (MPF) and the 40 kDa membrane-bound form of MSLN, which is restrictedly expressed on mesothelial cells of the pleura, peritoneum, and pericardium [73]. We and others show a high expression in several malignancies, particularly mesothelioma, epithelial ovarian cancer (EOC), and pancreatic ductal adenocarcinoma (PDAC) [74] (**Publication I: Reischer* & Leutbecher* et al.**). The physiological function of MSLN remains unknown, as MSLN-deficient mice show a normal phenotype [75]. Nevertheless, the interaction of MSLN with cancer antigen 125 (CA-125) is involved in tumor progression and metastasis development [76]. Thus, the restricted expression in normal tissues but high expression in solid cancers, supported by the beneficial blockade of the MSLN-CA-125 axis, highlights MSLN as a promising target for cancer therapies.
Various MSLN-targeting immunotherapeutic approaches, including mAbs [77], ADCs [78], and CAR T-cell therapies [79], have been evaluated in clinical trials. For instance, amatuximab, an αMSLN mAb, has been well-tolerated in $MSLN^+$ tumor patients [77]. In a phase II trial enrolling mesothelioma patients, the combination with pemetrexed and cisplatin chemotherapy was well tolerated, led to 90% disease control, and improved the median overall survival (OS) of 14.8 months compared favorably with 13.3 months in historical controls [80]. The ADC anetumab ravtansine, an αMSLN mAb conjugated to the maytansinoid tubulin inhibitor DM4, is currently evaluated as monotherapy in patients with advanced $MSLN^+$ solid tumors [78]. Its combination with doxorubicin chemotherapy is particularly beneficial in a phase Ib study enrolling platinum-resistant EOC patients [81].
Notably, MSLN can serve as a biomarker in various cancer entities [82], as high concentrations of soluble MSLN have been found in the serum of patients [83] (**Publication I: Reischer* & Leutbecher* et al.**). To maintain the therapeutic window even in the presence of shed MSLN, several approaches were developed, including bispecific or multifunctional antibodies [84,85] (**Publication I: Reischer* & Leutbecher* et al.**) or membrane-proximal MSLN-targeting bsAbs [86] and CAR-T cells [87].

1.2.4.2 CD123 is a therapeutically relevant hematologic tumor antigen

CD123, also known as the IL-3 receptor (IL-3R) α chain, binds IL-3 specifically with low affinity and forms, together with the common β chain, the heterodimeric high-affinity IL-3R. IL-3 regulates the differentiation and proliferation of myeloid cells, including granulocytes, monocytes, and particularly progenitor cells [88].
CD123 is expressed on $CD34^+$ hematopoietic progenitor cells and is maintained in the granulocytic lineage, in contrast to reduced expression in monocytes. Erythrocytes and megakaryocytes progressively lose CD123 expression during differentiation [89]. Nevertheless, CD123 expression on plasmacytoid DCs (pDCs), eosinophils, and neutrophils results in potential on-target off-tumor toxicity [90].
Jordan et al. found CD123 to be frequently expressed on leukemic stem cells (LSCs) in acute myeloid leukemia (AML), as opposed to normal bone marrow-derived hematopoietic cells [91]. The high expression in various hematologic malignancies, including AML, B-cell acute lymphoblastic leukemia, and blastic plasmacytoid dendritic cell neoplasm [92], makes it a promising therapeutic target for mAbs [93] (**Publication II: Tahk et al.**), ADCs [94], T-cell-engaging bsAbs [95], and CAR-T cell therapy [96].

1.2.5 Immune checkpoint inhibition led to a new wave in cancer immunotherapy

Immune checkpoints are regulatory pathways to maintain self-tolerance and prevent overactivation of immune responses. Tumor cells exploit these mechanisms by upregulating inhibitory immune checkpoints to evade immune surveillance. Checkpoint inhibition utilizes the immune system's ability to recognize and eliminate cancer cells [97]. To date, checkpoint inhibition focuses on the adaptive inhibitory pathways, with currently three FDA- or EMA-approved checkpoints, CTLA-4, PD-1/PD-L1, and lymphocyte-activation gene 3 (LAG-3), and more than 20 immune checkpoints being investigated in clinical trials [28]. However, irAEs restrict the therapeutic potential [98], and despite their striking efficacy in some entities, such as melanoma, non-small cell lung cancer, and renal cell carcinoma [99–102], various cancers show only limited responses [103,104]. As checkpoint inhibition only reactivates immune responses, cancers with low mutational burden and low PD-L1 expression, as well as an immunosuppressive TME, including exhausted and dysfunctional T cells, among other reasons, weaken this strategy [105–108]. Thus, innate immune checkpoint blockade is another promising concept.

1.2.5.1 CD47 is an important inhibitory innate immune checkpoint

CD47 is a 50kDa transmembrane protein with an extracellular single Ig superfamily domain [109]. It was first described as a novel TAA in ovarian cancer in 1986 [110] and later named OA3 [111]. In 1994, Mawby et al. [112] identified CD47 as an abundantly expressed glycoprotein identical to OA3 and the integrin-associated protein (IAP), another discovered protein expressed on hematopoietic cells [113]. Interaction of CD47 with its ligands, integrin and thrombospondin-1 (TSP-1), contributes to various mechanisms, including cell adhesion, migration, angiogenesis, and aging [114,115].
The most important role of CD47 as a “marker of self” on red blood cells (RBCs) was demonstrated by $CD47^{-/-}$ RBC elimination through splenic macrophages *in vivo* [116]. The binding of CD47 to its co-receptor SIRPα on myeloid cells, such as macrophages and DCs, inhibits phagocytosis by inducing a “don’t eat me” signal. SIRPα binding leads to downstream phosphorylation of intracellular immunoreceptor tyrosine inhibitory motifs (ITIMs), which recruit and activate Src-homology 2 tyrosine phosphatases, SHP-1, and SHP-2 to inhibit signaling in tyrosine kinase-dependent activation pathways required for phagocytosis [114–116].
The inhibitory checkpoint CD47 is expressed on almost every cell to mediate healthy homeostasis, especially in the life cycle of RBCs. However, tumor cells utilize that mechanism to escape the immune system by upregulating CD47 on the cell surface. AML was the first cancer entity, well characterizing the high CD47 expression [117], followed by a broad range of solid and hematologic malignancies [66] (**Publication I: Reischer* & Leutbecher* et al.**). High CD47 expression has also been shown to correlate with a poorer prognosis in various cancer patients, including AML and EOC [66,117]. Therefore, CD47 represents a viable target.

1.2.5.2 CD47 is a promising target in immunotherapy

CD47 targeting was validated as a promising immunotherapeutic approach for treating various hematological and solid tumor entities [118]. However, CD47 expression on healthy cells, notably RBCs, poses significant challenges for CD47 targeting. Multiple concepts were developed to block the CD47-SIRPα axis, including αCD47 mAbs with reduced RBC targeting [119], SIRPα fusion proteins with an intrinsically lower affinity to CD47 [120], and a human IgG4 isotype to minimize potential off-target effects [121].
The predominant mechanism of blocking the CD47-SIRPα axis was inducing macrophages to mediate ADCP [118]. However, further mechanisms might contribute to the immune response, including macrophage recruitment by secreted cytokines and chemokines [126,128], macrophage polarization [109], neutrophil activation [129], and an adaptive T-cell immune response induced by cross-presentation of phagocytic APCs [128]. By bridging innate and adaptive immunity, blockade of the CD47-SIRPα pathway is a highly promising strategy in cancer immunotherapy.

Liu et al. developed the humanized 5F9 IgG4 mAb (Hu5F9-G4, magrolimab), which bound human CD47 with 8 nM affinity, induced potent ADCP of AML cells *in vitro*, and eliminated AML blasts *in vivo* and toxicokinetic studies in non-human primates [121]. It was subsequently evaluated in clinical trials enrolling patients with r/r AML or myelodysplastic syndromes (MDS) and advanced solid cancers, and despite evidence of monotherapy activity, combination trials were enrolled to evaluate its optimal therapeutic efficacy [130].
In the last 10 years, various other CD47-targeting mAbs were evaluated as monotherapy in phase1/2 clinical trials, including advanced hematologic and solid cancer patients. Anti-CD47 IgG4 mAbs, such as IBI188 [131], CC-90002 [132], Ti-061 [133], lemzoparlimab (TJC4) [134], ligufalimab (AK117) [135], SRF231 [136], and IMC-002 [137], the anti-CD47 IgG2a mAb AO-176 [138], as well as SIRPα Fc fusion mAbs, such as TTI-621 (IgG1) [139], TTI-622 (IgG4) [140], timdarpacept (IMM01) [141] and evorpacept (ALX148) [142] were well tolerated and showed clinical activity. However, further development of, e.g., CC-90002 was discontinued due to a lack of monotherapy activity [143].

1.2.5.3 Combinatorial approaches enhance CD47-mediated phagocytosis

CD47 checkpoint blockade as monotherapy might not be sufficient, as additional pro-phagocytic signals are needed to induce significant ADCP [144]. One approach to synergize the antitumor efficacy is the addition of Fc-active mAbs to stimulate phagocytic cells by Fc-FcγR interaction as pro-phagocytic signals [145]. The combination with rituximab in non-Hodgkin's lymphoma (NHL) patients [122], daratumumab, an anti-CD38 mAb in myeloma [146], as well as GD2-targeting in glioblastoma [147] and trastuzumab, an anti-HER2 mAb, in breast cancer [148], demonstrated promising pre-clinical results *in vitro* and *in vivo*. Notably, the combination of rituximab and magrolimab showed safe and durable complete responses in a phase 1b/2 trial involving patients with aggressive r/r NHL without significant safety events. Interestingly, this combinatorial approach restored the sensitivity of rituximab, as 95% of the enrolled patients were rituximab-resistant [149]. Moreover, lemzoparlimab in combination with rituximab demonstrated anticancer activity and was well tolerated in a phase 1b study for r/r NHL [150]. For the treatment of solid tumors, including gastric cancer and HNSCC, the combination of evorpacept and trastuzumab was favorable with historic controls [142].
Another strategy is to induce immunogenic cell death, which leads to the upregulation of pro-phagocytic ligands, such as calreticulin, on the target cells [151]. In that regard, cytotoxic agents, including chemotherapy, poly ADP ribose polymerase inhibitors (PARPi), and stimulator of interferon genes (STING) agonists, synergized with CD47 blockade in solid tumors *in vitro* [152–154].
Moreover, magrolimab-mediated CD47 blockade combined with the hypomethylating agent azacytidine was pre-clinically and clinically demonstrated as an encouraging and synergistic approach for hematologic malignancies, particularly AML and MDS [155]. The combinatorial treatment demonstrated several benefits. It eliminated LSCs, potentially inducing a more durable response, and changed the bone marrow TME, including an increased T-cell frequency as evidence of adaptive immune activation. Furthermore, the response rates of TP53 mutant AML patients having a particularly poor prognosis were improved [156].
Azacytidine was well tolerated by MDS patients and showed clinically meaningful activity in combination with evorpacept [157], lemzoparlimab [158], and timdarpacept [159] in phase 2 trials, as well as IBI188 [160] and ligufalimab [161] in phase 1b trials.
Furthermore, AML patients were enrolled in phase 1/2 trials evaluating magrolimab in combination with the BCL-2 inhibitor, venetoclax, and azacytidine, showing remarkable response rates and a safe profile [162]. However, the randomized, double-blind, placebo-controlled, multicenter phase 3 ENHANCE-3 study (NCT05079230) evaluating magrolimab + venetoclax + azacytidine in AML patients was terminated due to futility. Although full reports are missing to date, the first preliminary data showed increased toxicity due to on-target off-leukemia toxicity. Previously untreated AML patients, ineligible for intensive chemotherapy due to an older age (>75) or having comorbidities, were enrolled. In that regard, the elderly, frail patient cohort was a major obstacle. Furthermore, one can speculate if an IgG4 construct combined with a hypomethylating agent is the ideal combination to provide the needed pro-phagocytic signal. However, all clinical trials for the application of magrolimab in

hematologic and solid malignancies are withdrawn, discontinued, or terminated (e.g., NCT05079230, NCT06046482, NCT05169944, NCT05738161, NCT05807126).
An alternative approach is the combination of innate and adaptive checkpoint blockade, which has been pre-clinically shown to be synergistic for several solid cancers [163]. In a phase 2 trial, timdarpacept plus αPD-1 mAb tislelizumab, showed a robust anti-tumor efficacy with a well-tolerated safety profile for lymphoma and solid tumor patients [164]. In a phase 1 trial enrolling advanced solid tumors, the combination of evorpacept and αPD-1 mAb pembrolizumab, was favorable to historical controls, supporting further investigation [142]. Ligufalimab plus cadonilimab, a PD-1/CTLA-4 bsAb, and chemotherapy demonstrated encouraging anti-tumor activity in a phase 1 trial enrolling gastric cancer patients [165].

1.2.5.4 On-target off-tumor binding can lead to CD47-induced toxicities

The ubiquitous expression of CD47 on healthy cells demonstrates a major risk for CD47-targeting. Higher doses are likely needed to overcome a potential antigen sink. Moreover, the particularly high expression of CD47 on RBCs can lead to RBC clearance, resulting in anemia as a serious CD47-induced toxicity [121,166].
Throughout the ~120-day lifespan of RBCs, high expression of CD47 diminishes during aging while simultaneously upregulating pro-phagocytic signals. In that regard, aged RBCs might be disposed to CD47 targeting. Magrolimab has been evaluated in several clinical trials, demonstrating manageable anemia. An initial low priming dose of 1 mg/kg of magrolimab was shown to mitigate anemia by eliminating aged RBCs but sparing young RBCs [156]. As a result, the transient mild and predictable anemia was followed by compensatory reticulocytosis, and the newly generated RBCs were unaffected by magrolimab [156]. Furthermore, a protective phenomenon named RBC pruning was detected, meaning that initially primed RBCs lost CD47 expression by CD47 shedding [167]. Thus, this priming dose, followed by a higher maintenance dose, reduced anemia in phase 1 clinical trials with advanced solid tumor and NHL patients [149,166].
In general, CD47-targeting mAbs were well tolerated by the patients in the clinical trials, and the common irAEs were manageable anemia, thrombocytopenia, and neutropenia. Furthermore, fatigue, nausea, and infusion-related reactions occurred [131,138,140,143]. The phase 1/2 combination trials of magrolimab and azacytidine resulted in an irAE profile similar to azacytidine monotherapy, mainly anemia, thrombocytopenia, and infusion reactions [155].
However, magrolimab showed no improved overall survival or response in the recent phase 3 ENHANCE-3 study (NCT05079230), and the higher incidence of serious irAEs resulted in the complete stop of further developing magrolimab. However, as the enrolled patients are already biased due to their older age or comorbidities and, therefore, overall difficult to treat, the conclusions might not reflect the true potential of CD47 checkpoint blockade [168].

1.2.5.5 Multispecific targeting improves CD47 checkpoint blockade

Synergism between blocking the CD47-SIRPα pathway and additional tumor targeting or adaptive checkpoint blockade has been shown. Consequently, novel concepts evolved by fusing different strategies into one molecule, leading to bifunctional or multifunctional antibody constructs. These include bsAbs bridging innate and adaptive immunity to maximize the anti-tumor efficacy and improve a long-term response, such as CD47×PD-L1 bsAbs (IBI322 and PF-07257876) [169,170], SIRPα-Fc-CD40L fusion protein (SL-172154) [171 172], and SIRPα×4-1BB bsAb (DSP107) [173], for advanced solid tumors and hematologic malignancies.
A major strategy is combining CD47 blockade with TAA-targeting to redirect the checkpoint blockade to tumor cells, thus reducing on-target off-tumor toxicities. Several bsAbs were developed pre-clinically to treat hematologic malignancies by co-targeting CD47 with CD20 [174], CD19 [175], CD38 [176], and CD70 [177]. Ponce et al. developed a multifunctional antibody construct targeting CD33 with high affinity and blocking CD47 by a fused low-affinity SIRPα domain [178]. We adapted this concept to target CD123 on AML LSCs (**Publication II: Tahk et al.**). Other examples are the humanized CD47×CD19 bsAb, TG-

1801, showing clinical activity as monotherapy and an acceptable preliminary safety profile in B-cell lymphoma patients in combination with the αCD20 mAb ublituximab patients [179]. The humanized CD47×CD20 BsAb, IMM0306, was well tolerated with robust anti-tumor activity in a phase 1/2 trial for treating r/r NHL patients as monotherapy [180] , and the combination trial with lenalidomide is currently ongoing, showing similar irAEs to monotherapy [181].
For the treatment of solid tumors, several bsAbs were developed pre-clinically, such as targeting human HER2 [182], Glypican-3 (GPC3) [183], CD24 [184], CD38 [185], EpCAM [186], B7-H3 [187], and EGFR [188]. For instance, the CD47×HER2 bsAb, IMM2902, demonstrated encouraging preliminary safety, tolerability, and anti-tumor activity in a phase 1/2 trial [189]. NI-1801, an MSLN×CD47 fully human IgG1 bsAb was developed as κλ-body format with an αMSLN λ-light chain and an αCD47 κ-light chain [86]. It is currently being studied in a clinical trial for patients with MSLN-expressing solid malignancies, including EOC, breast cancer, and PDAC, as monotherapy and in combination with pembrolizumab or paclitaxel [42]. We also developed an MSLN- and CD47-targeting construct. We translated the concept of Ponce et al. in AML [178] to solid tumors by targeting MSLN and CD47 by fusing the extracellular SIRPα domain to the full-length αMSLN mAb. The multivalent specificity of our construct is the major advantage compared to the MSLN×CD47 bsAb, leading to superior binding, ADCC, and ADCP (**Publication I: Reischer* & Leutbecher* et al.**).

1.3 Cancer entities in focus

Despite remarkable improvements in cancer treatment of a subset of patients, several entities, such as EOC, PDAC, and AML, do not benefit from immunotherapy [15,21,190]. Although EOC and AML differ fundamentally in cellular origin and affected physiological systems, each presenting unique challenges in diagnosis, treatment, and prognosis, both malignancies remain highly lethal, highlighting the urgent need for novel treatment strategies.

1.3.1 Epithelial ovarian cancer

Ovarian cancer is the fifth leading cause of cancer-related death in women worldwide [191]. It is a heterogeneous disease, with EOC accounting for the most frequent and lethal gynecological malignancy, as approximately 90% of the patients are affected. Malignant germ cell and sex-cord stromal tumors are less common. EOC is histologically classified into high-grade and low-grade serous, endometrioid, mucinous, and clear cell carcinomas, whereby high-grade serous ovarian carcinoma (HGSOC) is the predominant and most aggressive form [192,193].
An early diagnosis of EOC with a localized tumor stage leads to a high 5-year OS rate of 93%. In contrast, a late diagnosis, where metastases have already spread, reduces the 5-year OS to 30% [194]. Unfortunately, most patients are diagnosed at an advanced stage due to the combination of missing or nonspecific symptoms, such as back and abdominal pain, fatigue, and bloating [195], as well as inefficient screening and manifestation tools [196].
The standard treatment of EOC is debulking surgery and first-line platinum-based chemotherapy. Despite initial remission in 80% of the women, most advanced cancer patients relapse and additionally develop chemoresistance. Novel strategies such as targeted therapy, hormone therapy, and immunotherapy are evaluated [197]. The molecular heterogeneity of the disease further complicates the treatment options. P53 was aberrantly mutated, and in approximately 50% and 25% of HGSOC patients, homologous recombination deficiency (HRD) and BRCA1/2 mutations were detected, respectively [198]. Based on this, novel strategies impeding DNA repair pathways, such as PARPi to induce synthetic lethality, have been developed. Since 2014, four different PARPi have been approved by the FDA and EMA for treating recurrent and newly diagnosed BRCA-mutated EOC patients, significantly improving these patients' survival [199]. Furthermore, two years ago, the FDA approved the folate receptor α (FolRα)-targeting ADC, mirvetuximab soravtansine, for platinum-resistant FolRα-expressing ovarian cancer [200].

However, immunotherapeutic approaches, such as PD-1/PD-L1 checkpoint blockade, have not been beneficial [201]. Although EOC was the first tumor to detect intratumoral T cells as a prognostic factor [202], an immunosuppressive TME, including abundant Tregs [203] and exhausted T cells [204,205], may contradict the immune response. Several ongoing clinical studies evaluate novel immunotherapeutic strategies to fight this challenging disease.

1.3.2 Acute myeloid leukemia

Acute leukemias are characterized by the accumulation of aberrantly differentiated hematopoietic stem cells that disrupt regular hematopoiesis [206]. AML is a highly aggressive and the most frequent form of acute leukemia in adults, with a median age of 65 years. It is described by the uncontrolled proliferation of immature myeloid precursor cells in the bone marrow and peripheral blood [207,208]. The accumulation of immature blasts in the bone marrow leads to anemia, thrombocytopenia, and neutropenia [209]. The clinical symptoms range from fatigue, pallor, bleeding, and an increased risk of infections [210].

AML is driven by a rare population of LSC clones with different sequentially acquired mutations, leading to a heterogeneous mutational landscape of several common genetic mutations, such as fms-related tyrosine kinase 3 (FLT3), nucleophosmin 1 (NPM1), DNA methyltransferase 3 α (DNMT3A), isocitrate dehydrogenase 1 (IDH1), IDH2, TP53, and Wilm's tumor 1 (WT1), and thousands of additional rarely mutated genes [211]. LSCs are often chemotherapy-resistant, thereby initiating relapse. This highlights them as important targets to induce durable responses in AML patients [190].

The standard treatment involves chemotherapy, followed by active immune surveillance, including assessment of post-treatment measurable residual disease (MRD) and maintenance therapy to prevent relapse. Nevertheless, approximately 40% of MRD-negative patients relapse within 5 years with a poor prognosis [212]. High-risk patients characterized by an unfavorable cytogenetic profile may be considered for allogeneic hematopoietic stem cell transplantation (HSCT), currently the only potentially curative option, by inducing a graft-versus-leukemia effect. However, HSCT is not eligible for all patients, and relapse rates remain high [213].

As current advances in understanding AML biology and genetics have identified novel targets and deregulated pathways, several targeted therapies were developed and recently approved by the FDA, including small molecules targeting FLT3, gilteritinib [214], and midostaurin [215], ADCs targeting CD33, such as gemtuzumab ozogamicin [216], and the combination of the BCL-2 inhibitor venetoclax with the hypomethylating agents azacytidine or decitabine [217] .

Immunotherapeutic approaches, including bispecific T-cell engagers targeting CD33, such as flotetuzumab and AMG 330 [218], and CAR-T cells, [219] are currently under investigation, showing partially promising early results in clinical trials with r/r AML patients. Despite recent advances, the prognosis for AML remains poor, with a 5-year OS rate of ~30% [211], highlighting the need for novel therapies to improve patient outcomes.

1.4 Aim

Despite favorable progress in treating various cancer entities in the last decades, several malignancies, such as EOC and AML, have not yet benefited and often remain lethal. Thus, novel treatment strategies are urgently needed. The overexpression of the innate immune checkpoint CD47 on tumor cells emphasizes its targeting as a promising strategy. However, ubiquitous CD47 expression on healthy cells poses a therapeutic risk. We aimed for the development of a multifunctional mAb construct, which combines low-affinity CD47 checkpoint blockade with high-affinity tumor binding, thereby (1) reducing on-target off-tumor toxicity by improved tumor targeting and (2) mediating a robust immune response in solid tumors and hematologic cancers.

2. Summary of publications

2.1 Publication I: Targeted CD47 checkpoint blockade using a mesothelin-directed antibody construct for enhanced solid tumor-specific immunotherapy [220]

In this study, we developed a novel multifunctional antibody construct as an immunotherapeutic approach to improve solid tumor treatment. Despite promising results in some cancer entities, several solid tumors, like EOC and PDAC, do not respond to blockade with adaptive checkpoint inhibitors, often resulting in poor prognosis. Effective treatment options remain limited, highlighting the need for novel therapeutic approaches. The innate immune checkpoint CD47 represents a promising target due to its widespread overexpression on cancer cells. However, its expression on healthy cells poses challenges, including a potential antigen sink and on-target off-tumor toxicity. This necessitates strategies to enhance specificity and therapeutic efficacy. Thus, we combined low-affinity CD47 blockade with high-affinity tumor targeting in a single multifunctional mAb using MSLN as an established TAA for solid cancers.

For this purpose, a local inhibitory checkpoint monoclonal antibody (LicMAb) was generated by fusing the endogenous *N*-terminal SIRPα Ig V-like domain, characterized by a lower affinity to CD47, to a high-affinity anti-human MSLN IgG1 mAb. Two mAb clones, 4D8 and M4F5, were generated using hybridoma technology following mouse and rat immunization, respectively. Both SIRPα-αMSLN LicMAb clones were evaluated for binding, CD47 blocking, and their functional capacity mediating ADCC and ADCP of solid tumor cells. The EOC cancer cell line OVCAR-3 and the MSLN-transduced PDAC cell line SUIT-2-MSLN were used as model systems with different levels of CD47 and MSLN expression. First, we analyzed the RNA expression of CD47 and MSLN in various cancer entities and found both to be highly upregulated in several solid tumor entities, particularly in EOC and PDAC. Moreover, we confirmed their protein expression in primary EOC cells derived from tumor tissue and ascites.

Next, we demonstrated the SIRPα-αMSLN LicMAb binding to the OVCAR-3, SUIT-2-MSLN, and $MLSN^+$ primary EOC cells but not $MSLN^-$ cells. Importantly, the binding capacity was dependent on the MSLN expression levels. Despite the low-affinity binding of the fused SIRPα domain, LicMAbs blocked CD47 on the target cells, but to a lesser extent than high-affinity αCD47 mAbs.

As CD47-expressing RBCs are the most abundant cells in the blood and anemia was the most common CD47-related toxicity in clinical studies with magrolimab, we evaluated the risk of on-target off-tumor binding. The LicMAbs did not bind to RBCs and neutrophils nor induce platelet aggregation. However, lymphocytes were bound by the LicMAbs but to a significantly lesser extent than by high-affinity αCD47 mAbs. Importantly, in competitive binding assays with excess RBC and lymphocytes, the LicMAbs bound specifically to the $MSLN^+$ cancer cells and avoided binding to RBC or lymphocytes in contrast to high-affinity αCD47 mAbs.

Next, the functional capacity of LicMAbs to induce NK cell-mediated cytotoxicity of EOC and PDAC cell lines was evaluated. The LicMAbs induced E: T-ratio- and dose-dependent lysis of OVCAR-3 and PDAC cells, superior to the αMSLN mAb (4D8 and M4F5) and amatuximab. The NK-cell activation and degranulation correlated with the dose-dependent lysis. Notably, shed MSLN is a common phenomenon known to diminish MSLN-targeting. Therefore, we analyzed the binding and cytotoxic capacity of LicMAbs in the presence of soluble MSLN. While the capability of conventional αMSLN mAb has been highly affected, the LicMAbs were still effective, albeit with higher concentrations.

As a next step, the improved phagocytosis by blocking the CD47-SIRPα axis in addition to the IgG1 prophagocytic signal was demonstrated in EOC and PDAC entities. The LicMAbs induced dose-dependent phagocytosis of OVCAR-3 and SUIT-2-MSLN cells, dependent on the MSLN levels expressed on the target cells. Interestingly, the combinatorial targeting of LicMAbs showed enhanced ADCP to CD47 blockade mediated by αCD47 (h5F9) and magrolimab.

Lastly, we demonstrated the LicMAb-mediated killing of MSLN$^+$ EOC cells in a 3D organoid system as a more advanced pre-clinical research model.
Taken together, we established a novel strategy to redirect the CD47 blockade to solid cancer entities. CD47-related on-target off-tumor toxicities were avoided by restricting the innate immune reaction to MSLN-expressing tumor cells.

My contribution:

The shared co-authorship is due to the project initiation and the first two rounds of LicMAb expression (clone 4D8) done by A.R. My contribution to this publication is based on designing, planning, performing, analyzing, and interpreting the *in vitro* experiments. More precisely, I isolated the EOC single-cell suspensions by dissociating the primary EOC tissue samples derived from surgery or cultivation of ascites fluid, and I analyzed the antigen expression pattern and LicMAb binding capability by flow cytometry. I evaluated the binding and blocking specificity of the expressed mAbs and LicMAbs on the cell lines by flow cytometry. Furthermore, I took care of the continuous cultivation of the cell lines and the collection and isolation of the HD PBMCs used for the experiments.
Additionally, I analyzed on-target off-tumor toxicities induced by hematopoietic cell binding and competition assays with both cell lines OVCAR-3 and SUIT-2-MSLN. I conducted and analyzed all cytotoxicity assays of OVCAR-3 cells and SUIT-2-MSLN cell lines (clone 4D8 and M4F5) by impedance measurement (xCELLigence) and flow cytometry, as well as the respective evaluation of the NK-cell activation and degranulation. Likewise, I performed and analyzed the phagocytosis assays of OVCAR-3 cells and SUIT-2-MSLN cells (clone 4D8 and M4F5) evaluated by imaging flow cytometry and classical flow cytometry. Furthermore, I compared the LicMAbs and the CD47xMSLN bsAb in the ADCC and ADCP assays. Besides, I was involved in the preparation, evaluation, and interpretation of the *ex vivo* EOC organoid cytotoxicity assays.
In addition, I designed all the figures, wrote the first manuscript draft, and organized and handled the complete submission and revision process.
(Figures 1-6; and Supplementary Figures S1-8)

2.2 Publication II: SIRPα-αCD123 fusion antibodies targeting CD123 in conjunction with CD47 blockade enhance clearance of AML-initiating cells [221]

In this study, published by Tahk et al., we developed a dual-targeting immunotherapeutic strategy to treat AML. A major challenge in AML treatment is the persistence of the chemo-refractory AML-initiating LSCs. In that regard, LSC targeting is a promising strategy to avoid AML relapse and achieve sustained remission. As the innate checkpoint CD47 and the TAA CD123 are highly expressed on bulk AML and LSC cells, a dual targeting approach was developed by binding CD123-expressing cells and locally blocking the CD47-SIRPα axis.

In that regard, we fused an αCD123 mAb with the extracellular SIRPα domain, generating a single-fused 1 x SIRPα-αCD123 and a double-fused 2 x SIRPα-αCD123 antibody construct. The specific binding and CD47 blocking properties, as well as the functional capacity to induce ADCC and ADCP of AML, were characterized *in vitro* and *in vivo*.

First, binding and CD47 blocking studies were performed. Both fusion constructs bound the $CD123^{+}CD47^{+}$ AML cell line MOLM-13 more strongly than the αCD123 mAb. Despite the low-affinity binding of the SIRPα domain, the single fusion enabled CD47 blockade, which was enhanced by the double fusion. As expected, the high-affinity αCD47 mAb blocked the majority of CD47 on the MOLM-13 cell surface. To evaluate the risk of on-target off-tumor toxicities and an antigen sink, competitive binding assays with excess RBCs or PBMCs were performed. RBCs, which are highly abundant in the blood, were not bound by the constructs. The fusion constructs bound PBMCs, including $CD123^{+}$ pDCs, in the presence of AML cells. The 2 x SIRPα-αCD123 showed a similar binding strength to PBMCs compared to the high-affinity αCD47 mAb. Nevertheless, PBMC binding by the fusion constructs was significantly reduced compared to the high-affinity αCD47 control antibodies Hu5F9-G4 and commercially available B6H12. Platelets were less bound and aggregated by the fusion constructs than the CD47-targeting control antibodies.

Next, the phagocytic capacity of the constructs was evaluated by blocking the CD47-SIRPα axis in combination with the prophagocytic FcR stimulation. The enhanced phagocytosis of the MOLM-13 cell line and primary patient-derived AML (pAML) blasts was demonstrated in an allogeneic and autologous setting. Thereby, 1 x and 2 x SIRPα-αCD123 induced comparable ADCP frequencies superior to αCD47 or the combination of αCD47 and αCD123. Furthermore, the NK cell-mediated lysis of the MOLM-13 cell line and pAML cells was analyzed. Both fusion constructs induced specific lysis of MOLM-13 and pAML cells with enhanced lysis mediated by the double fusion. The αCD47 did not lead to the lysis of pAML cells. Interestingly, a fusion construct targeting the TAA CD33 (SIRPα-αCD33) mediated less lysis than its SIRPα-αCD123 counterpart. The 1 x and 2 x SIRPα-αCD123 markedly increased lysis of AML patient-derived xenografts (PDX) compared to αCD123.

As a last step, the cytotoxic capability of the fusion constructs was evaluated by an *in vivo* engraftment assay. To this end, residual AML PDX cells surviving an *ex vivo* ADCC assay served as a surrogate for LSCs and were transplanted into NSG mice. The 2 x SIRPα-αCD123 mediated tumor control and significantly longer survival of the PDX-engrafted mice compared to the αCD123-treated mice. The preferred targeting of LSCs over bulk AML cells was detected using the extreme limiting dilution algorithm.

Overall, by developing the dual-targeting SIRPα-αCD123 fusion constructs, we localized the disruption of the CD47-SIRPα axis to AML cells and thus enhanced the elimination of LSC cells without on-target off-leukemia toxicities.

My contribution:

My contribution to this publication is based on performing, evaluating, and interpreting the experiments concerning on-target off-tumor toxicities. I collected and isolated PBMCs derived from HD whole blood. Primarily, I analyzed the CD123 and CD47 antigen expression on the cell surface of HD PBMCs. I established a multicolor flow cytometry panel and evaluated the CD47 expression levels on PBMCs and, in greater detail, on $CD4^+$ and $CD8^+$ T cells, B cells, NK cells, pDCs, and monocytes. Moreover, I conducted binding assays of the antibody fusion constructs and proper controls to HD PBMCs, depicted in Figure 2F.

3. Publication I

Cancer Immunology, Immunotherapy (2025) 74:214
https://doi.org/10.1007/s00262-025-04032-0

RESEARCH

Targeted CD47 checkpoint blockade using a mesothelin-directed antibody construct for enhanced solid tumor-specific immunotherapy

Anna Reischer[1,2] · Alexandra Leutbecher[1,2] · Björn Hiller[3] · Enrico Perini[3] · Kieron White[2] · Alejandra Hernández-Cáceres[3] · Alexandra Schele[3] · Benjamin Tast[1,2] · Lisa Rohrbacher[1,2] · Lis Winter[1,2] · Bastian Czogalla[4] · Sven Mahner[4] · Heinrich Flaswinkel[5] · Heinrich Leonhardt[5] · Lorenza Wyder[3] · Christian Wichmann[6] · Denis Maenner[6] · Fabian Trillsch[4] · Mirjana Kessler[4] · Karl-Peter Hopfner[3] · Nadja C. Fenn[3] · Marion Subklewe[1,2]

Received: 24 September 2024 / Accepted: 24 March 2025

Abstract
The immune checkpoint CD47 is highly upregulated in several cancers as an innate immune escape mechanism. CD47 delivers a "don't eat me" signal to its co-receptor signal regulatory protein α (SIRPα), thereby inhibiting phagocytosis. Blocking the CD47–SIRPα axis is a promising immunotherapeutic strategy against cancer. However, early trial data has demonstrated on-target off-leukemia toxicity. In addition, the ubiquitous expression pattern of CD47 might contribute to an antigen sink. In this study, we combined low-affinity CD47 checkpoint blockade and specific tumor targeting in a multivalent and multifunctional antibody construct to prevent CD47-related toxicities. First, we established a local inhibitory checkpoint monoclonal antibody (LicMAb) by fusing two *N*-terminal extracellular domains of SIRPα to a full-length anti-human mesothelin (MSLN)-IgG1 antibody, a well-described tumor-associated antigen in epithelial ovarian cancer (EOC) and pancreatic ductal adenocarcinoma (PDAC). Next, we evaluated the SIRPα-αMSLN LicMAb for mediating a tumor-restricted immune response as observed by antibody-dependent cellular cytotoxicity (ADCC) and phagocytosis (ADCP). Our data validates CD47 and MSLN as highly upregulated targets expressed on various solid cancer entities, particularly EOC. We show tumor-specific binding and CD47 blocking by the SIRPα-αMSLN LicMAb even in the presence of healthy CD47-expressing cells. Furthermore, the LicMAb induces NK-cell-mediated cytotoxicity and improves phagocytosis of EOC and PDAC tumor cells. Moreover, cell death in EOC-derived organoids was specifically LicMAb-driven. Hence, the SIRPα-αMSLN LicMAb combines a tumor-restricted blockade of the CD47–SIRPα axis with a specific antitumor response while preventing on-target off-tumor toxicities. Our data supports the multifunctional SIRPα-αMSLN LicMAb as a promising approach to treating solid tumors.

Anna Reischer, Alexandra Leutbecher, Nadja C. Fenn and Marion Subklewe: Contributed equally.

✉ Nadja C. Fenn
nfenn@genzentrum.lmu.de

✉ Marion Subklewe
marion.subklewe@med.uni-muenchen.de

[1] Department of Medicine III, University Hospital, LMU Munich, Munich, Germany

[2] Laboratory of Translational Cancer Immunology, LMU Gene Center, Munich, Germany

[3] Gene Center and Department of Biochemistry, LMU Munich, Munich, Germany

[4] Department of Obstetrics and Gynecology, Comprehensive Cancer Center Munich, University Hospital, LMU Munich, Munich, Germany

[5] Faculty of Biology and Center for Molecular Biosystems (BioSysM), Human Biology and BioImaging, LMU Munich, Munich, Germany

[6] Division of Transfusion Medicine, Cell Therapeutics and Haemostaseology, University Hospital, LMU Munich, Munich, Germany

Published online: 22 May 2025

Graphical abstract

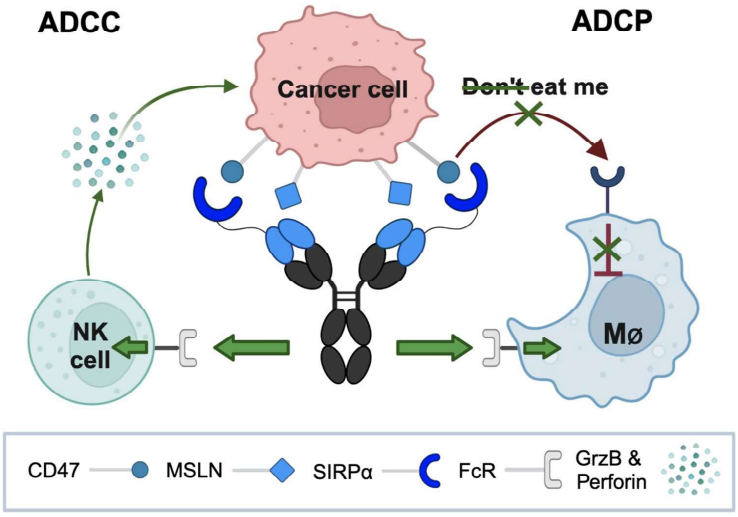

The local inhibitory checkpoint monoclonal antibody (LicMAb) binds mesothelin (MSLN) with high affinity and simultaneously blocks CD47 on MSLN-expressing tumor cells to inhibit the "don't eat me" signal. CD47 is blocked by the fused extracellular SIRPα domain that intrinsically has a low affinity. Furthermore, the SIRPα-αMSLN LicMAb is based on a human IgG1 backbone to provide an Fc receptor (FcR)-activating stimulus to enable direct NK-cell-mediated killing by granzyme B (GrzB) and perforin secretion, and an additional pro-phagocytic signal to phagocytic cells, such as macrophages (MØ). This leads to tumor-restricted antibody-dependent cellular cytotoxicity (ADCC) and antibody-dependent cellular phagocytosis (ADCP) of cancer cells. This scheme was created with BioRender (BioRender.com/g77u465).

Keywords CD47–SIRPα · Innate immune checkpoints · Mesothelin · Multifunctional antibodies · Solid tumors

Abbreviations

SIRPα	Signal regulatory protein α
LicMAb	Local inhibitory checkpoint monoclonal antibody
MSLN	Mesothelin
EOC	Epithelial ovarian cancer
PDAC	Pancreatic ductal adenocarcinoma
ADCC	Antibody-dependent cellular cytotoxicity
ADCP	Antibody-dependent cellular phagocytosis
FcR	Fc receptor
GrzB	Granzyme B
MØ	Macrophages
mAbs	Monoclonal antibodies
ICIs	Immune checkpoint inhibitors
RBCs	Red blood cells
TAA	Tumor-associated antigen
V_L	Variable light chain
V_H	Variable heavy chain
$(G_4S)_4$	Polyglycine-serine linker of 4 repeats
E	T ratio: Effector: target ratio
PDOs	Patient-derived organoids
MPFC	Multiparametric flow cytometry
MFI	Median fluorescence intensity
SPR	Surface plasmon resonance
AUC	Area under curve
rhMSLN	Recombinant human MSLN
BF	Brightfield
CT	Cell Trace™
EpCAM	Epithelial cell adhesion molecule
bsAb	Bispecific antibody
HER2	Human epidermal growth factor receptor 2
EGFR	Epidermal growth factor receptor
GPC3	Glypican-3
PD-L1	Programmed death ligand 1
ADC	Antibody–drug conjugate
CART	Chimeric antigen receptor T cell
PARPi	Poly ADP ribose polymerase inhibitors
STING	Stimulator of interferon genes

Introduction

Immunotherapy has revolutionized the therapeutic landscape of oncology for most tumor entities. In recent decades, monoclonal antibodies (mAbs) targeting immune checkpoints have reformed treatment algorithms for various cancer entities [1]. However, some solid cancer entities such as epithelial ovarian cancer (EOC) or pancreatic ductal adenocarcinoma (PDAC) show only limited response to the blockade of adaptive immune checkpoint inhibitors (ICIs). As the patient outcome remains poor in these disease entities, novel treatment options are highly sought after [2, 3].

The inhibitory innate checkpoint molecule CD47 is known as a "marker of self" and is expressed on almost every cell in the body. The interaction of CD47 with its co-receptor signal inhibitory regulatory protein α (SIRPα) on phagocytes sends a "don't eat me" signal that is necessary for healthy homeostasis, especially in the life cycle of red blood cells (RBCs) [4]. Interestingly, CD47 has been reported to be overexpressed in many different hematological and solid tumors as an immune escape mechanism [5, 6].

Targeting CD47 with mAbs has been shown to block the CD47–SIRPα signaling axis and thus, leads to enhanced phagocytosis of tumor cells. The first-in-class IgG4 CD47-targeting mAb magrolimab, followed by others, demonstrated robust anticancer activity in patients with hematologic and solid cancers [7, 8]. Nevertheless, as CD47 is ubiquitously expressed on healthy cells, its targeting leads to CD47-induced toxicities, such as anemia and thrombocytopenia [9]. Additionally, high doses of CD47-targeting mAbs are required due to a large antigen sink [8]. Clinical trials with magrolimab in hematologic and solid malignancies were discontinued due to on-target off-tumor toxicity rendering further investigation futile (e.g. NCT05079230, NCT06046482). To reduce CD47 targeting on healthy cells, other strategies to block the CD47–SIRPα axis were developed such as αCD47 mAbs with reduced RBC targeting [10–12] or SIRPα fusion proteins [13, 14]. The overall concept of the CD47 blockade has been proven more effective when combined with a pro-phagocytic stimulus, such as rituximab, an αCD20 IgG1 mAb [15].

One strategy to combine the benefits of a tumor-restricted CD47 blockade with a pro-phagocytic stimulus in a single molecule is to fuse SIRPα with a tumor-associated antigen (TAA)-specific IgG1 antibody. This approach has been validated preclinically in hematologic malignancies [16, 17].

The TAA mesothelin (MSLN) is highly expressed in several solid cancer types, particularly in EOC, PDAC, and mesothelioma [18]. Hence, to improve the treatment options for these disease entities, we fused the endogenous SIRPα immunoglobulin V-like domain to the *N*-terminus of the light chain of an anti-human MSLN IgG1 mAb generating a SIRPα–αMSLN local inhibitory checkpoint monoclonal antibody (LicMAb).

Our in vitro studies demonstrated successful clearance of MSLN-expressing cancer cells by IgG1-mediated activation of innate immune cells inducing cytotoxicity and phagocytosis. Moreover, we confirmed the preclinical efficacy of SIRPα-αMSLN LicMAb in primary EOC samples and patient-derived organoids.

Methods

RNAseq and genomic alteration analysis

Transcriptomic data and corresponding clinical data from the Cancer Genome Atlas PanCancer Studies data collection (TCGA-PanCancer Atlas) were downloaded from cBioportal (https://www.cbioportal.org). Samples were filtered based on the availability of mRNA expression data (n = 10,071 samples, 91% of TCGA-PanCancer Atlas cohort). mRNA expression z-scores relative to all samples (log RNAseq V2 RSEM) were used to assess the expression of MSLN and CD47 across cancer types. The cancer types and relative sample numbers are described in Supplementary Table S1. The package ggplot2 tool in R was used for data visualization. To assess the genomic changes across cancer types, MSLN and CD47 were manually selected. Within the cBioportal visualization tool, "Mutation count" and "Genes with the highest frequency in any group" were selected. The mutation count for each cancer type was plotted on a boxplot and the 10 most frequently mutated genes for each cancer type were plotted on a bar graph.

Generation of local inhibitory checkpoint monoclonal antibody (LicMAb)

Human MSLN antibodies were generated by immunizing mice and rats with the extracellular domain of MSLN (amino acids 296–606). A detailed description of the SIRPα-αMSLN LicMAb generation is provided in the supplementary methods. In brief, RNA was isolated from hybridoma cells, variable light (V_L) and variable heavy (V_H) chains were amplified, and genes were synthesized and cloned into expression vectors containing the constant human IgG1 framework. The *N*-terminal Ig V-like domain of SIRPα was linked to the αMSLN light chain by a flexible polyglycine–serine four-repeat linker $(G_4S)_4$ to clone a SIRPα-αMSLN LicMAb. All proteins were produced in Expi293F cells and purified. The αCD33 mAb and SIRPα-αCD33 LicMAb, as well as high-affinity αCD47 IgG4 and αCD47 IgG1 mAb (h5F9-G4 and h5F9-G1, respectively), served as controls.

Antibody-dependent cellular cytotoxicity (ADCC)

For the impedance-based readout, target cells were seeded in a sterile 96-well real-time cell analysis (RTCA) E-plate (Agilent) and cultured in the xCELLigence (Agilent) for 24 h. NK cells were isolated from fresh peripheral blood mononuclear cells (PBMCs) using the human NK Cell Isolation Kit (Miltenyi Biotec). NK cells were co-cultured with target cells and antibodies for 24 h. Cytotoxicity was calculated after 4 h of co-culture as overall lysis [%] = {1 − (normalized cell index of condition)/(normalized cell index of condition w/o Ab)} × 100. For the multiparametric flow cytometry (MPFC)-based readout, isolated NK cells were co-cultured with CellTrace CFSE-labeled target cells and antibodies for 4 h. Cells were stained with LIVE/DEAD Near-IR Dead Cell Staining Kit (Invitrogen) and lysis was calculated as percentage of dead cells or overall lysis [%] = {1 − (cell count of condition)/(cell count of condition w/o Ab)} × 100. NK-cell activation was evaluated by CD69 and CD107a expression.

Antibody-dependent cellular phagocytosis (ADCP)

Monocytes were isolated using the Classical Monocyte Isolation Kit (Miltenyi Biotec) and differentiated into macrophages in the presence of M-CSF (100 ng/ml; Biolegend) for 7 days.

CellTrace Calcein Red–Orange- or Far-Red-labeled macrophages were incubated with CellTrace CFSE-labelled target cells at an effector:target (E:T) ratio of 1:1 and a serial dilution of the antibodies (0.01–10 nM) for 4 h. Analysis was performed using either the Amnis® Imagestream® MKII (Cytek Biosciences) or the Cytoflex LX (Beckman Coulter) flow cytometer. After doublet exclusion, the double-positive population represented the phagocytosed population.

ADCC with primary EOC patient-derived organoids

As previously described [19], patient-derived organoids (PDOs) were derived from fresh tumor tissue by enzymatic digestion and isolation of progenitors, followed by differential seeding in Cultrex RGF Basement Membrane Extract, Type 2 (Bio-Techne), and growth media matrix to identify optimal patient-specific growth conditions.

The assay was performed on a co-culture of freshly isolated NK cells (5:1 E:T ratio) and PDOs with the antibodies (50 nM) and IL-2 (10 nM) for 48 h. PDOs were retrieved from the 3D extracellular matrix by washing with ice-cold ADF F12 medium, supplemented with HEPES and Glutamax, and resuspended in growth medium. Technical replicates were digested with TrypLE to determine the number of single cells per PDO as approximately 2×10^4 cells per well. Phase contrast images were taken after 24 and 48 h. Cell viability was quantified by luminescence-based CellTiter-Glo 3D Assay (Promega), in independent quintuplicates per condition. Fluorescence images were obtained using a fully motorized Keyence BZ X-810 microscope, equipped with a Tokai stage-top incubator. Phenotypic characterization of the PDOs has been performed by immunofluorescence staining [19] (Supplementary Table S3).

Results

EOC shows enriched MSLN expression and the highest CD47 mRNA expression across 30 cancer entities

MSLN and CD47 are promising targets for immunotherapy [5, 18]. This was confirmed by a pan-cancer analysis of the TCGA cohort to evaluate the MSLN and CD47 mRNA expression levels across 30 cancer entities. MSLN mRNA was highly enriched in EOC and PDAC (Fig. 1a) in contrast to healthy ovarian tissue (Supplementary Figure S1a, b). MSLN protein expression was validated on primary EOC cells isolated from tumor tissue and ascites by MPFC (median MFI ratios 2.2 and 4.0, respectively; Fig. 1b, Supplementary Figure S1c, d). As expected, CD47 mRNA was highly abundant in all cancer entities evaluated and, interestingly, displayed the highest expression in EOC (Fig. 1c, Supplementary Figure S1a, b). Robust CD47 protein expression was validated in EOC cells by MPFC and is particularly prominent on tissue-derived cancer cells (median MFI ratio 41.8; Fig. 1d, Supplementary Figure S1c, d). Moreover, 73–75% of EOC patients express CD47 and MSLN (Supplementary Figure S1e). Analysis of the genomic alteration frequencies demonstrated the highest proportion of MSLN amplification in breast cancer and EOC (4%, and 2%, respectively; Supplementary Figure S1f). Moreover, EOC displayed the highest CD47 amplification frequency at 6% (Supplementary Figure S1g). These data further support MSLN and CD47 as promising targets for novel immunotherapeutic approaches in EOC.

Generation and characterization of SIRPα-αMSLN LicMAb demonstrating MSLN-specificity and CD47-blocking capacity

We generated anti-human MSLN mAbs using the hybridoma technique to identify two clones (4D8 and M4F5). The SIRPα-αMSLN^{4D8} and SIRPα-αMSLN^{M4F5} LicMAbs were generated by fusing two *N*-terminal SIRPα immunoglobulin V-like domains to the V_L chain of the antibody via a flexible $(G_4S)_4$ linker (Fig. 2a). First, we investigated the impact of the *N*-terminal SIRPα fusion on the binding to MSLN by determining the K_D value using surface plasmon resonance (SPR). The

Cancer Immunology, Immunotherapy (2025) 74:214 Page 5 of 16 214

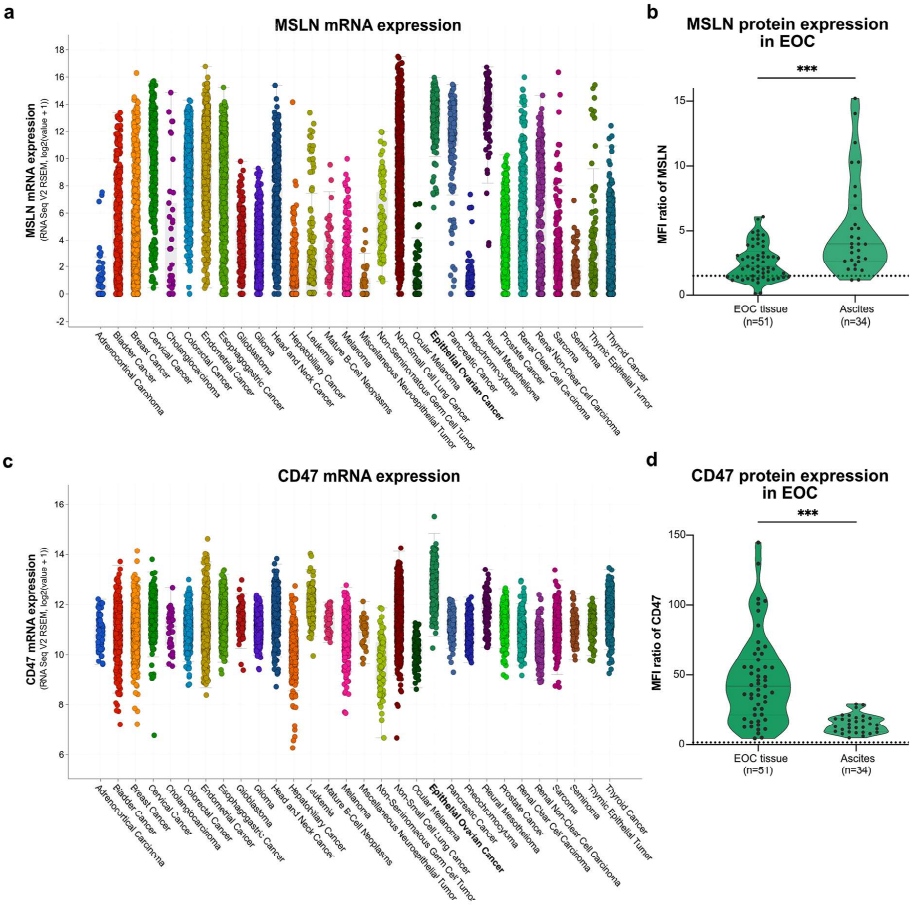

Fig. 1 EOC features high MSLN and CD47 mRNA and protein levels. The mRNA expression of MSLN (**a**) and CD47 (**c**) was evaluated across 30 cancer entities using the TCGA-derived pan-cancer cohort (10,953 patients; 10,967 samples). The protein expression levels of MSLN (**b**) and CD47 (**d**) on primary EOC cells derived from EOC tissue (n = 51) and ascites (n = 34) are depicted as median fluorescence intensity (MFI) ratio in violin plots with median (gray line) and quartiles (dashed gray line). The black dashed line represents the threshold MFI ratio of 1.5. Statistical analysis was performed using an unpaired t-test, $^{***}p \leq 0.001$

K_D values were in the low nanomolar range for all constructs, indicating the affinity for MSLN was unaffected by the fusion of the SIRPα domain (Supplementary Figure S3a). Binding to CD47 occurred with lower affinity ($K_D = 1$ µM), consistent with previously measured affinities of SIRPα for CD47 [20].

We also analyzed binding to the MSLN-expressing EOC cell line OVCAR-3 and the MSLN-transduced PDAC cell line SUIT-2-MSLN by MPFC (Fig. 2b, c). The SIRPα–αMSLN^{4D8} LicMAb and the αCD47 mAb (h5F9-G4) mAb bound to OVCAR-3 cells similarly, with MFI ratios of 117.2 and 119.5, respectively. By contrast, the αMSLN^{4D8} mAb showed a lower MFI ratio of 10.2, which can be explained by a 2.7-fold higher CD47 antigen density on the OVCAR-3 cell surface (Supplementary Figure S2). As expected, the SIRPα–αMSLN^{4D8} LicMAb bound the SUIT-2-MSLN cells similarly to the αMSLN^{4D8} and αCD47 mAb (h5F9-G4) mAb with MFI ratios of 27.5, 21.6, and 31.2, respectively (Fig. 2b, c). Furthermore, primary EOC cells derived from ascites (Fig. 2d) and tumor tissue (Supplementary Figure S3b) were bound by the SIRPα–αMSLN^{4D8} LicMAb (MFI ratios 2.1 and 3.3, respectively), αMSLN^{4D8}

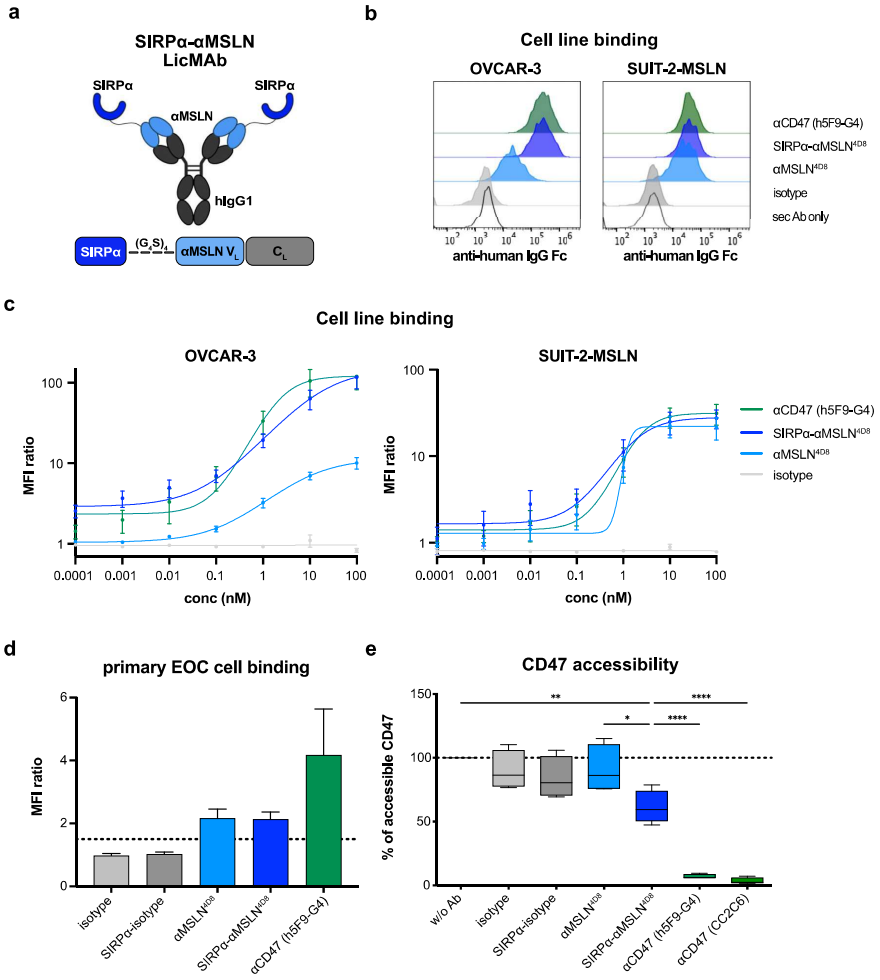

Fig. 2 The engineered SIRPα-αMSLN LicMAb is characterized by MSLN-specific targeting and CD47-blocking capacities. (**a**) A scheme of the SIRPα-αMSLN LicMAb targeting MSLN and simultaneously blocking CD47 on the cancer cells to switch on an "eat me" signal to the phagocytosing effector cells. The extracellular SIRPα domain that intrinsically has low affinity is fused to the IgG1 antibody light chains (V_L) via a flexible $(G_4S)_4$ linker. This scheme was created with BioRender (BioRender.com/g77u465). (**b**) A representative example of binding to OVCAR-3 (left) and SUIT-2-MSLN (right) cells by the indicated antibodies was evaluated by flow cytometry. (**c**) The binding to OVCAR-3 (left) and SUIT-2-MSLN cells (right) in a serial dilution of the indicated antibodies (0.0001–100 nM) was evaluated by flow cytometry (n = 3–4). (**d**) The binding of the indicated antibodies to primary EOC cells derived from ascites was evaluated using flow cytometry (n = 3). (**e**) The frequency of accessible CD47 on SUIT-2-MSLN cells was evaluated by flow cytometry using an APC-conjugated CD47-targeting antibody after incubation with the indicated antibodies (100 nM, n = 4). Data represents the mean ± SEM. Statistical analysis was performed using an ordinary one-way ANOVA, $^{*}p \leq 0.05$, $^{**}p \leq 0.01$, and $^{****}p \leq 0.0001$

mAb (MFI ratios 2.2 and 3.3, respectively), and αCD47 mAb h5F9-G4 (MFI ratios 4.2 and 6.0, respectively). Importantly, the SIRPα–αMSLN^{4D8} LicMAb did not bind to MSLN^{neg} patient-derived EOC cells (Supplementary Figure S3c).

One reason to generate LicMAbs is to retain the therapeutic benefit of blocking the CD47–SIRPα interaction, specifically on tumor cells. To evaluate the CD47-blocking capacity, we analyzed the accessible CD47 on SUIT-2-MSLN cells by MPFC (Fig. 2e). In contrast to the high-affinity αCD47 mAbs h5F9-G4 and CC2C6, which blocked the majority of CD47 sites (6.2% and 2.3% accessible CD47, respectively), the SIRPα–αMSLN^{4D8} LicMAb was less efficacious in blocking CD47 (59.5% accessible CD47). To determine the specificity of MSLN targeting, we also evaluated the binding (Supplementary Figure S3d) and blocking capacity (Supplementary Figure S3e) of the SIRPα–αMSLN^{4D8} LicMAb to the MSLN^{neg}/CD33^{pos} AML cell line MOLM-13. The SIRPα–αMSLN^{4D8} LicMAb neither binds to MOLM-13 cells nor blocks CD47. By contrast, the isotype control SIRPα–αCD33 LicMAb bound to CD33^{pos}/CD47^{pos} MOLM-13 cells and blocked CD47 (47% accessible CD47). These data show that the SIRPα–αMSLN LicMAb binds to the MSLN-expressing EOC and PDAC cells while simultaneously blocking CD47.

The SIRPα-αMSLN LicMAb avoids on-target off-tumor binding

We postulated that the SIRPα-αMSLN LicMAb specifically blocks CD47 on MSLN^{pos} cancer cells. Consequently, the risk for potential adverse events by on-target off-tumor binding, such as anemia, neutropenia, and thrombocytopenia [9], is reduced. To this end, we examined the SIRPα-αMSLN LicMAb binding to hematologic MSLN^{neg}/CD47^{pos} cells. In contrast to the high-affinity αCD47 (h5F9-G4) mAb, the SIRPα-αMSLN LicMAb did not bind to RBCs (Fig. 3a, Supplementary Figure S4b) or neutrophils (Fig. 3b). Furthermore, unlike control molecules targeting CD47, the SIRPα-αMSLN LicMAb did not elicit platelet aggregation (Supplementary Figure S4c). Interestingly, lymphocytes, which express CD47 at higher levels than RBCs and neutrophils (Supplementary Figure S4a), were bound by the SIRPα-αMSLN LicMAb. However, compared to the high-affinity αCD47 (h5F9-G4) mAb with an EC_{50} value of 0.26 nM, a fourfold lower MFI ratio was detected with a 40-fold higher EC_{50} value of 12.0 nM. Unexpectedly, we found that the αMSLN mAb binds to lymphocytes at a high concentration of 100 nM. This result might explain the affinity of SIRPα-αMSLN LicMAb as an avidity effect of binding at MSLN and CD47. Further experiments are needed to precisely understand the mode of binding.

Next, we hypothesized that the SIRPα-αMSLN^{4D8} LicMAb specifically binds to tumor cells in the presence of RBCs or lymphocytes. Even with a 20-fold excess of RBCs or tenfold excess of lymphocytes, the SIRPα-αMSLN^{4D8} LicMAb was specifically bound to tumor cells. By contrast, the αCD47 mAb bound significantly more RBCs than tumor cells (Fig. 3d) and did not discriminate between tumor cells and lymphocytes (Fig. 3e).

These data show that the SIRPα-αMSLN LicMAb binds specifically to MSLN-expressing tumor cells, a profile for potentially minimizing CD47-related on-target off-tumor toxicity.

The SIRPα-αMSLN LicMAb mediates ADCC against tumor cells

Next, we investigated the potency of LicMAbs to induce NK-cell-mediated ADCC by noninvasive, real-time cellular impedance measurements (xCELLigence). Reproducible ADCC against OVCAR-3 cells was monitored as decreased impedance values (normalized cell index) over time (Fig. 4a). For comparability reasons, the area under curve (AUC) was calculated per condition and showed an E: T-dependent decrease, particularly pronounced for the SIRPα-αMSLN^{4D8} LicMAb. A high-affinity αCD47 IgG1 mAb (h5F9-G1) served as a positive control and gave the lowest and E: T-independent AUC (Fig. 4b). After 4 h in co-culture with NK cells, the OVCAR-3 cells had lysed in a dose-dependent manner. The SIRPα-αMSLN^{4D8} and SIRPα-αMSLN^{M4F5} LicMAbs achieved 92% lysis ($EC_{50} = 0.003$ nM) and 100% lysis ($EC_{50} = 0.003$ nM), respectively, which was comparable to the αCD47 (h5F9-G1) mAb (96.4%). The αMSLN^{4D8} and αMSLN^{M4F5} showed lower maximum overall lysis (79.5% and 81.1%, respectively) and up to 70-fold higher EC_{50} values, underlining the greater cytotoxic potency of the LicMAbs (0.216 and 0.019 nM, respectively; Fig. 4c).

In parallel, we confirmed NK-cell-mediated lysis by MPFC (Supplementary Figure S5). SIRPα-αMSLN LicMAbs induced comparable dose-dependent killing of OVCAR-3 and SUIT-2-MSLN cells. Due to high CD47 expression on OVCAR-3 cells, h5F9-G1 exhibited robust cytotoxicity of OVCAR-3 cells at lower concentrations. However, the SIRPα-αMSLN LicMAb achieved comparable maximum lysis (Supplementary Figure S5a). In contrast, h5F9-G1 mediated decreased dose-dependent lysis of SUIT-2-MSLN cells based on a lower CD47 expression (Supplementary Figure S5b). As expected, magrolimab did not induce cytotoxicity of SUIT-2-MSLN cells as the IgG4 scaffold minimizes Fc-dependent effector functions [21]. Nevertheless, CD47^{high} OVCAR-3 cells are lysed by magrolimab similarly to αMSLN mAbs (Supplementary Figure S5a). In that regard, high levels of CD47 seem to support ADCC by targeting IgG4 molecules [22]. The cytotoxicity data is further supported by a dose-dependent activation and degranulation of NK cells in co-culture with OVCAR-3 and SUIT-2-MSLN cells (Fig. 4d,e; Supplementary Figure S5c,d). Notably, the αMSLN^{4D8} and αMSLN^{M4F5} mAbs showed improved cytotoxicity as well as NK-cell activation and degranulation in comparison to the αMSLN IgG1 mAb amatuximab (Fig. 4, Supplementary Figure S5). These data

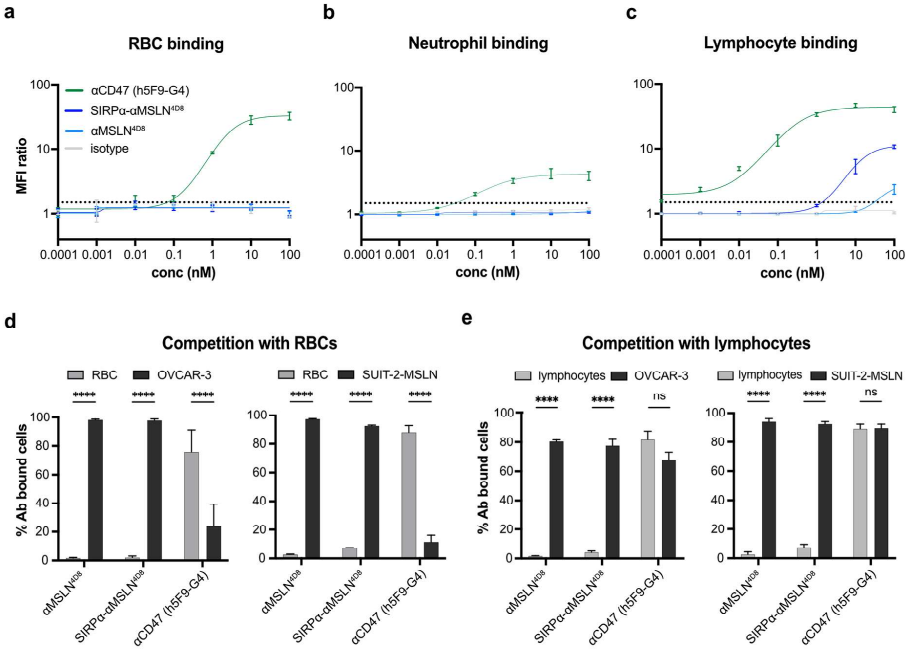

Fig. 3 The SIRPα-αMSLN LicMAb avoids on-target off-tumor binding. The binding to red blood cells (RBCs, **a**), neutrophils (**b**), or lymphocytes (**c**) in a serial dilution (0.001–100 nM) of the indicated antibodies was evaluated by flow cytometry (n = 3–6). In competitive binding assays, a 20-fold excess of CD47^{pos} RBCs (d, gray bar) or tenfold excess of lymphocytes (e, gray bar) was co-cultured with OVCAR-3 (left) or SUIT-2-MSLN (right) target cells (black bars). Binding was evaluated by flow cytometry in the presence of antibodies (100 nM; n = 5). Data represent the mean ± SEM. Statistical analysis was performed using a 2way ANOVA and Šídák's multiple comparisons test. ns = not significant; ****$p \leq 0.0001$

demonstrate the robust capacity of the SIRPα-αMSLN LicMAb to kill solid tumor cell lines.

The SIRPα-αMSLN LicMAb is effective in the presence of soluble MSLN

MSLN is anchored to the plasma membrane by a glycosyl-phosphatidylinositol linkage. However, shed MSLN can be found in sera from EOC and mesothelioma patients and, thus, represents a potential antigen sink to MSLN-targeting therapies [23]. First, we measured the MSLN concentrations in the serum and ascites of EOC patient samples and in the supernatant of cultured ascites and patient-derived organoids (Supplementary Figure S6a). We detected a median of 26.3 ng/ml soluble MSLN in the serum of EOC patients. Unexpectedly, reduced soluble MSLN was detected in fresh and cultured ascites of EOC patients and patient-derived organoids (median 5.4 ng/ml, 5.0 ng/ml, and 260 pg/ml, respectively). Next, we aimed to mimic shed MSLN using recombinant human MSLN (rhMSLN) and evaluate the functional capacity of the SIRPα-αMSLN LicMAb in its presence. To induce competition in vitro, we titrated rhMSLN to detect the saturated concentration, which inhibited MSLN binding. A concentration of 2.5 µM rhMSLN, at least 2000-fold higher than published data, completely abolished the binding of αMLSN^{M4F5} mAb to SUIT-2-MSLN cells, whereas binding of the SIRPα-αMSLN^{M4F5} LicMAb was detected, albeit 40% reduced and with a 20-fold lower EC_{50} value (Supplementary Figure S6b, c). Subsequently, we analyzed the impact of rhMSLN in functional assays. Most strikingly, and consistent with the LicMAb concept, the SIRPα-αMSLN^{M4F5} LicMAb was still effective in NK-cell-mediated killing of SUIT-2-MSLN cells in the presence of rhMSLN, albeit at higher concentrations (Supplementary Figure S6d).

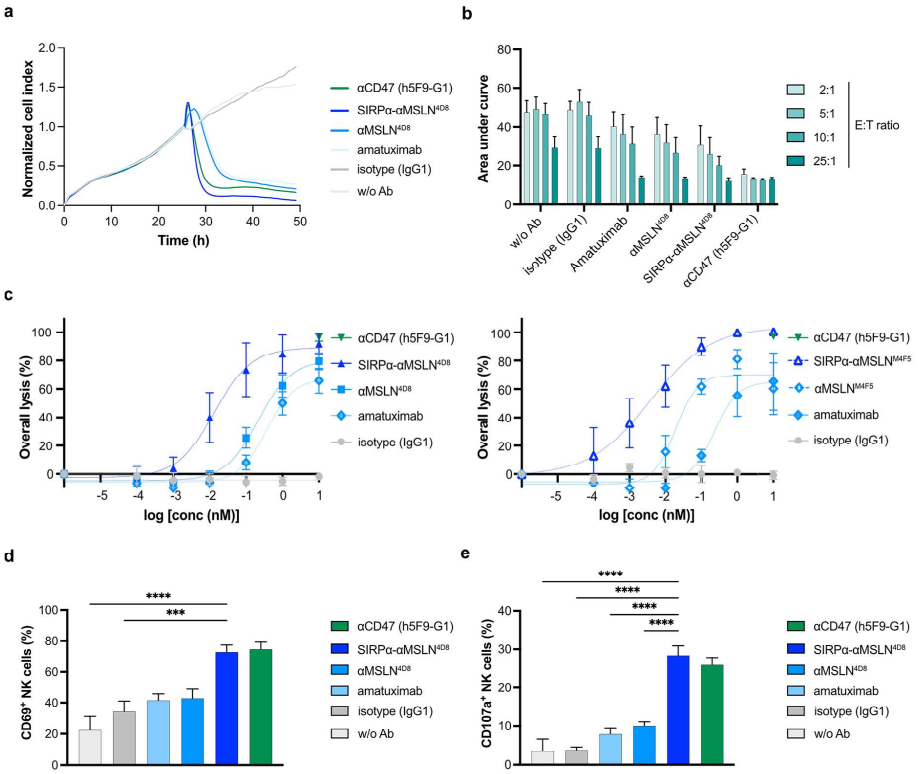

Fig. 4 The SIRPα-αMSLN LicMAb mediates dose-dependent and E:T ratio-dependent ADCC of tumor cells. (**a**) A representative example of NK-cell-mediated ADCC against OVCAR-3 cells in a 2:1 E:T ratio in the presence of the indicated antibodies (10 nM). ADCC was evaluated over time using the xCELLigence system. The cell indices were normalized to the timepoint of antibody and NK-cell addition. (**b**) The area under the curve (AUC) of the co-culture of OVCAR-3 cells and NK cells is shown for each antibody (10 nM) and the indicated E:T ratios. (**c**) The overall lysis after 4 h co-culture with serial dilutions of the indicated antibodies (0.1 pM–10 nM) was calculated based on the background NK-cell-mediated cytotoxicity of OVCAR–3 cells (5:1 E:T ratio; n = 4–5). The expression of CD69 (**d**) and CD107a (**e**) on the surface of NK cells after 4 h co-culture with OVCAR-3 cells (5:1 E:T ratio) is evaluated by flow cytometry (n = 8 and n = 6, respectively). Data represent the mean ± SEM. Statistical analysis was performed using an ordinary one-way ANOVA; $^{***}p \leq 0.001$, $^{****}p \leq 0.0001$

The maximum lysis was reduced from 57.5% to 45.0% with rhMSLN, and the EC_{50} values were increased from 0.007 to 0.239 nM. Importantly, rhMSLN almost completely abolished the cytotoxicity of the conventional αMLSN^{M4F5} mAb. Taken together, our data support the hypothesis that soluble MSLN entirely affects the efficacy of standard αMLSN mAbs but not the multifunctional SIRPα-αMSLN LicMAb.

The SIRPα-αMSLN LicMAb mediates dose-dependent ADCP of tumor cells

Next, we hypothesized that LicMAbs increase the phagocytic activity of macrophages due to the combination of CD47–SIRPα blockade and an IgG1 pro-phagocytic stimulus. Figure 5a shows the visualization of SIRPα-αMSLN^{4D8}-induced phagocytosis of OVCAR-3 cells by imaging flow cytometry. Single cells were validated as brightfield (BF) images and successful phagocytosis as double-positive macrophages. Approximately one-third (31.8%) of OVCAR-3 cells were phagocytosed in the presence of the

SIRPα-αMSLN^{4D8} LicMAb, which is enhanced versus the αCD47 (25.4%) and αMSLN^{4D8} (15.7%) mAbs (Fig. 5b). The h5F9-G4 served as the positive control to address the maximum phagocytosis mediated by the CD47-SIRPα blockade. In parallel, traditional flow cytometry was used for high-throughput multi-parameter analysis of LicMAb-associated phagocytosis as a double-positive macrophage population (Fig. 5c). OVCAR-3 and SUIT-2-MSLN cells treated with SIRPα-αMSLN LicMAbs underwent comparable dose-dependent phagocytosis (Fig. 5d, e; left). The SIRPα-αMSLN^{4D8}-induced ADCP of MSLN^{low}CD47^{high} OVCAR-3 cells was significantly greater (92.5%) compared to the action of αCD47 mAb (72.7%) and particularly αMSLN^{4D8} mAb (26.1%; Fig. 5d, right). By contrast, the SIRPα-αMSLN^{M4F5} and αMSLN^{M4F5} induced similar phagocytosis of MSLN-transduced SUIT-2-MSLN cells. Notably, magrolimab mediated only 27.1% ADCP (Fig. 5e, right).

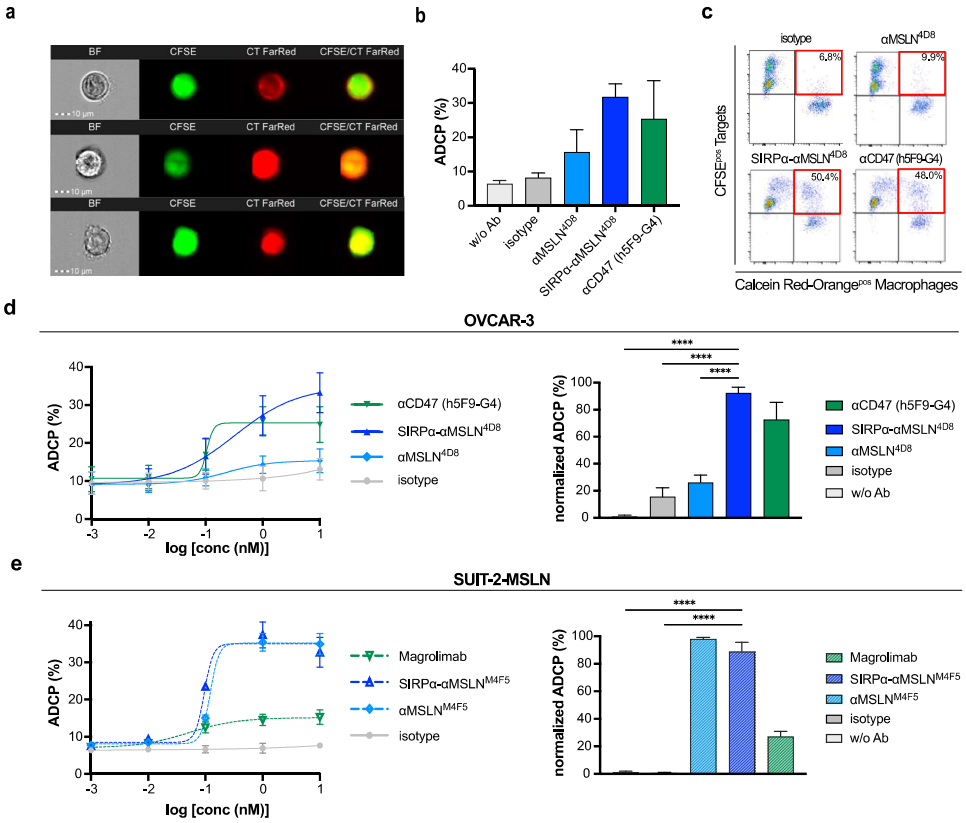

Fig. 5 The SIRPα-αMSLN LicMAb mediates dose-dependent ADCP of tumor cells. (**a**) Representative images of SIRPα-αMSLN^{4D8}-mediated phagocytosis of CFSE^{pos} OVCAR-3 cells by Cell Trace (CT) FarRed^{pos} macrophages evaluated by imaging flow cytometry. Each row shows one representative example per donor. BF: brightfield. (**b**) The phagocytosed CFSE^{pos}/CT FarRed^{pos} OVCAR-3 population was quantified by imaging flow cytometry in the presence of the indicated antibodies (10 nM; n = 3). (**c**) Representative FACS plots depict ADCP in the presence of the indicated antibodies (10 nM). The phagocytosed population is discriminated as CFSE^{pos}/Calcein Red-Orange^{pos} population (red rectangle). (**d**) The frequency of phagocytosed OVCAR-3 cells with serial dilutions of the indicated antibodies (left; 0.1 pM–10 nM) and the normalized ADCP in the presence of antibodies (right; 10 nM) was evaluated by flow cytometry after 4 h co-culture (n = 7). (**e**) The frequency of phagocytosed SUIT-2-MSLN cells with serial dilutions of the indicated antibodies (left; 0.1 pM–10 nM) and the normalized ADCP in the presence of antibodies (right; 10 nM) was evaluated by flow cytometry after 4 h co-culture (n = 4). Data represent the mean ± SEM. Statistical analysis was performed using a one-way ANOVA; ****$p \leq 0.0001$

These data underline the enhanced phagocytic capacity of the SIRPα-αMSLN LicMAbs by blocking CD47.

The SIRPα-αMSLN LicMAb is superior to a CD47xMSLN bispecific antibody

Further, we compared the SIRPα-αMSLN LicMAb with a CD47xMSLN bispecific antibody (bsAb) similar to the published κλ body from Hatterer et al. [24]. First, we analyzed binding to SUIT-2-MSLN cells by MPFC (Supplementary Figure S7a). The CD47xMSLN bsAb reached similar MFI ratios as the SIRPα–αMSLN^{M4F5} LicMAb (16.1 and 19.3, respectively), however, with an 18-fold higher EC_{50} value, due to monovalent versus bivalent MLSN binding sites, respectively. Particularly, saturating concentrations of soluble MSLN as an alias for MSLN shedding reduced the binding of the CD47xMSLN bsAb by 87% in contrast to the SIRPα–αMSLN^{M4F5} LicMAb showing 53% reduced binding (MFI ratio 2.2 and 9.1, respectively). Next, we compared the NK-cell-mediated lysis of OVCAR-3 and SUIT-2-MSLN in a dose-dependent manner by MPFC (Supplementary Figure S7b). In contrast to the CD47xMSLN bsAb, the SIRPα-αMSLN^{4D8} LicMAb exhibited robust cytotoxicity of OVCAR-3 and SUIT-2-MSLN cells at low concentrations with a clear benefit in efficacy for the LicMAb as shown by an up to 900-fold reduced EC_{50} value. The CD47xMSLN bsAb and SIRPα-αMSLN^{4D8} LicMAb achieved similar maximum lysis of OVCAR-3 cells (39.6% and 38.1%, respectively) and SUIT-2-MSLN cells (33.7% and 46.9%, respectively). Moreover, we evaluated the phagocytic capacity of the antibody constructs (Supplementary Figure S7c, d). The CD47xMSLN bsAb induced lower dose-dependent phagocytosis of OVCAR-3 and SUIT-2-MSLN cells than the SIRPα-αMSLN LicMAbs. While the CD47xMSLN bsAb induced 51.0% and 59.3% ADCP of OVCAR-3 cells and SUIT-2-MSLN cells, respectively, the LicMAbs phagocytosed 85.2% and 92.0%, respectively. These data underline the superiority of the SIRPα-αMSLN LicMAbs to a CD47xMSLN bsAb.

The SIRPα-αMSLN LicMAb induces NK-cell-mediated cytotoxicity of EOC organoids

To evaluate the SIRPα-αMSLN LicMAb in a model closer to the clinical context, we assessed its cytotoxic efficacy in primary EOC PDOs. The expression of MSLN (red) and epithelial cell adhesion molecule (EpCAM; green) was confirmed by immunofluorescence staining and flow cytometry (Fig. 6a, Supplementary Figure S8). Histochemistry revealed a more variable MSLN staining in the native tissue compared to an overall high MSLN expression in the respective organoid (Supplementary Figure S8). Assessment of viability in a co-culture of PDOs and NK cells in a multi-well format ensured the technical robustness of the experimental setting. It demonstrated the high potential of SIRPα-αMSLN^{M4F5} to induce NK-cell-mediated organoid cell death (Fig. 6b, c). A visual inspection of the interaction between NK cells and PDOs at 24 h revealed a characteristic pattern of cellular debris and decomposed fragments in SIRPα-αMSLN^{M4F5}-containing conditions (Fig. 6b). The ability of the SIRPα-αMSLN^{M4F5} LicMAb to activate NK cells and initiate organoid disintegration and cytotoxicity was also visualized by live-cell imaging (Supplemental video). Furthermore, after 48 h of SIRPα-αMSLN^{M4F5} LicMAb treatment, the total luminescence intensity was consistently lower than with magrolimab or αMSLN^{M4F5}, confirming the largest decrease in living cells (Fig. 6c). These data validate the cytotoxic capacity of the SIRPα-αMSLN LicMAb in a more clinically relevant model.

Discussion

In this study, we prepared two preclinical LicMAb constructs (4D8 and M4F5) that induced an innate immune response restricted to MSLN-expressing solid cancers. Moreover, by cancer-directed CD47 blockade, we abolished CD47-related on-target off-tumor toxicities.

CD47 was first reported as a promising target antigen in the context of hematologic malignancies. In this context, antibodies blocking CD47 indicated phagocytosis as a primary mode of action and showed robust antitumor efficacy [7, 8]. However, based on recent phase III trial data on magrolimab in the context of AML, further development was deemed futile and terminated. Although we await full reports, the first preliminary data of the multi-center international trial revealed increased toxicity due to on-target off-leukemia effects [25]. Furthermore, the combination with a hypomethylating agent to provide the pro-phagocytic signal [25], necessary to enable high phagocytosis rates [26], might not be the optimal approach. Other combinatorial approaches using mAbs as additional pro-phagocytic stimuli showed synergistic antitumor efficacy in hematologic [15] and solid cancers [27, 28]. Subsequently, bsAbs targeting a TAA and blocking the CD47–SIRPα axis to dampen on-target off-tumor toxicities in solid tumors, were developed. Targeted TAAs include human epidermal growth factor receptor 2 (HER2) [29], epidermal growth factor receptor (EGFR) [30], and programmed death ligand 1 (PD-L1) [31]. CD47xMSLN bsAbs have been generated as κλ bodies with an αMSLN λ-light chain and an αCD47 κ-light chain [32, 33], which are currently being investigated in a phase I clinical trial [24].

We translated the concept of multifunctionality from hematologic [16, 17, 34] to solid tumors by fusing the low-affinity SIRPα domains to an antibody targeting MSLN

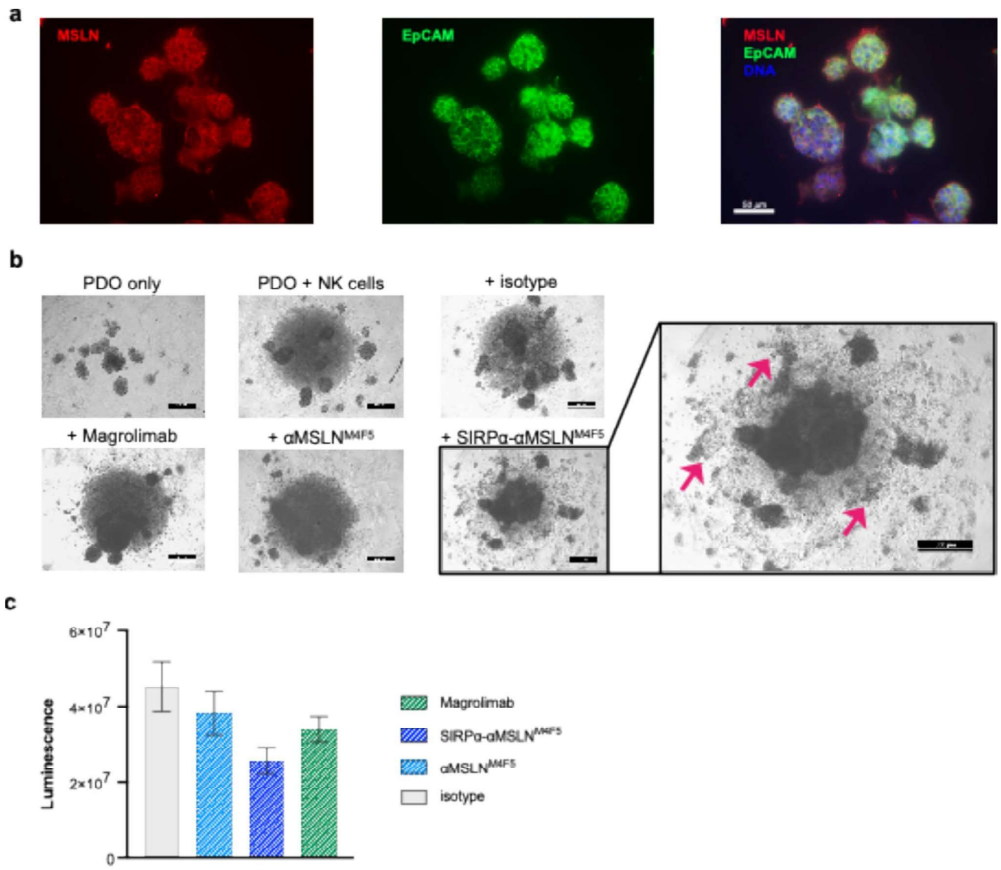

Fig. 6 The SIRPα-αMSLN LicMAb enables NK-cell-mediated cytotoxic effects of EOC patient-derived organoids. (**a**) Representative immunofluorescence images of EOC patient-derived organoids (PDOs; biobank reference HGSO_6) expressing MSLN (red, left) and epithelial cell adhesion molecule (EpCAM, green, middle) and a merged image with DNA (blue, right). Scale bar: 50 µm. (**b**) Representative phase-contrast images of EOC PDOs (biobank reference HGSOC_35) after 24 h co-culture with NK cells (E:T ratio 5:1) and indicated antibodies (50 nM). Red arrows indicate cellular debris from organoids, as killing leads to the breakage of cell junctions and loss of epithelial architecture. The experiment is representative of 10 independent experiments with three different donor PDO lines showing the same pattern of SIRPα-αMSLN^{M4F5} activity. Scale bars: 500 µm (**c**) Quantification of viable cells by Cell Titer glow depicting the total luminescence intensity after incubation of EOC PDOs with NK cells at an E: T ratio of 5:1 and indicated antibodies (50 nM) after 48 h (n = 3, biobank reference HGSOC_35, HGSO_20, HGSO_6). Data represent the mean ± SEM.

with high affinity. MSLN is a promising TAA as its expression levels are high on solid tumors, such as EOC and PDAC but limited on healthy cells. Furthermore, targeting MSLN prevents its interaction with cancer antigen CA-125, which has been implicated in supporting metastases [18]. Hence, several MSLN-targeting strategies, such as mAbs [35], antibody–drug conjugates (ADCs) [36], or chimeric antigen receptor T cell (CAR T) cells, [37] have been evaluated in clinical trials. Although amatuximab was well tolerated in MSLN^{pos} tumor patients [35], only its combination with chemotherapy gave beneficial results in mesothelioma patients [38].

Notably, MSLN shedding is a mechanism by which high concentrations of MSLN accumulate in the serum of EOC and mesothelioma [23]. Indeed, we detected soluble MSLN in the EOC patients' serum, in line with the literature [23, 39], and fivefold less in the ascites. Interestingly, Okła et al. detected nearly tenfold greater levels

of soluble MSLN in peritoneal fluid (622.8 pg/ml) versus plasma (81.6 pg/ml) of advanced EOC patients [40]. However, these plasma concentrations are 300-fold lower than our data. To address the risk of shed MSLN acting as an antigen sink, we evaluated the binding and cytotoxicity of SIRPα-αMSLN LicMAb in the presence of soluble rhMSLN. As the clinically relevant concentrations are rather low and vary between patients and samples, a saturating concentration of rhMSLN was used to ensure challenging assay conditions in vitro. Although the functional capacity of an αMSLN mAb is highly reduced, the SIRPα-αMSLN LicMAb was still effective, albeit at higher concentrations. We suppose the avidity effects by binding MSLN and CD47 multivalently as the reason for maintaining the binding of the LicMAbs to target cells. Thus, bifunctional approaches such as using LicMAbs might maintain the therapeutic window even in the presence of shed MSLN and support MSLN and CD47 as promising targets to treat EOC. Furthermore, the clinical evaluation of CD47xMSLN κλ bodies [24] highlights the combined targeting of MSLN and CD47 as an encouraging strategy. Importantly, compared to the CD47xMSLN bsAb, SIRPα-αMSLN LicMAbs demonstrated enhanced binding, particularly in the presence of soluble MSLN, as well as increased cytotoxicity and phagocytosis.

The antitumor efficacy of the SIRPα-αMSLN LicMAb is based on IgG1-induced NK-cell activation to effect ADCC and the simultaneous stimulation of phagocytic cells, such as macrophages, to mediate ADCP. Indeed, we confirm consistent cytotoxic and phagocytic activity against EOC and PDAC cell lines. Furthermore, we demonstrate the effective induction of cell death in organoids derived from EOC patients in co-culture with NK cells. Importantly, the SIRPα-αMSLN LicMAb induced more cytotoxicity and phagocytosis than the controls amatuximab and magrolimab. Using two different tumor cell lines emphasizes the reliable potency of the LicMAbs, independent of the antigen expression level. We hypothesize that these findings are transferrable to other MSLN-expressing solid tumor entities.

Notably, MSLN was more uniformly expressed in patient-derived organoids than in respective native cancer tissue. As organoids are derived from the tumor's progenitor population, our data suggest that MSLN is associated with the stemness compartment driving tumor growth. Hence, the specific and enhanced killing activity against PDO cells of the LicMAb in comparison to magrolimab supports the interpretation that this multifunctional antibody may be advantageous to treat long-term tumor growth potential.

Elevated expression levels of CD47 on healthy cells, notably RBCs, thrombocytes, and PBMCs, pose a concern for on-target off-tumor toxicity [4]. Thus, phagocytic anemia was one of the most adverse events in patients receiving CD47-targeting agents, and neutropenia and thrombocytopenia were also frequently observed [9]. Not surprisingly, highly CD47-expressing lymphocytes were targeted at high concentrations of the SIRPα-αMSLN LicMAb but less prominent than the high-affinity αCD47 mAb. Moreover, based on the unspecific binding of the αMSLN mAb at high concentrations, the LicMAb binding might rely on avidity effects by binding sites to MSLN and CD47. However, the SIRPα-αMSLN LicMAb did not bind to RBCs, the most abundant cells in the blood, nor to neutrophils. Most importantly, in competition, tumor cells were specifically targeted while binding to RBCs and lymphocytes was absent. In addition, reduced platelet aggregation lowers the risk of thrombocytopenia. This is in sharp contrast to a high-affinity αCD47 construct [41] and underlines the potential of the LicMAb to minimize toxicity. Furthermore, a potential antigen sink effect is avoided because the low-affinity binding characteristics of the fused SIRPα domain prevent unspecific CD47 binding. This further enhances the efficacy of the SIRPα-αMSLN LicMAb therapeutic approach.

CD47-targeting synergizes with the cytotoxicity of agents such as chemotherapies [42], stimulator of interferon genes (STING) agonists [43], and poly (ADP-ribose) polymerase inhibitors (PARPi) [44] that are known to induce immunogenic cell death and thereby lead to upregulation of pro-phagocytic ligands [44]. Thus, combinatorial approaches might increase the response rates of EOC and PDAC patients. Moreover, as adaptive ICIs such as αPD-1/αPD–L1 did not improve response rates in these patients [2, 3], the combination with innate CD47 blockade using LicMAbs might synergize analogously with other cancer entities [45, 46]. It is known that CD47-targeting leads to an adaptive immune reaction by T cells [47]. In that regard, the LicMAb might also induce cross-presentation to T cells by antigen-presenting cells, resulting in long-lasting antitumor effects. Future studies are awaited to validate this mechanism, which might lead to long-term tumor control. Furthermore, an inflammatory microenvironment with high IL-2 levels can activate NK cells and induce SIRPα upregulation as an inhibitory pathway [48]. This additional mode of action could be targeted by the LicMAbs, further highlighting them as a promising concept.

A limitation of our study is the focus on ex vivo data. Immunotherapy is beset by the lack of suitable immunocompetent animal models that allow human-specific binding domains to be tested. Hence, either humanized NSG mouse models injected with human cancer cell lines and effector cells serve as surrogates or murine antibody constructs would have been necessary. Each model system has limitations, and we opted for validation in the human organoid model, an advantageous research tool over mouse models regarding applicability and practicability, laboratory workload and costs, ethics, and high-throughput screening options [49]. Accordingly, the efficient cytotoxic effects of

primary EOC organoids validate the LicMAb in a more clinically relevant 3D model. However, humanized NSG mouse models with orthotopic cancer inoculation remain important for future studies to expand the preclinical evaluation and toxicity assessments of LicMAbs.

In summary, our SIRPα-αMSLN LicMAb constructs show promising activity without on-target off-tumor toxicity in preclinical models. Hence, our data supports the further development of a SIRPα-αMSLN LicMAb for evaluation in early clinical trials on advanced ovarian and pancreatic cancer patients.

Supplementary Information The online version contains supplementary material available at https://doi.org/10.1007/s00262-025-04032-0.

Acknowledgements We thank Sabine Sandner-Thiede and Simone Pentz (University Hospital, LMU Munich) for their excellent technical support and the study nurses, Bettina Ganseder and Natalie Kronthaler (University Hospital Munich), for their assistance in patient recruitment and sample collection. We acknowledge Maria Fischer for her assistance in the live-cell imaging of the EOC organoid-killing assay and Martina Rahmeh for the immunohistochemistry stainings. We acknowledge Elisabeth Kremmer for supporting the MSLN generation. We thank Prof. Dr. Sebastian Kobold for generously providing the SUIT-2-MSLN cell line used in this study. The graphical abstract and Figure 2a were created with BioRender (Neumann, A. (2023) BioRender.com/g77u465). This work was supported by the BMBF in the framework of the Cluster4Future program (Cluster for Nucleic Acid Therapeutics Munich, CNATM) (Project ID: (03ZU1201AA). We thank our thrombocyte apheresis collection center in the division of Transfusion Medicine, Cell Therapeutics and Haemostaseology, LMU Munich, for providing us with the leukoreduced single-donor platelet concentrate chambers. We acknowledge the iFlow Core Facility of the University Hospital, LMU Munich (INST 409/225-1 FUGG) for assistance in generating flow cytometry data and the Core Facility Flow Cytometry at the Biomedical Center, LMU Munich, for providing equipment, services, and expertise.

Author contributions A.L., N.F., A.R., M.S.: manuscript writing and editing. A.L., B.H., E.P., K.W., N.C.F., M.K., A.R.: experiment performance and data acquisition and analysis. A.L., B.H., E.P., K.W., N.C.F., M.K., A.R., B.T., A.H.C., A.S., L.R., L.Wi., L.Wy. B.C., F.T., S.M.: involved in research design and data interpretation. N.C.F., M.S., K-P.H.: study design and supervision. H.F., H.L. involved in MSLN antibody generation. C.W., D.M. provided the leukoreduction chamber material. All authors read and approved the final manuscript.

Funding Open Access funding enabled and organized by Projekt DEAL. The work was supported by the Bavarian Elite Graduate School "i-target" (A.L., A.H-C., L.R.), the Else-Kröner-Fresenius Forschungskolleg CSP Cancer Immunotherapy (A.R.), the Sonderforschungsbereich SFB 338 (M.S.), Deutsche Forschungsgemeinschaft (DFG) 451580403 (M.S., K-P.H.), 452881907 (M.S.) and Exist Transfer of Research I grant (N.F.).

Availability of data and materials The datasets analyzed during the current study are available from the corresponding author upon reasonable request.

Declarations

Ethics approval and consent to participate PB samples from HDs or leukoreduction system chambers (LRSC) from plate-apheresis were collected with written consent following the Declaration of Helsinki and with approval from the Institutional Review Board of LMU Munich (23–0283). The collection of ovarian cancer tissue for biobanking and generation of organoids has been approved by the Ethics Commission of LMU University (17–0471), and written consent of each patient has been obtained.

Consent for publication Not applicable.

Competing interests K-P.H., M.S., and N.C.F. are inventors of a patent application regarding the SIRPα-antibody fusion proteins. M.S. has received industry research support from Amgen, Gilead, Miltenyi Biotec, Morphosys, Roche, and Seattle Genetics, and has served as a consultant/advisor to Amgen, BMS, Celgene, Gilead, Pfizer, Novartis, and Roche. She sits on the advisory boards of Amgen, Celgene, Gilead, Janssen, Novartis, Pfizer, and Seattle Genetics, and serves on the speakers' bureau at Amgen, Celgene, Gilead, Janssen, and Pfizer. F.T.: grants and personal fees from AbbVie, AstraZeneca, Eisai, GSK, ImmunoGen, MSD, Roche, and SAGA diagnostics S.M.: Research funding, advisory board, honorary or travel expenses: AbbVie, AstraZeneca, Clovis, Eisai, GlaxoSmithKline, Hubro, Immunogen, Medac, MSD, Novartis, Nykode, Olympus, PharmaMar, Pfizer, Roche, Seagen, Sensor Kinesis, Teva. M.K.: inventor of the European Patent for ovarian cancer organoid culture. B.C.: Honoraria from AstraZeneca. A.L., A.R., B.H., E.P., K.W., B.T., A.H-C.; A.S., L.R., L.Wi., L.Wy., C.W., D.M., declare no relevant conflicts of interest.

References

1. Luke JJ, Flaherty KT, Ribas A, Long GV (2017) Targeted agents and immunotherapies: optimizing outcomes in melanoma. Nat Rev Clin Oncol 14:463–482. https://doi.org/10.1038/nrclinonc.2017.43
2. Balsano R, Zanuso V, Pirozzi A et al (2023) Pancreatic ductal adenocarcinoma and immune checkpoint inhibitors: the gray curtain of immunotherapy and spikes of lights. Curr Oncol 30:3871–3885. https://doi.org/10.3390/curroncol30040293
3. Zeng S, Liu D, Yu Y et al (2023) Efficacy and safety of PD-1/PD-L1 inhibitors in the treatment of recurrent and refractory ovarian cancer: A systematic review and a meta-analysis. Front Pharmacol 14:1–10. https://doi.org/10.3389/fphar.2023.1111061
4. Oldenborg PA, Zheleznyak A, Fang YF et al (2000) Role of CD47 as a marker of self on red blood cells. Science (80-) 288:2051–2054. https://doi.org/10.1126/science.288.5473.2051
5. Willingham SB, Volkmer J-P, Gentles AJ et al (2012) The CD47-signal regulatory protein alpha (SIRPa) interaction is a therapeutic target for human solid tumors. Proc Natl Acad Sci 109:6662–6667. https://doi.org/10.1073/pnas.1121623109

6. Jaiswal S, Jamieson CHM, Pang WW et al (2009) CD47 is upregulated on circulating hematopoietic stem cells and leukemia cells to avoid phagocytosis. Cell 138:271–285. https://doi.org/10.1016/j.cell.2009.05.046
7. Chao MP, Takimoto CH, Feng DD et al (2019) Therapeutic targeting of the macrophage immune checkpoint CD47 in myeloid malignancies. Front Oncol 9:1380. https://doi.org/10.3389/fonc.2019.01380
8. Sikic BI, Lakhani N, Patnaik A et al (2019) First-in-human, first-in-class Phase I trial of the anti-CD47 antibody Hu5F9-G4 in patients with advanced cancers. J Clin Oncol 37:946–953. https://doi.org/10.1200/JCO.18.02018
9. Sallman DA, Al Malki MM, Asch AS et al (2023) Magrolimab in combination with Azacitidine in patients with higher-risk myelodysplastic syndromes: final results of a Phase Ib study. J Clin Oncol Off J Am Soc Clin Oncol 41:2815–2826. https://doi.org/10.1200/JCO.22.01794
10. Burris HA III, Spira AI, Taylor MH et al (2021) A first-in-human study of AO-176, a highly differentiated anti-CD47 antibody, in patients with advanced solid tumors. J Clin Oncol 39:2516. https://doi.org/10.1200/JCO.2021.39.15_suppl.2516
11. Daver NG, Stevens DA, Hou J-Z et al (2022) Lemzoparlimab (lemzo) with venetoclax (ven) and/or azacitidine (aza) in patients (pts) with acute myeloid leukemia (AML) or myelodysplastic syndromes (MDS): a phase 1b dose escalation study. J Clin Oncol 40:TPS7067–TPS7067. https://doi.org/10.1200/JCO.2022.40.16_suppl.TPS7067
12. Wang T, Wang S-Q, Du Y-X et al (2024) Gentulizumab, a novel anti-CD47 antibody with potent antitumor activity and demonstrates a favorable safety profile. J Transl Med 22:220. https://doi.org/10.1186/s12967-023-04710-6
13. Ansell SM, Maris MB, Lesokhin AM et al (2021) Phase I study of the CD47 blocker TTI-621 in patients with relapsed or refractory hematologic malignancies. Clin Cancer Res Off J Am Assoc Cancer Res 27:2190–2199. https://doi.org/10.1158/1078-0432.CCR-20-3706
14. Lakhani NJ, Chow LQM, Gainor JF et al (2021) Evorpacept alone and in combination with pembrolizumab or trastuzumab in patients with advanced solid tumours (ASPEN-01): a first-in-human, open-label, multicentre, phase 1 dose-escalation and dose-expansion study. Lancet Oncol 22:1740–1751. https://doi.org/10.1016/S1470-2045(21)00584-2
15. Advani R, Flinn I, Popplewell L et al (2018) CD47 blockade by Hu5F9-G4 and rituximab in non-Hodgkin's lymphoma. N Engl J Med 379:1711–1721. https://doi.org/10.1056/NEJMoa1807315
16. Ponce LP, Fenn NC, Moritz N et al (2017) SIRPα-antibody fusion proteins stimulate phagocytosis and promote elimination of acute myeloid leukemia cells. Oncotarget 8:11284–11301. https://doi.org/10.18632/oncotarget.14500
17. Tahk S, Vick B, Hiller B et al (2021) SIRPα-αCD123 fusion antibodies targeting CD123 in conjunction with CD47 blockade enhance the clearance of AML-initiating cells. J Hematol Oncol 14:1–17. https://doi.org/10.1186/s13045-021-01163-6
18. Weidemann S, Gagelmann P, Gorbokon N et al (2021) Mesothelin expression in human tumors: a tissue microarray study on 12,679 tumors. Biomedicines. https://doi.org/10.3390/biomedicines9040397
19. Trillsch F, Czogalla B, Kraus F et al (2023) Protocol to optimize the biobanking of ovarian cancer organoids by accommodating patient-specific differences in stemness potential. STAR Protoc 4:102484. https://doi.org/10.1016/j.xpro.2023.102484
20. Weiskopf K, Ring AM, Ho CCM et al (2013) Engineered SIRPα variants as immunotherapeutic adjuvants to anticancer antibodies. Science 341:88–91. https://doi.org/10.1126/science.1238856
21. Liu J, Wang L, Zhao F et al (2015) Pre-clinical development of a humanized anti-CD47 antibody with anti-cancer therapeutic potential. PLoS ONE 10:137345. https://doi.org/10.1371/journal.pone.0137345
22. Steplewski Z, Sun LK, Shearman CW et al (1988) Biological activity of human-mouse IgG1, IgG2, IgG3, and IgG4 chimeric monoclonal antibodies with antitumor specificity. Proc Natl Acad Sci USA 85:4852–4856. https://doi.org/10.1073/pnas.85.13.4852
23. Hassan R, Remaley AT, Sampson ML et al (2006) Detection and quantitation of serum mesothelin, a tumor marker for patients with mesothelioma and ovarian cancer. Clin Cancer Res 12:447–453. https://doi.org/10.1158/1078-0432.CCR-05-1477
24. Romano E, Medioni J, Rouge TDLM et al (2022) A Phase 1, open-label, dose finding study of NI-1801, a bispecific mesothelin x CD47 engaging antibody, in patients with mesothelin expressing solid cancers. J Immunother Cancer 10:A740 LP. https://doi.org/10.1136/jitc-2022-SITC2022.0707
25. Naval D, Paresh V, Gerwin H et al (2024) Magrolimab vs placebo in combination with Venetoclax and Azacitidine in previously untreated patients with acute myeloid leukemia who are ineligible for intensive chemotherapy: the ENHANCE-3 study. EHA Libr 422242:138
26. Osorio JC, Smith P, Knorr DA, Ravetch JV (2023) The antitumor activities of anti-CD47 antibodies require Fc-FcγR interactions. Cancer Cell 41:2051-2065.e6. https://doi.org/10.1016/j.ccell.2023.10.007
27. Theruvath J, Menard M, Smith BAH et al (2022) Anti-GD2 synergizes with CD47 blockade to mediate tumor eradication. Nat Med 28:333–344. https://doi.org/10.1038/s41591-021-01625-x
28. Liu B, Guo H, Xu J et al (2018) Elimination of tumor by CD47/PD-L1 dual-targeting fusion protein that engages innate and adaptive immune responses. MAbs 10:315–324. https://doi.org/10.1080/19420862.2017.1409319
29. Zhang B, Shi J, Shi X et al (2024) Development and evaluation of a human CD47/HER2 bispecific antibody for Trastuzumab-resistant breast cancer immunotherapy. Drug Resist Updat 74:101068. https://doi.org/10.1016/j.drup.2024.101068
30. Hendriks MAJM, Ploeg EM, Koopmans I et al (2020) Bispecific antibody approach for EGFR-directed blockade of the CD47-SIRPα "don't eat me" immune checkpoint promotes neutrophil-mediated trogoptosis and enhances antigen cross-presentation. Oncoimmunology. https://doi.org/10.1080/2162402X.2020.1824323
31. Wang Y, Ni H, Zhou S et al (2021) Tumor-selective blockade of CD47 signaling with a CD47/PD-L1 bispecific antibody for enhanced anti-tumor activity and limited toxicity. Cancer Immunol Immunother 70:365–376. https://doi.org/10.1007/s00262-020-02679-5
32. Hatterer E, Chauchet X, Richard F et al (2020) Targeting a membrane-proximal epitope on mesothelin increases the tumoricidal activity of a bispecific antibody blocking CD47 on mesothelin-positive tumors. MAbs. https://doi.org/10.1080/19420862.2020.1739408
33. Dheilly E, Moine V, Broyer L et al (2017) Selective blockade of the ubiquitous checkpoint receptor CD47 is enabled by dual-targeting bispecific antibodies. Mol Ther 25:523–533. https://doi.org/10.1016/j.ymthe.2016.11.006
34. Piccione EC, Juarez S, Liu J et al (2015) A bispecific antibody targeting CD47 and CD20 selectively binds and eliminates dual antigen expressing lymphoma cells. MAbs 7:946–956. https://doi.org/10.1080/19420862.2015.1062192
35. Fujisaka Y, Kurata T, Tanaka K et al (2015) Phase I study of amatuximab, a novel monoclonal antibody to mesothelin, in Japanese patients with advanced solid tumors. Invest New Drugs 33:380–388. https://doi.org/10.1007/s10637-014-0196-0

36. Santin AD, Vergote I, González-Martín A et al (2023) Safety and activity of anti-mesothelin antibody-drug conjugate anetumab ravtansine in combination with pegylated-liposomal doxorubicin in platinum-resistant ovarian cancer: multicenter, phase Ib dose escalation and expansion study. Int J Gynecol Cancer 33:562–570
37. Hassan R, Butler M, O'Cearbhaill RE et al (2023) Mesothelin-targeting T cell receptor fusion construct cell therapy in refractory solid tumors: phase 1/2 trial interim results. Nat Med 29:2099–2109. https://doi.org/10.1038/s41591-023-02452-y
38. Hassan R, Kindler HL, Jahan T et al (2014) Phase II clinical trial of amatuximab, a chimeric antimesothelin antibody with pemetrexed and cisplatin in advanced unresectable pleural mesothelioma. Clin Cancer Res 20:5927–5936. https://doi.org/10.1158/1078-0432.CCR-14-0804
39. Huang CY, Cheng WF, Lee CN et al (2006) Serum mesothelin in epithelial ovarian carcinoma: A new screening marker and prognostic factor. Anticancer Res 26:4721–4728
40. Okła K, Surówka J, Frąszczak K et al (2018) Assessment of the clinicopathological relevance of mesothelin level in plasma, peritoneal fluid, and tumor tissue of epithelial ovarian cancer patients. Tumor Biol 40:1–15. https://doi.org/10.1177/1010428318804937
41. Velliquette RW, Aeschlimann J, Kirkegaard J et al (2019) Monoclonal anti-CD47 interference in red cell and platelet testing. Transfusion 59:730–737. https://doi.org/10.1111/trf.15033
42. Lo J, Lau EYT, So FTY et al (2016) Anti-CD47 antibody suppresses tumour growth and augments the effect of chemotherapy treatment in hepatocellular carcinoma. Liver Int 36:737–745. https://doi.org/10.1111/liv.12963
43. Kosaka A, Ishibashi K, Nagato T et al (2021) CD47 blockade enhances the efficacy of intratumoral STING-targeting therapy by activating phagocytes. J Exp Med. https://doi.org/10.1084/jem.20200792
44. Al-Sudani H, Ni Y, Jones P et al (2023) Targeting CD47-SIRPa axis shows potent preclinical anti-tumor activity as monotherapy and synergizes with PARP inhibition. npj Precis Oncol 7:1–10. https://doi.org/10.1038/s41698-023-00418-4
45. Kauder SE, Kuo TC, Harrabi O et al (2018) ALX148 blocks CD47 and enhances innate and adaptive antitumor immunity with a favorable safety profile. PLoS ONE 13:1–33. https://doi.org/10.1371/journal.pone.0201832
46. Tao H, Qian P, Wang F et al (2017) Targeting CD47 enhances the efficacy of anti-PD-1 and CTLA-4 in an esophageal squamous cell cancer preclinical model. Oncol Res 25:1579–1587. https://doi.org/10.3727/096504017X14900505020895
47. Liu X, Pu Y, Cron K et al (2015) CD47 blockade triggers T cell-mediated destruction of immunogenic tumors. Nat Med 21:1209–1215. https://doi.org/10.1038/nm.3931
48. Deuse T, Hu X, Agbor-Enoh S et al (2021) The SIRPα-CD47 immune checkpoint in NK cells. J Exp Med. https://doi.org/10.1084/JEM.20200839
49. Chenchula S, Kumar S, Shodan Babu V (2019) Comparative efficacy of 3dimensional (3D) cell culture organoids vs. 2dimensional (2D) cell cultures vs experimental animal models in disease modeling, drug development, and drug toxicity testing. Int J Curr Res Rev 11:11–17. https://doi.org/10.31782/IJCRR.2019.11242

4. Publication II

Tahk *et al. J Hematol Oncol* (2021) 14:155
https://doi.org/10.1186/s13045-021-01163-6

Journal of Hematology & Oncology

RESEARCH Open Access

SIRPα-αCD123 fusion antibodies targeting CD123 in conjunction with CD47 blockade enhance the clearance of AML-initiating cells

Siret Tahk[1], Binje Vick[2,3], Björn Hiller[1], Saskia Schmitt[1], Anetta Marcinek[4,5], Enrico D. Perini[1], Alexandra Leutbecher[4,5], Christian Augsberger[4,5], Anna Reischer[4,5], Benjamin Tast[4,5], Andreas Humpe[6], Irmela Jeremias[2,3,7], Marion Subklewe[3,4,5], Nadja C. Fenn[1*] and Karl-Peter Hopfner[1*]

Abstract

Background: Acute myeloid leukaemia (AML) stem cells (LSCs) cause disease relapse. The CD47 "don't eat me signal" is upregulated on LSCs and contributes to immune evasion by inhibiting phagocytosis through interacting with myeloid-specific signal regulatory protein alpha (SIRPα). Activation of macrophages by blocking CD47 has been successful, but the ubiquitous expression of CD47 on healthy cells poses potential limitations for such therapies. In contrast, CD123 is a well-known LSC-specific surface marker utilized as a therapeutic target. Here, we report the development of SIRPα-αCD123 fusion antibodies that localize the disruption of CD47/SIRPα signalling to AML while specifically enhancing LSC clearance.

Methods: SIRPα-αCD123 antibodies were generated by fusing the extracellular domain of SIRPα to an αCD123 antibody. The binding properties of the antibodies were analysed by flow cytometry and surface plasmon resonance. The functional characteristics of the fusion antibodies were determined by antibody-dependent cellular phagocytosis and antibody-dependent cellular cytotoxicity assays using primary AML patient cells. Finally, an in vivo engraftment assay was utilized to assess LSC targeting.

Results: SIRPα-αCD123 fusion antibodies exhibited increased binding and preferential targeting of $CD123^+$ $CD47^+$ AML cells even in the presence of $CD47^+$ healthy cells. Furthermore, SIRPα-αCD123 fusion antibodies confined disruption of the CD47-SIRPα axis locally to AML cells. In vitro experiments demonstrated that SIRPα-αCD123 antibodies greatly enhanced AML cell phagocytosis mediated by allogeneic and autologous macrophages. Moreover, SIRPα-αCD123 fusion antibodies efficiently targeted LSCs with in vivo engraftment potential.

Conclusions: SIRPα-αCD123 antibodies combine local CD47 blockade with specific LSC targeting in a single molecule, minimize the risk of targeting healthy cells and efficiently eliminate AML LSCs. These results validate SIRPα-αCD123 antibodies as promising therapeutic interventions for AML.

Keywords: CD47, Acute myeloid leukaemia, CD123, Leukemic stem cells, Phagocytosis, Immunotherapy

Background

Therapeutic options for acute myeloid leukaemia (AML) are limited, and the majority of patients relapse due to persistent chemorefractory LSCs [1–3]. Targeting and eradicating the leukemic stem cell (LSC) population is therefore a prerequisite for sustained

*Correspondence: nfenn@genzentrum.lmu.de; hopfner@genzentrum.lmu.de
[1] Gene Center and Department of Biochemistry, Ludwig-Maximilians-Universität München, Feodor-Lynen-Straße 25, 81377 Munich, Germany
Full list of author information is available at the end of the article

remission. CD47 is an innate immune checkpoint upregulated on LSCs, where it functions as a "don't eat me" signal by interacting with SIRPα on myeloid cells [4–6]. The first in class CD47-blocking antibody, magrolimab (Hu5F9-G4), was evaluated as a monotherapy in AML in a phase 1 trial (NCT02678338) [7, 8]. However, preclinical data support the combination of magrolimab with pro-phagocytic signals, such as activation of Fcγ receptors (FcγR) on macrophages or expression of calreticulin on target cells [8–12]. Magrolimab has consequently been combined with calreticulin-inducing azacytidine in a phase 1b trial including untreated AML patients unfit for chemotherapy and patients with intermediate to very high-risk myelodysplastic syndrome (MDS) [8, 13]. The combination demonstrated encouraging results; 64% of AML patients achieved an objective response (OR), while 56% achieved complete remission (CR) or CR with incomplete haematological recovery. In patients with high-risk MDS, 91% had an OR, and 42% had a CR (NCT03248479).

Nevertheless, CD47 is ubiquitously expressed on healthy cells as well, which generates an antigen sink lowering the effective dose and comprising a potential site of toxicity for αCD47 therapies [14, 15]. Combining the CD47 blocking domain, such as endogenous SIRPα, with a cancer-specific antibody in a single molecule can restrict the blockade of CD47 locally on antigen-expressing cells [16–18].

Similar to CD47, the interleukin-3 receptor alpha chain (CD123) is upregulated on AML LSCs and is associated with increased proliferation of AML cells and a poor prognosis [19–21]. Furthermore, high CD47 and CD123 coexpression has been demonstrated to correlate with AML chemoresistance [22]. These studies suggest that dual targeting of CD123 and CD47 could reduce the LSC count and enhance the rate and duration of response in AML patients.

To improve AML LSC targeting and clearance, we fused an αCD123 antibody with the endogenous N-terminal SIRPα immunoglobulin V-like domains and generated 1 × SIRPα-αCD123 and 2 × SIRPα-αCD123 fusion antibodies. Both of our antibodies exhibited improved binding to $CD123^+$ $CD47^+$ cells and stimulated efficient natural killer (NK) cell-mediated lysis of AML compared to the conventional αCD123 antibody in vitro. Importantly, SIRPα-αCD123 fusion antibodies blocked CD47 locally on $CD123^+$ cells and induced phagocytosis of primary AML cells by allogeneic and autologous macrophages in vitro. Finally, the 2 × SIRPα-αCD123 antibody targeted LSCs that are capable of engrafting and reinitiating AML in an in vivo model.

Materials and methods

Expression and purification of the antibodies

αCD123 antibody light and heavy chain plasmids were generated by cloning the αCD123 variable light (V_L) and variable heavy (V_H) sequences of talacotuzumab [23] into the respective pFUSE2-CLIg-hK and pFUSE-CHIg-hG1 vectors (InvivoGen). For 1 × SIRPα-αCD123 and 2 × SIRPα-αCD123, one or two N-terminal SIRPα variant 1 immunoglobulin V-like domains (amino acids 31-149) were subcloned from a previously described construct [18] into the N-terminus of the αCD123 V_L using a $(Gly_4Ser)_4$ linker. The αCD19 V_L and V_H plasmids (clone 4G7) were cloned to generate the control molecules. The αCD47 (clone Hu5F9) V_L and V_H sequences [24] were subcloned into pFUSE2-CLIg-hK and pFUSE-CHIg-hG4, respectively. The SIRPα-Fc fusion construct (similar to TTI-621) [25] was generated by fusing the N-terminal V domain of human SIRPα variant 2 [26] to the human IgG1 Fc region of a pFUSE-CHIg-hG1 vector (InvivoGen). The plasmids were transfected into Expi293F cells (Thermo Fisher Scientific) according to the manufacturer's protocol. After five to seven days, the supernatant was harvested, and antibodies were purified by protein A affinity chromatography followed by size exclusion chromatography using a Superdex 200 increase 10/300 GL column (GE Healthcare). Antibodies were analysed by sodium dodecyl sulphate (SDS) polyacrylamide gel electrophoresis, and stability was measured using a Tycho NT.6 (NanoTemper Technologies). The coding sequence for the CD123 extracellular domain was amplified by PCR from complementary DNA of L-428 cells and subcloned into pSecTag2/HygroC containing a His_6-tag (Thermo Fisher Scientific). CD123 was expressed in Expi293F cells and purified by nickel affinity chromatography and size exclusion chromatography.

Surface plasmon resonance analysis

Binding of the αCD123 antibodies to CD123 was measured using a Biacore X100 (Biacore). Antibodies were captured on a CM5 sensor chip using the Human Antibody Capture Kit (both GE Healthcare). CD123 was used at concentrations of 3.91–1000 nM, and equilibrium dissociation constants (K_D) were calculated from the ratio of the rate constants (k_{off}/k_{on}) of the multicycle kinetics measurements using Biacore Evaluation software.

Cell lines

All cell lines were cultured under standard conditions. MOLM-13 and Raji cells were purchased from the Deutsche Sammlung von Mikroorganismen und Zellkulturen (DSMZ). Chinese hamster ovary (CHO) cells stably overexpressing human CD47 were previously generated [18]. Expi293F cells were obtained from Thermo Fisher

Scientific. Cell lines were routinely screened for mycoplasma contamination.

Patient and healthy donor material

At initial diagnosis or relapse, AML patient samples were characterized at the Laboratory for Leukemia Diagnostics of the Klinikum der Universität München as previously described [27–29]. Peripheral blood mononuclear cells (PBMCs) were isolated from healthy donor (HD) blood or residual cells of leukoreduction chambers by Biocoll (Biochrom). RBCs were collected from HD peripheral blood. Platelet-rich plasma (PRP) was isolated from HD peripheral blood by centrifugation at 200×*g* for 20 min at 25 °C. In the binding studies, platelets were isolated from PRP in the presence of prostaglandin E1 (Merck). For patient-derived xenograft (PDX) cells, AML patient cells were serially transplanted into NOD/SCID gamma null mice (NOD.Cg-Prkdc^{scid} IL2rg^{tm1Wjl}/SzJ, NSG). PDX cells were transduced with luciferase and mCherry lentiviral constructs for bioluminescence imaging [23]. For ex vivo experiments, PDX cells were grown in StemPro-34 medium with 2% FBS, L-glutamine and penicillin–streptomycin (all Gibco) supplemented with rhIL3, rhTPO, rhSCF (all Peprotech) and rhFLT3-ligand (R&D Systems). Patient characteristics are summarized in Table 1 and Additional file 1: Table S1.

Antibodies and flow cytometry

Commercial antibodies were from Biolegend (San Diego) unless otherwise stated. Human IgG1 isotype control (QA16A12) and αCD47 (B6H12, eBioscience) were used in binding, CD47 blocking and functional experiments. FITC or APC α human IgG (αhIgG, HP6017) was used for binding, and FITC αCD47 (B6H12, eBioscience) was used in CD47 blocking experiments for secondary staining. APC and FITC isotype (MOPC-21), APC αCD123 (6H6) and FITC αCD47 (B6H12) were used for surface expression analysis. Surface antigen density was evaluated using QIFIKIT (Agilent Technologies). Flow cytometry was performed using the Guava easyCyte 6HT (Merck Millipore), the Cytoflex LX (Beckman Coulter) or the BD LSRFortessa (Becton Dickinson). As a measure

Table 1 Patient characteristics

Patient	Age	Sex	Disease status	Karyotype	ELN genetic group	*FLT3*-ITD	*NPM1*
0276	29	F	ID	Aberrant	Adverse	wt	wt
2562	52	M	ID	Intermediate aberrant	n.a.	wt	wt
3140	74	M	ID	Normal	Intermediate	wt	wt
3073	54	M	R	Normal	Favourable	wt	wt
1233	49	F	ID	Complex aberrant	Adverse	mut	mut
3826	85	M	ID	Aberrant	Adverse	wt	wt
2449	30	F	ID	Aberrant	Favourable	wt	wt
4169	20	M	ID	Aberrant	Intermediate	wt	wt
0178	56	F	ID	Complex aberrant	Favourable	wt	wt
3386	52	M	ID	Normal	Favourable	wt	mut
3776	35	F	ID	Normal	Favourable	wt	wt
3221	59	M	ID	Normal	Favourable	wt	mut
3495	58	M	ID	Normal	Favourable	mut	wt
0885	74	F	ID	Normal	Intermediate	mut	mut
4321	50	F	ID	Normal	Intermediate	mut	mut
6789	68	M	ID	Normal	Favourable	mut	wt
0252	84	F	ID	Aberrant	Favourable	mut	mut
1421	66	F	ID	Aberrant/normal	Adverse	wt	wt
0682	56	F	ID	Complex aberrant	Adverse	wt	wt
7782	76	M	ID	Complex aberrant	Adverse	wt	wt
5964	87	F	ID	Complex aberrant	Adverse	wt	wt
AML-491 [3]	53	F	R	del(7)(q21)	Adverse	wt	wt
AML-579 [3]	51	M	R	Normal	Adverse	mut, LOH	mut
AML-640	79	M	R	t(11;15)	Intermediate	mut	mut
AML-979	56	F	R	Normal	n.a.	wt + mut subclone	mut

European LeukemiaNet (ELN), initial diagnosis (ID), relapse (R), not available (n.a.), wild type (wt), mutated (mut), loss of heterozygosity (LOH), female (F), male (M)

of antibody binding, the median fluorescence intensity (MFI) ratio was calculated by dividing the MFI of the tested antibody by the MFI of the corresponding isotype. Antibodies were considered to bind the cells if the intensity exceeded an MFI ratio of 1.5.

Competitive binding assays

PKH26 (Sigma-Aldrich)-labelled MOLM-13 was incubated with a 20-fold excess of red blood cells (RBCs) and antibodies. APC αhIgG (HP6017) or APC αmIgG (Poly4053) was used for secondary labelling. For assays with PBMCs, calcein AM (Thermo Fisher Scientific) or CellTrace™ calcein red-orange AM (Thermo Fisher Scientific)-labelled MOLM-13 cells were incubated with a fivefold excess of PBMCs and antibodies. APC or FITC αhIgG (HP6017) was used for secondary antibody labelling.

Platelet aggregation

PRP was centrifuged at 15,000×*g* for 2 min to obtain platelet-poor plasma (PPP). PRP was incubated in the presence of 100 nM antibodies, and absorbance was measured at 595 nm using an Infinite M100 plate reader (TECAN) for 16 min. The percentage of aggregation was calculated as $(\text{platelet aggregation}[\%] = 100 \times \frac{(\text{OD PRP - OD sample})}{(\text{OD PRP - OD PPP})})$ [30].

Antibody-dependent cellular phagocytosis (ADCP) assay

Monocytes were enriched using a classical monocyte isolation kit (Miltenyi) and were differentiated into macrophages in the presence of 100 ng/ml MCSF (Biolegend) for 5–7 days. Macrophages were labelled with calcein AM and incubated with CellTrace™ calcein red-orange AM-labelled target cells and antibodies at 50 pM or 50 nM for 3 h at 37 °C at a 1:1 effector-to-target (E:T) ratio.

Antibody-dependent cellular cytotoxicity (ADCC) assays

NK cells were enriched using a NK cell isolation kit (Miltenyi). MOLM-13 cells were labelled with calcein AM and incubated with NK cells and antibodies for 4 h at 37 °C at a 5:1 E:T ratio. In the competitive ADCC assay, NK cells were incubated with labelled MOLM-13 or Raji cells mixed with unlabelled Raji or MOLM-13 cells, respectively, at a 5:1:1 E:T:T ratio. Triton X-100 (2.5%, Sigma-Aldrich) was used for maximum lysis. Fluorescence intensity (FI) from calcein AM release was measured using an Infinite M100 plate reader, and lysis was calculated as $(\text{specific lysis}[\%] = 100 \times \frac{\text{FI(antibody stimulation)} - \text{FI(untreated)}}{\text{FI(max)} - \text{FI(target)}})$. Data were fitted to a four-parameter dose–response curve.

ADCC assays of AML patient samples were performed in α-MEM (Thermo Fisher Scientific) supplemented with 12.5% foetal calf serum, 12.5% horse serum, 1% penicillin, 1% streptomycin, 1% glutamine (Invitrogen) and a distinct cytokine cocktail on irradiated MS-5 cells in a long-term culture as described elsewhere [31, 32]. AML cells were incubated with HD NK cells and 10 nM antibodies for 20 h at 37 °C at a 5:1 E:T ratio. Dead cells were excluded as 7-AAD (BioLegend) or LIVE/DEAD™ Fixable Aqua (Thermo Fisher Scientific)-positive cells. $CD33^+$ or $CD123^+$ AML cells were determined by BV421, APC αhCD33 (WM53) or PE αhCD123 (6H6) labelling, respectively. Additionally, APC-Cy7 or FITC αhCD69 (FN50) and the corresponding isotype control (MOPC-21) were used to determine the percentage of $CD69^+$ cells. In some experiments, NK cells were labelled with CellTrace™ CFSE or CellTrace™ Far Red (both Thermo Fisher Scientific) according to the manufacturer's recommendations. Cell populations were assessed by flow cytometry, and the percentage of viable $CD33^+$ or $CD123^+$ AML cells was normalized to the human IgG1 isotype control sample. The percentage of $CD69^+$ cells was normalized to the human IgG1 isotype control sample.

In the AML PDX ADCC, AML-491, AML-979, and AML-640 were incubated with NK cells and 100 nM antibodies for 20 h at 37 °C at a 5:1 E:T ratio. Cells were labelled with LIVE/DEAD Fixable Aqua, and the proportion of live $mCherry^+$ cells was determined by flow cytometry and normalized to the isotype control.

In vivo engraftment experiments

To evaluate the targeting of AML cells with leukaemia-initiating properties, ex vivo NK cell-mediated ADCC was performed using the αCD123 antibody, the 2 × SIRPα-αCD123 fusion antibody or isotype antibody as a control, and surviving cells were used in an in vivo engraftment experiment. To this end, PDXs AML-491 and AML-579 [33, 34] were incubated with HD NK cells at an E:T ratio of 5:1 and antibodies for 20 h. After ADCC, residual $mCherry^+$ PDX cells were separated from NK cells and quantified by fluorescence-activated cell sorting (FACS) using a FACSAria III (BD Biosciences). According to previous data [34] and assuming that the isotype control antibody did not alter LIC frequency, we injected cell numbers corresponding to 10 leukaemia-initiating cells (10 × LIC, $n = 5$) and 100 × LIC ($n = 5$) for AML-491 or 14 × LIC ($n = 4$) and 140 × LIC ($n = 2$) for AML-579 by counting and diluting sorted cells of the isotype control suspensions. To enable comparison between the groups, equal volumes of αCD123 and 2 × SIRPα-αCD123 antibody ex vivo cell suspensions were sorted and injected intravenously into 10- to 12-week-old male (AML-491) or female (AML-579) NSG mice. Positive AML engraftment was analysed by in vivo

bioluminescence imaging (BLI), and total flux was quantified as previously described [33]. Mice exhibiting a total flux greater than 5×10^7 photons per second were classified as exhibiting positive engraftment; mice displaying no positive imaging signal within 28 weeks after transplantation were classified as negative for engraftment. To evaluate the percentage of human $CD33^+$ cells in peripheral blood, PE anti-human CD33 (WM53, BD Biosciences) and PE isotype control (MOPC-21, BD Biosciences) were used. Mice exhibiting any clinical signs of illness or end-stage leukaemia (total flux > 2×10^{10} photons/s; $hCD33^+$ cells in peripheral blood > 50%) were euthanized. Three mice died in narcosis during imaging and were counted as positive according to the last imaging signal or were excluded if not engrafted.

Data analysis

Statistical evaluation was performed using GraphPad Prism versions 6.07 and 8.1.2 (GraphPad). Datasets were analysed using one-way analysis of variance (ANOVA) including a test to determine equal variances within the groups and correction for multiple testing using Holm-Sidak's test. Chi-squared test was used to determine whether there is a statistically significant difference in the growth of engrafted AML PDX cells. A Kaplan–Meier plot was generated to depict AML engraftment and survival by treatment group, and significance was assessed using the log-rank Mantel-Cox test. Extreme limiting dilution analysis was performed using the injected cell number and number of AML engrafted mice as inputs as previously described [35] (Figure 7; Additional file 1: Table S2). The results were considered statistically significant at the following values and are marked in the figures as follows: p value < 0.05 (*), < 0.01 (**), < 0.001 (***), < 0.0001 (****).

Results

Generation and characterization of SIRPα-αCD123 fusion antibodies

The 1 × SIRPα-αCD123 recombinant antibody was generated by fusing the N-terminal SIRPα immunoglobulin V-like domain to the αCD123 antibody light chain via a flexible polypeptide linker (Fig. 1A). Likewise, for 2 × SIRPα-αCD123, a second SIRPα domain was connected to the N-terminus of 1 × SIRPα-αCD123 (Fig. 1A). Antibodies were produced in Expi293F cells, purified from cell culture supernatants and analysed by size exclusion chromatography and SDS–polyacrylamide gel electrophoresis (Additional file 1: Figure S1A-B). Thermal stability was assessed by measuring changes in the intrinsic fluorescence of the proteins using Tycho NT.6 (Additional file 1: Figure S1C). To investigate whether the N-terminal fusion of the SIRPα domains alters the binding to CD123, we determined the K_D values using a Biacore assay. The K_D values were in the low nanomolar range for all constructs, indicating that the high affinity for CD123 was not affected by the fusion of the SIRPα domains (Fig. 1B). We further evaluated binding of the antibodies to CHO cells stably overexpressing human CD47 (hCD47) by flow cytometry (Table 2). As expected, 1 × SIRPα-αCD123 and 2 × SIRPα-αCD123 bound to $^+$CHO_$hCD47^+$ cells but not to $^-$CHO_$hCD47^-$ cells (Fig. 1C). These binding experiments indicate that the αCD123 and SIRPα domains can bind to their respective targets in the fusion antibody.

SIRPα-αCD123 fusion antibodies specifically bind to $CD123^+CD47^+$ AML cells

Next, we used the $CD123^+$ $CD47^+$ AML cell line MOLM-13 in a flow cytometry-based binding assay to study the dual targeting properties of the antibody constructs (Fig. 2A, Table 2). The binding of 1 × SIRPα-αCD123 and 2 × SIRPα-αCD123 to MOLM-13 cells was stronger than that of the αCD123 antibody, indicating a contribution by the SIRPα domain. The αCD19 SIRPα fusion antibodies mediated only weak binding to $CD19^-$ MOLM-13 cells due to some low binding of the SIRPα domains (Fig. 2A, Table 2). In summary, we hypothesize that the strong binding of the SIRPα-αCD123 antibodies to MOLM-13 cells is due to avidity-dependent binding to both CD123 and CD47.

The physiological interaction of the SIRPα domain and CD47 is approximately 100-fold weaker than the affinity of the αCD123 antibody for CD123 [26, 36]. Therefore, we postulated that the high affinity αCD123 drives the preferential binding of SIRPα-αCD123 fusion antibodies onto $CD123^+CD47^+$ leukemic cells over $CD123^-CD47^+$ healthy cells. To test this hypothesis, we first utilized RBCs as highly abundant healthy cells expressing CD47 (Fig. 2B, Table 2).

We observed selective binding to MOLM-13 cells using the 1 × SIRPα-αCD123 antibody even in the presence of a 20-fold excess of RBCs (Fig. 2B, C). 2 × SIRPα-αCD123, on the other hand, was also detected on the surface of RBCs, indicating that the additional SIRPα domains can increase the competition between $CD47^+$ MOLM-13 cells and RBCs (Fig. 2B, C). Nevertheless, the RBC targeting observed for 2 × SIRPα-αCD123 was very weak, with a binding intensity far below an MFI ratio of 1.5 (Fig. 2D). In contrast, the high affinity αCD47 B6H12 antibody demonstrated a substantial on-target off-leukaemia effect, as it primarily bound to RBCs with a high MFI ratio (Fig. 2B–D). We concluded that despite carrying the SIRPα domains, the SIRPα-αCD123 fusion antibodies target MOLM-13 cells more than the high affinity αCD47 and avoid the antigen sink generated by the RBCs.

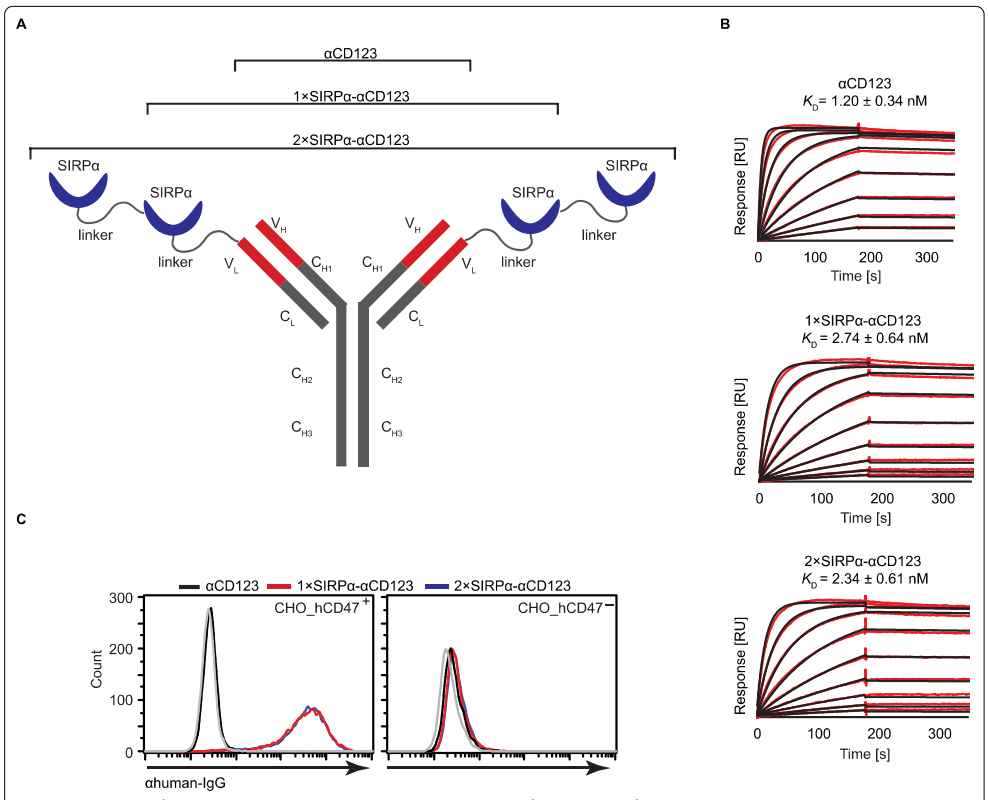

Fig. 1 SIRPα-αCD123 fusion antibodies bind to CD123 and CD47. **A** Structure of SIRPα-αCD123 fusion antibodies. V_H—variable heavy, C_L—constant light, C_{H1}—constant heavy 1, C_{H2}—constant heavy 2, C_{H3}—constant heavy 3. **B** Different CD123 concentrations binding to the antibody constructs measured using SPR. Raw data are shown in red; black curves were fitted to a 1:1 interaction. K_D values represent mean values from $n = 3$ independent experiments ± standard error of the mean (SEM). **C** Binding of antibodies to CHO_hCD47$^+$ and CHO_hCD47$^-$ cells at 100 nM concentration measured by flow cytometry. The grey line indicates nonspecific staining of the isotype control and secondary antibody. Histograms show 1 of 3 experiments with similar results

Table 2 Antigen expression levels

Cell type	CD123	CD47	CD19
MOLM-13	13 723 ± 1 108	67 703 ± 3 784	30 ± 2
Raji	94 ± 95	170 868 ± 37 029	141 688 ± 19 997
CHO^{CD47+}	104 ± 68	1 424 894 ± 329 869	n. d.
CHO^{CD47-}	159 ± 50	532 ± 35	n. d.
RBC	106 ± 33	33 841 ± 2 221	n. d.

Determined using QIFIKIT. Data are shown as the means ± SEM ($n = 2$–3). Not determined (n. d.)

In another set of experiments, we investigated the selective binding of our antibodies to MOLM-13 cells in the presence of HD PBMCs (Fig. 2E). From PBMCs, plasmacytoid dendritic cells express CD123 and are targeted by the αCD123 antibody CSL362 [37]. We also found that some of our αCD123 binds to PBMCs; however, the majority of the antibodies still bound to MOLM-13 cells (Fig. 2E). The 1 × SIRPα-αCD123 antibody bound PBMCs to a considerable extent, but higher selective binding to MOLM-13 cells was observed compared to the αCD47 Hu5F9-G4 clone. 2 × SIRPα-αCD123 targeted MOLM-13 cells similarly to αCD47 Hu5F9-G4. However, when we analysed binding of the antibodies to PBMCs

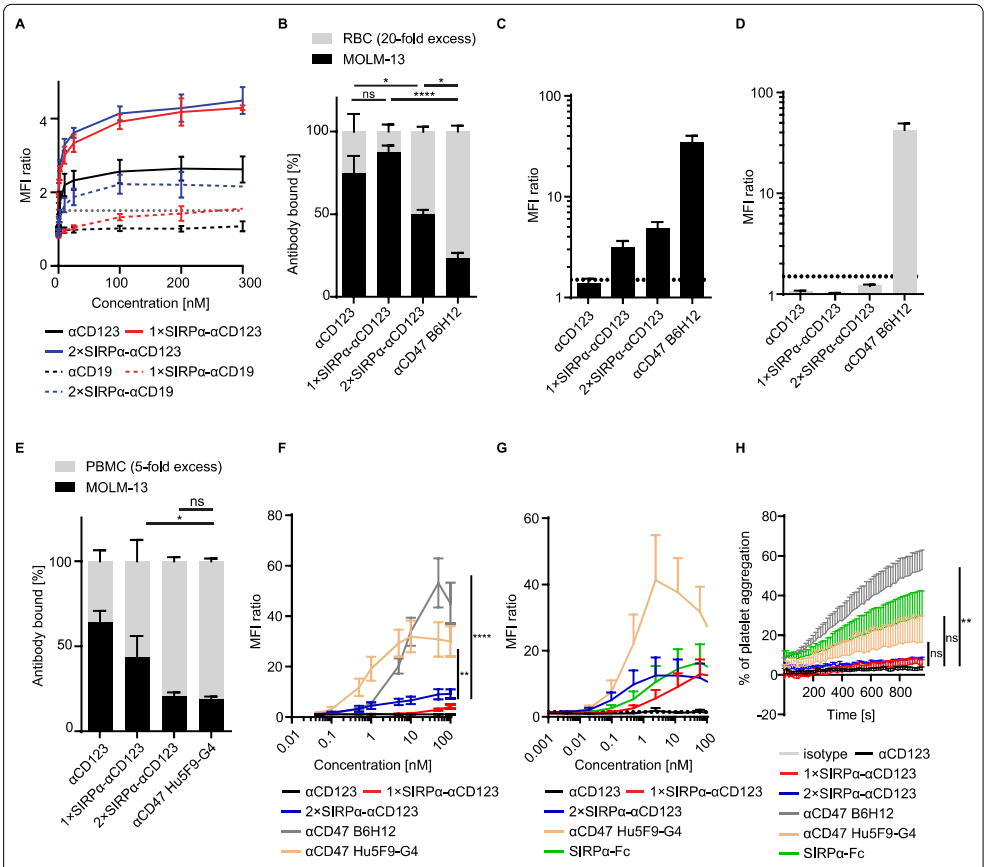

Fig. 2 SIRPα-αCD123 fusion antibodies preferentially bind to MOLM-13 cells in the presence of RBCs. **A** Binding of SIRPα-αCD123 fusion antibodies to MOLM-13 cells assessed by flow cytometry-based MFI ratio. The dotted line indicates an MFI ratio of 1.5 as the cut-off for positivity. Shown are the mean values from $n = 2$–3 independent experiments ± SEM. **B** Percentage of 100 nM antibodies targeting MOLM-13 cells or RBCs measured by flow cytometry at a 20-fold excess of RBCs. **C** MFI ratios of antibody binding to MOLM-13 cells in the presence of a 20-fold excess of RBCs. **D** MFI ratios of antibody binding to RBCs in the presence of MOLM-13 cells. The results of independent experiments with 4 different RBC donors represented as the mean ± SEM are shown. **E** Percentage of 100 nM antibodies targeting MOLM-13 cells or PBMCs measured by flow cytometry at a fivefold excess of PBMCs. Shown are mean values from $n = 6$ donors ± SEM. **F** Binding of SIRPα-αCD123 fusion antibodies to PBMCs assessed by flow cytometry-based MFI ratio. Shown are mean values from $n = 5$ donors ± SEM. **G** Binding of SIRPα-αCD123 fusion antibodies to platelets assessed by flow cytometry-based MFI ratio. Mean values from $n = 4$ donors ± SEM are shown. **H** Platelet aggregation induced by 100 nM antibody over time. Mean values from $n = 4$ donors ± SEM are shown. **F** and **H** p values are the same for both SIRPα-αCD123 fusion antibodies. Statistical differences were determined by one-way ANOVA using Holm–Sidak's post hoc test. *$p < 0.05$, **$p < 0.01$, ***$p < 0.001$, ****$p < 0.0001$

alone, we observed that our fusion antibodies bound PBMCs significantly less than the αCD47 Hu5F9-G4 and B6H12 antibodies (Fig. 2F). These data indicate that although our fusion antibodies seem to target PBMCs more than RBCs, they bind to PBMCs to a lesser extent than the high affinity αCD47 antibodies.

In addition to binding to RBCs, CD47-targeting agents have been reported to bind platelets and interfere with their function [38, 39]. We therefore investigated whether our SIRPα-αCD123 fusion antibodies target platelets and induce their aggregation (Fig. 2G–H). Indeed, SIRPα-αCD123 fusion antibodies bound to platelets similarly to

the SIRPα-Fc construct but less than the αCD47 Hu5F9-G4 control (Fig. 2G). However, SIRPα-αCD123 antibodies did not induce aggregation of platelets, unlike SIRPα-Fc, αCD47 Hu5F9-G4 and especially αCD47 B6H12 antibodies (Fig. 2H). These experiments suggest that binding of the constructs does not directly correlate with a functional effect and indicate that our SIRPα-αCD123 fusion antibodies do not stimulate platelet aggregation.

SIRPα-αCD123 fusion antibodies block CD47 and induce phagocytosis of MOLM-13 cells in vitro

SIRPα-αCD123 fusion antibodies were designed to inhibit the CD47-SIRPα axis locally on CD123$^+$ cells. To examine this, we performed a blocking assay using labelled αCD47 antibodies that interfere with the binding of SIRPα. Despite the weak affinities of the SIRPα domains, 1 × SIRPα-αCD123 and 2 × SIRPα-αCD123 were able to block CD47 molecules on MOLM-13 cells. Not surprisingly, maximum blockade was observed with the high affinity αCD47 antibody. In comparison, 1 × SIRPα-αCD123 did not block CD47 on CD123$^-$ Raji cells, and 2 × SIRPα-αCD123 minimally blocked CD47 (Additional file 1: Figure S2A), indicating that binding of the αCD123 moiety to target cells is required for efficient disruption of the CD47-SIRPα axis.

We next examined whether CD47 blockade with concomitant engagement of FcγRs stimulates the ADCP of MOLM-13 cells by HD-derived macrophages (Fig. 3B). Indeed, phagocytosis was significantly boosted by 1 × SIRPα-αCD123 compared to αCD123. 2 × SIRPα-αCD123 also induced elevated phagocytosis, but this was not statistically significant. In contrast, αCD47 did not stimulate phagocytosis either alone or in combination with αCD123 in this setting. The respective αCD19 controls did not have an effect on phagocytosis. In summary, SIRPα-αCD123 fusion antibodies boost ADCP in MOLM-13 cells, whereas αCD123 and αCD47 antibodies alone lack this ability.

SIRPα-αCD123 fusion antibodies induce enhanced phagocytosis of patient-derived AML cells by allogeneic and autologous macrophages in vitro

We further investigated the stimulation of phagocytosis by SIRPα-αCD123 antibodies using primary AML patient-derived blasts as targets and allogeneic or autologous monocyte-derived macrophages as effector cells (Fig. 4A, B). We observed enhanced overall phagocytosis by primary AML cells compared to MOLM-13 cells. Allogeneic macrophages from HDs mediated significantly higher ADCP with the 1 × SIRPα-αCD123 fusion antibody compared to αCD123. The 2 × SIRPα-αCD123 had a similar effect (Fig. 4A). More importantly, these results were confirmed in the autologous setting (Fig. 4B). Phagocytosis mediated by 1 × SIRPα-αCD123 and 2 × SIRPα-CD123 was significantly higher than that mediated by αCD123. αCD47 antibodies B6H12 and Hu5F9-G4 alone or in combination with αCD123 antibody induced similar ADCP as SIRPα-αCD123 fusion antibodies. When comparing SIRPα-CD123 fusion antibodies to similar αCD33-based constructs [18], we did not observe significant differences in the ability to induce phagocytosis of AML cells (Fig. 4B). Taken together, these data reveal that SIRPα-αCD123 fusion antibodies

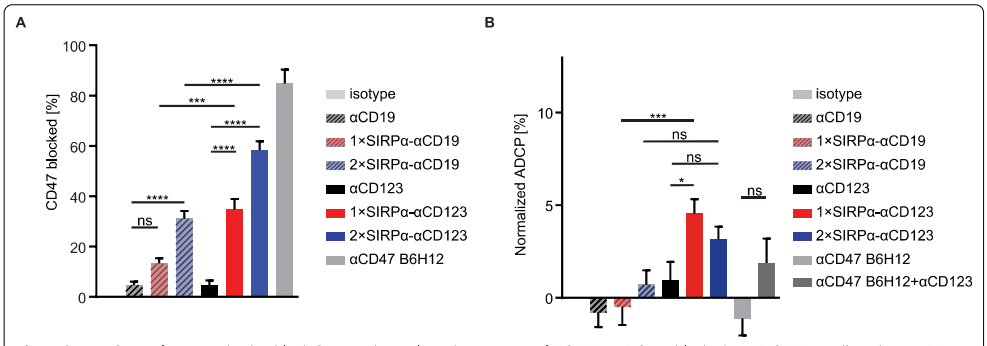

Fig. 3 SIRPα-αCD123 fusion antibodies block CD47 and stimulate phagocytosis of MOLM-13. **A** CD47 blockade on MOLM-13 cells with 100 nM antibodies determined by FITC αCD47 binding using flow cytometry. Background fluorescence was subtracted from the FITC αCD47 signal and normalized to isotype to calculate the CD47 blockade. Mean ± SEM of $n = 4$ independent experiments. **B** ADCP of MOLM-13 cells at a 50 pM concentration of antibodies after 3 h at an E:T ratio of 1:1. ADCP was measured as the percentage of double-positive cells from macrophages and normalized to the isotype control. Bar charts represent the mean ± SEM from $n = 7$ different donors. Statistical differences were determined by one-way ANOVA using Holm-Sidak's post hoc test. *$p < 0.05$, ***$p < 0.001$, ****$p < 0.0001$, not significant (ns)

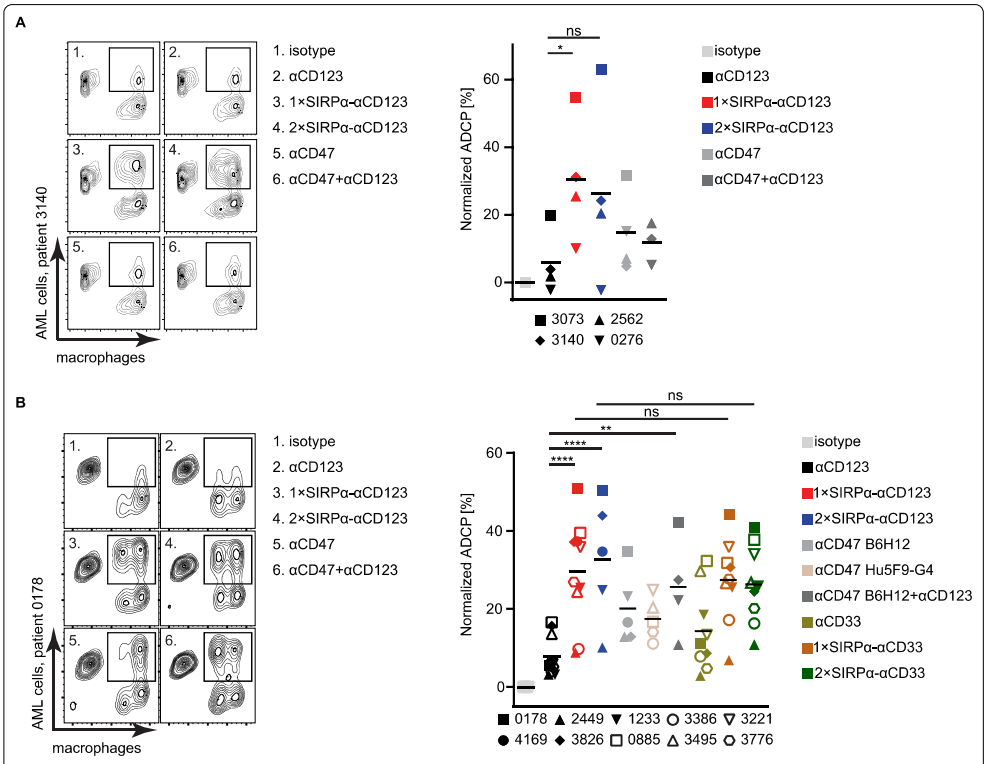

Fig. 4 SIRPα-αCD123 fusion antibodies stimulate phagocytosis of AML patient cells by allogeneic and autologous macrophages. AML target cells and macrophages were incubated with 50 nM antibody for 3 h at an E:T ratio of 1:1. ADCP was measured as the percentage of double-positive cells (gated) from all macrophages. Each symbol represents one patient (Table 1). **A** Phagocytosis of AML patient cells by allogeneic macrophages ($n = 4$). **B** Phagocytosis of AML patient cells by autologous macrophages ($n = 10$). Statistical differences were determined by one-way ANOVA using Holm-Sidak's post hoc test. *$p < 0.05$, ****$p < 0.0001$, not significant (ns)

represent an effective tool to overcome the CD47-mediated inhibition of phagocytosis in AML.

SIRPα-αCD123 fusion antibodies induce NK cell-mediated specific lysis of AML cells in vitro

ADCC by NK cells is one of the primary mechanisms by which IgG1 antibodies induce the elimination of antibody-bound cells in addition to macrophage-mediated ADCP [40]. Therefore, we analysed specific lysis of MOLM-13 cells by HD-derived NK cells (Fig. 5A). αCD123 induced moderate dose-dependent lysis of MOLM-13, whereas 1 × SIRPα-αCD123 and 2 × SIRPα-αCD123 were more potent. We postulated that SIRPα-αCD123 fusion antibodies are more efficient due to the avidity-dependent targeting of both CD123 and CD47. The respective αCD19 controls induced lysis of MOLM-13 cells only at high concentrations, which can be attributed to autonomous targeting of CD47 by the fused SIRPα domain. Nevertheless, the half maximal effective concentration (EC_{50}) was considerably lower for 2 × SIRPα-αCD123 (19.1 pM) than for the 2 × SIRPα αCD19 analogue (192.1 pM), demonstrating target antigen-specific cytotoxicity. This was further demonstrated in a competitive ADCC assay in which $CD123^{+}$ MOLM-13 cells were mixed with $CD123^{-}$ Raji cells (Additional file 1: Figure S2B). In this setting, Raji cells were not lysed by 1 × SIRPα-αCD123 and 2 × SIRPα-αCD123 only exerted an effect at high concentrations. In summary, although independent binding of the SIRPα domains can cause some lysis of target cells at high concentrations, we

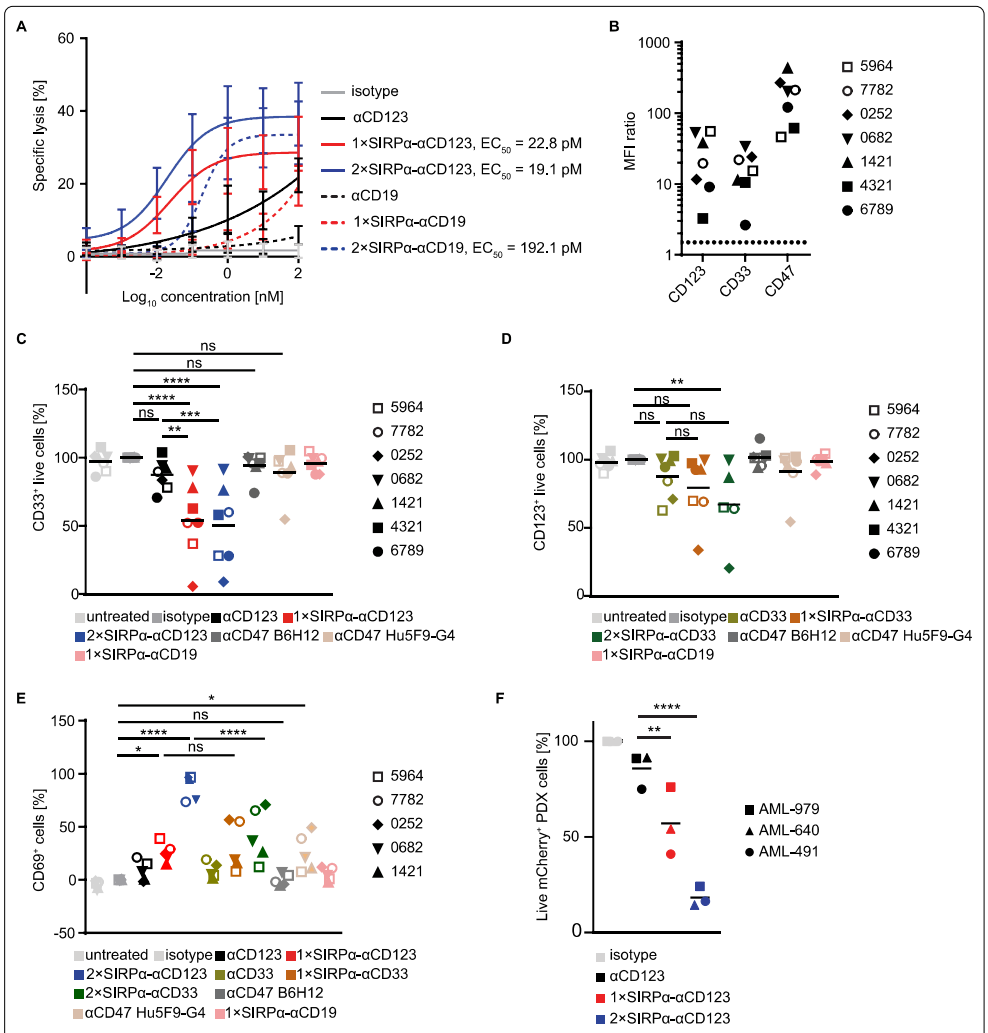

Fig. 5 SIRPα-αCD123 fusion antibodies enhance NK cell-mediated lysis of MOLM-13 and PDX AML cells. **A** NK cell-mediated dose-dependent lysis of MOLM-13 cells after 4 h at an E:T ratio of 5:1 measured by calcein AM release. Mean values ± SEM for $n = 6$ different NK cell donors are shown. EC_{50} values were calculated where possible. **B** Expression of CD123, CD33 and CD47 in primary AML samples assessed by flow cytometry. **C**, **D** NK cell-mediated lysis of AML cells in long-term culture at a 10 nM antibody concentration after 20 h at an E:T ratio of 5:1 measured by flow cytometry. The results from $n = 7$ different AML patient samples are represented as different symbols, and their mean values are shown. **E** Percentage of $CD69^+$ cells measured by flow cytometry. **F** NK cell-mediated lysis of PDX cells at 100 nM antibody concentration after 20 h at an E:T ratio of 5:1 measured by flow cytometry. The results from $n = 3$ different AML patient samples are represented as different symbols, and their mean values are shown. Statistical differences were determined by one-way ANOVA using Holm-Sidak's post hoc test. *$p < 0.05$, **$p < 0.01$, ***$p < 0.001$, ****$p < 0.0001$

consider high affinity αCD123 binding to be a prerequisite for targeting by SIRPα-αCD123 fusion antibodies.

The ability of SIRPα-αCD123 fusion antibodies to activate NK cells was further investigated using AML patient cells. First, we used blasts from primary AML patients (Fig. 5B) in a long-term culture system with HD-derived NK cells as effectors [31]. Compared to isotype controls and αCD123, 1 × SIRPα-αCD123 and 2 × SIRPα-αCD123 antibodies significantly boosted the cytotoxicity by NK cells, leading to reduced numbers of AML cells (Fig. 5C). As expected, the αCD47 antibodies B6H12 and Hu5F9-G4 and the 1 × SIRPα αCD19 control molecule did not stimulate lysis of AML cells (Fig. 5C). From the αCD33 constructs, only the 2 × SIRPα αCD33 analogue induced significant lysis of AML cells compared to the isotype control (Fig. 5D). When analysing the NK cell population of the ADCC samples, we observed a significant upregulation of the activation marker CD69 with 1 ×- and 2 × SIRPα-αCD123 (Fig. 5E). Treatment with 2 × SIRPα-αCD123 induced especially potent CD69 upregulation, which was also significantly greater than that induced by the 2 × SIRPα αCD33 analogue (Fig. 5E). Interestingly, the αCD47 antibody Hu5F9-G4 induced slight upregulation of CD69 (Fig. 5E). Together, these results demonstrate that in addition to highly effective FcγR-dependent ADCC stimulation, SIRPα-αCD123 antibodies might further activate NK cells via mechanisms related to CD47 blockade.

Next, we used AML PDX cells as target cells. Here, we observed that 1 × SIRPα-αCD123 and 2 × SIRPα-αCD123 both dramatically increased the lysis of AML PDX cells compared to αCD123 (Fig. 5E). This again highlights that our fusion antibodies enhance NK cell-mediated lysis of patient-derived AML cells.

SIRPα-αCD123 fusion antibodies have the potential to target AML stem cells

Specific targeting of AML LSCs is needed to prevent relapse and enhance the rate and duration of response to therapy in patients. We hypothesized that SIRPα-αCD123 fusion antibodies would efficiently eliminate $CD123^{high}$ $CD47^{high}$ LSCs due to the avidity-dependent binding of the αCD123 and SIRPα moieties. Xenograft mouse models have been widely used to investigate leukaemia-initiating cells (LICs) as surrogates for LSCs [41, 42]. To evaluate the impact of HD NK cell-dependent cytotoxicity of our antibodies on LICs, we performed an in vivo engraftment assay using residual AML PDX cells that survived an ex vivo ADCC assay (Fig. 6A). We expect that LICs are killed more efficiently with SIRPα-αCD123 fusion antibodies than with αCD123 antibodies in the ex vivo ADCC assay and thus lead to reduced engraftment of AML cells. To this end, PDX cells from two AML patients were incubated with NK cells and isotype control, αCD123 or 2 × SIRPα-αCD123 (Additional file 1: Figure S3). Only the 2 × SIRPα-αCD123 fusion antibody was used as it showed superior killing of AML PDX cells (Fig. 5F). After this ADCC, surviving PDX cells were sorted and injected into NSG mice at two doses corresponding to 10 leukaemia-initiating cells (10 × LIC) or 100 × LIC. AML engraftment was analysed by in vivo BLI and peripheral blood analysis.

As expected, all mice that received residual cells from isotype control-treated AML-491 ADCC culture exhibited PDX cell engraftment soon after transplantation [10 × LIC: 28–49 days post injection (dpi), $n = 5$; 100 × LIC: 33 dpi, $n = 5$], whereas treatment with the αCD123 antibody slightly delayed the time to positive engraftment (10 × LIC: 62–91 dpi, $n = 5$; AML-491 100 × LIC: 49 dpi, $n = 4$) (Fig. 6B–F). Importantly, residual cells from 2 × SIRPα-αCD123 ADCC cultures exhibited a dramatically reduced engraftment capacity, with only one animal in the 10 × LIC group (114 dpi) and none in the 100 × LIC group showing positive engraftment (Fig. 6B–F). All mice with positive engraftment reached end-stage leukaemia with high BLI signals and $hCD33^{+}$ cells in peripheral blood (Fig. 6; Additional file 1: Figure S5). AML-579 cells were injected at slightly higher doses of 14 × LIC and 140 × LIC, but the results were similar to those observed for AML-491 (Additional file 1: Figures S4 and S5).

We used the extreme limiting dilution analysis algorithm to determine whether the nearly absent engraftment in the 2 × SIRPα-αCD123 condition was due to specific LIC targeting or a lower number of injected residual cells [35]. Even though all mice in the isotype and αCD123 treatment groups exhibited engraftment, a significant difference in the estimated LIC frequencies was detected between αCD123 and 2 × SIRPα-αCD123 for AML-491 (Fig. 7A, B; Additional file 1: Table S2). We concluded that while 2 × SIRPα-αCD123 markedly reduces the number of bulk AML cells, it targets leukemic stem cells with an even higher preference.

Discussion

The ubiquitously expressed surface marker CD47 interacts with the SIRPα receptor to inhibit myeloid cell-mediated phagocytosis of autologous cells [4, 14, 15]. Blocking the CD47-SIRPα checkpoint as an anticancer therapy is under intense investigation since CD47 is overexpressed on AML as well as on various other cancer types [5, 10, 43]. However, ubiquitous expression of CD47 creates an antigen sink that can sequester CD47-targeting agents and reduce the effective dose. Moreover, nonspecific targeting can cause toxicities to healthy cells, as CD47 has various roles in physiological tissue homeostasis [44]. For

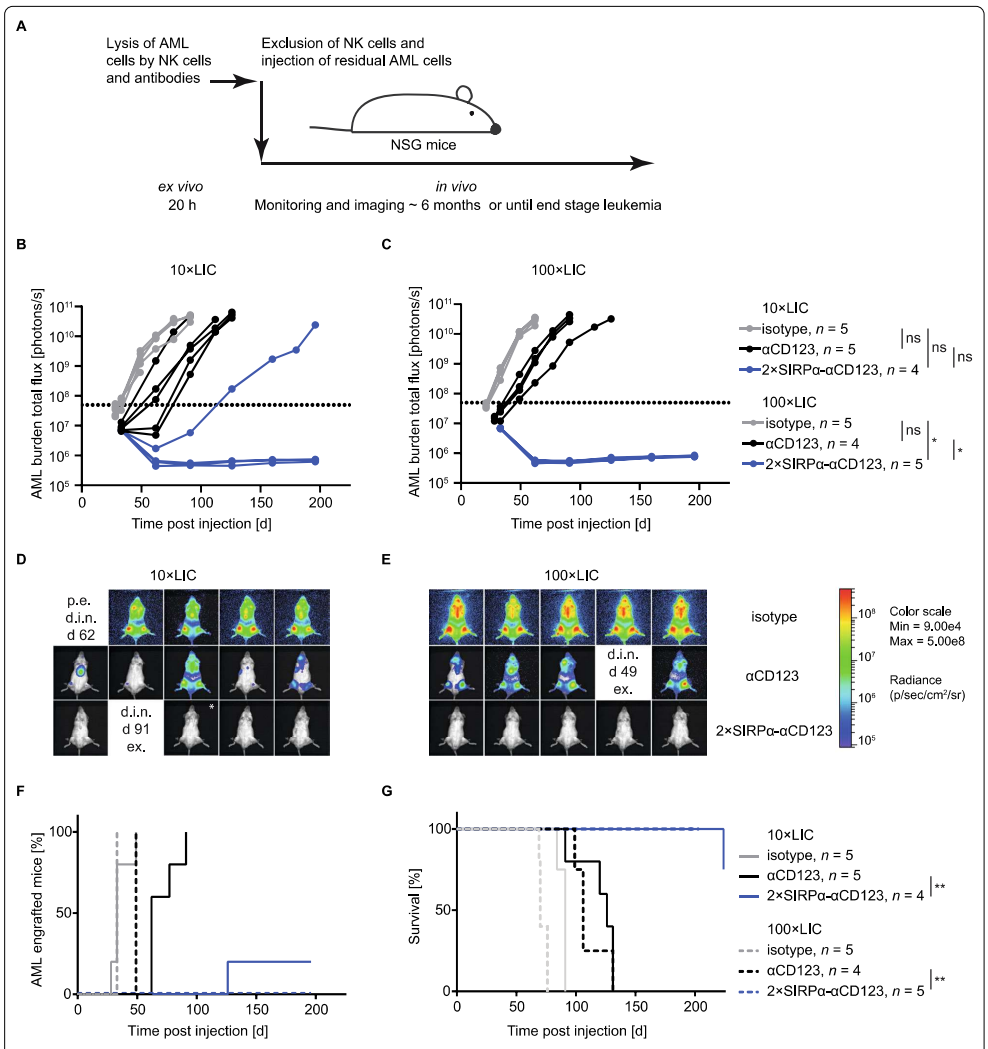

Fig. 6 Ex vivo treatment with 2 × SIRPα-αCD123 prevents outgrowth of AML-491 PDX cells in vivo. **A** Experimental design of the engraftment assay. Residual AML cell from ADCC in (Additional file 1: Figure 3A, B) was FACS sorted, and equal volumes were injected intravenously into NSG mice. Mice were monitored using in vivo BLI. **B**, **C** AML burden in individual mice of the 10 × LIC and 100 × LIC groups measured by BLI. The dotted line indicates a total flux of 5×10^7 photons/s as the cut-off for evaluating positive AML engraftment. Statistical analysis was performed using Chi-squared test. Representative images of mice injected with 10 × LIC (**D**) and 100 × LIC (**E**) on day (d) 62. Mice that died in narcosis during imaging (d.i.n.) were counted as positive if the last imaging signal showed positive engraftment (p. e.) or were excluded from analysis (ex.) if not engrafted. **F** Kaplan–Meier curve of AML-491 engraftment analysed by BLI. (**G**) Kaplan–Meier curves showing survival of mice. Statistical significance was calculated using the log-rank test. $*p < 0.05$, $**p < 0.01$, not significant (ns)

A

	Injected cells	Mice injected / engrafted	Estimated LIC frequency (95% confidence interval)
isotype	180 000	5 / 5	1/1 (1/1-1/22 575)
	18 000	5 / 5	
αCD123	26 000	4 / 4	1 / 1 (1/1-1/3 261)
	2 600	5 / 5	
2×SIRPα-αCD123	4 000	5 / 0	1 / 21 399 (1/2 786-1/164 397)
	400	4 / 1	

B

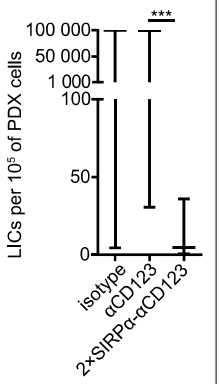

Fig. 7 LIC frequencies of AML-491 after NK cell-mediated lysis with the 2 × SIRPα-αCD123 fusion antibody. **A** Engraftment at each injected cell dose for each antibody. Residual AML cells were counted during cell sorting before injection. **B** LIC frequencies were estimated using extreme limiting dilution analysis software [35]. Horizontal lines indicate the estimated LIC frequencies, and the bars indicate 95% confidence intervals

example, the CD47 ligand SIRPγ is expressed on human T cells, and targeting CD47 with a mAb has been shown to affect human T cell responses [45].

The most serious side effects reported from CD47-targeting agents in clinical trials are anaemia and thrombocytopenia [39, 46–49]. The SIRPα-αCD123 antibodies presented here specifically bind to the AML cell line MOLM-13 in the presence of excess RBCs, in contrast to the high-affinity CD47-targeting antibody B6H12. These results agree with previous reports where similar constructs targeting CD33 and CD20 avoid the CD47 sink generated by RBCs [17, 18]. We also observed that SIRPα-αCD123 antibodies targeted PBMCs more than RBCs. The low-affinity SIRPα-dependent binding to PBMCs might, however, not lead to activation of macrophages or NK cells based on our results with SIRPα-αCD19 control molecules in experiments with MOLM-13 cells and primary AML cells. Importantly, although the SIRPα-αCD123 fusion antibodies also bind platelets, they do not induce any aggregation, unlike other CD47-targeting molecules tested herein. The underlying reason for this might be a combination of relatively low-affinity binding of the SIRPα domain to CD47 as well as different steric features of the antibody constructs.

Despite the low-affinity binding of the SIRPα domains, SIRPα-αCD123 fusion antibodies were able to induce the same or even higher phagocytosis than high affinity αCD47 either alone or in combination with αCD123. This is in line with the well-known synergy between CD47-SIRPa axis disruption and prophagocytic signals [8, 10, 50–52] and supports the rationale of combining CD47 blockade and FcγR stimulation into one molecule.

AML LSCs reside in specific niches in the bone marrow [53]. Antibodies can freely access the bone marrow through sinusoidal clefts and therefore represent a promising therapeutic strategy for targeting LSCs in their microenvironment [54]. CD33-targeting gemtuzumab ozogamicin is currently the only antibody-based therapy approved for AML [55]. Unfortunately, only some patients are likely to benefit from gemtuzumab ozogamicin [56, 57]. CD33/CD47 cotargeting has been previously preclinically investigated [18, 58]. However, bivalent mAbs against CD33 have been shown to internalize upon cross-linking, which can compromise the immune response [59, 60]. Expression of CD33 on LSCs is also associated with variability, which might affect therapeutic outcomes [20, 61]. Our results indicate that the SIRPα-αCD123 constructs are comparable to αCD33-based fusion antibodies in inducing autologous ADCP or allogenic ADCC. Interestingly, we observed much higher activation of NK cells in response to 2 × SIRPα-αCD123 than with the αCD33 analogue. Whether this was due to CD33-related internalization effects or other reasons remains to be investigated, but we consider αCD123-based constructs promising candidates next to αCD33-targeting antibodies.

Because chemorefractory LSCs build a reservoir for relapse, elimination of these cells is essential for AML treatment [1, 2]. In younger adults, a lower percentage of $CD123^+$ LSCs at diagnosis is correlated with a better response to treatment and survival [62]. Similarly, in

older patients who are fit for intensive chemotherapy, survival was higher in those who displayed lower levels of CD123$^+$ LSCs [63]. Therefore, eliminating or reducing the numbers of CD123$^+$ LSCs might lead to more durable responses and prolonged survival. We show here that compared to αCD123, SIRPα-αCD123 antibodies exhibit increased targeting efficacy of CD123$^+$ CD47$^+$ AML cells due to avidity-dependent binding to both antigens. Our fusion antibodies could take advantage of the high expression of both CD123 and CD47 on LSCs and effectively address this population. Indeed, we observed an extreme reduction in the engraftment of AML after an ex vivo ADCC assay with the 2 × SIRPα-αCD123 antibody, as our antibodies stimulated NK cell-mediated cytotoxic lysis of AML LSCs. The increased avidity of SIRPα-αCD123 antibodies thus provides the opportunity to preferentially target and eliminate AML LSCs.

Because of avidity-dependent binding to CD123 and CD47, SIRPα-αCD123 antibodies could further target malignant LSCs cells over healthy haematopoietic stem cells, which express low levels of CD47 and minimal amounts of CD123 [5, 19, 21, 64]. The 2 × SIRPα-αCD123 fusion antibody facilitated the most potent NK cell activation in our assays, and only this antibody was evaluated in LSC targeting experiments. To further analyse the safety and efficacy of the molecules and to determine whether the 1 ×- or 2 × SIRPα-αCD123 fusion format would be favourable in future clinical trials, assessing competitive targeting of patient-derived LSCs and healthy haematopoietic stem cells would be very pertinent.

While we are the first to combine CD123 and CD47 targeting, other therapeutic molecules have been developed against CD123 alone [65–67]. Talacotuzumab is an αCD123 antibody with a modified Fc region for enhanced ADCC [37, 68]. Unfortunately, talacotuzumab showed limited in vivo efficacy in clinical studies, which has been associated with the compromised NK cell activity in MDS and AML [69–71]. This suggests that recruiting other immune cells, such as macrophages, could stimulate a broader response to antibody-based CD123-targeting therapies. The benefit of activating macrophages in AML has been demonstrated by the αCD47 antibody magrolimab in combination with azacytidine [8]. Recent data additionally suggest that upon activation, NK cells can upregulate SIRPα, which leads to strong inhibition of cytotoxicity when interacting with CD47 on the surface of target cells [72]. An effective blockade of CD47 signalling could therefore be the reason we observed an extremely potent upregulation of CD69 on NK cells in response to 2 × SIRPα-αCD123 treatment. This was also indicated by the slight increase in the percentage of CD69$^+$ cells when the αCD47 antibody Hu5F9-G4 was used. A growing body of evidence indicates that adaptive immunity, especially the activation of CD8$^+$ T cells, further contributes to the effects observed in response to CD47-SIRPα inhibition [73–75]. As SIRPα-αCD123 fusion antibodies improve phagocytosis of AML patient cells compared to αCD123 while still initiating strong NK cell activation, we propose that SIRPα-αCD123 fusion antibodies stimulate a much broader immune response, including a long-lasting T-cell response.

Conclusions

In summary, we demonstrated that SIRPα-αCD123 antibodies specifically target LSCs, mediate their efficient clearance and stimulate phagocytosis of AML while restricting CD47-related on-target off-leukaemia toxicity. These encouraging results establish SIRPα-αCD123 antibodies as a promising approach for LSC targeting for prolonged remission in AML patients. Future in vivo studies using an appropriate AML mouse model are necessary for the translation of this approach into a clinical setting.

Abbreviations

AML: Acute myeloid leukaemia; LSC: Leukemic stem cell; SIRPα: Signal regulatory protein alpha; FcγR: Fcγ receptor; MDS: Myelodysplastic syndrome; OR: Objective response; CR: Complete remission; NK: Natural killer; V_L: Variable light; V_H: And variable heavy; SDS: Sodium dodecyl sulphate; EC_{50}: Half maximal effective concentration; PCR: Polymerase chain reaction; K_D: Equilibrium dissociation constant; CHO: Chinese hamster ovary; PBMC: Peripheral blood mononuclear cells; PDX: Patient-derived xenograft; NSG: NOD/SCID gamma null mice; MFI: Median fluorescence intensity; RBC: Red blood cells; E:T: Effector-to-target; LIC: Leukaemia-initiating cell; BLI: Bioluminescence imaging; ANOVA: Analysis of variance; ADCP: Antibody-dependent cellular phagocytosis; ADCC: Antibody-dependent cellular cytotoxicity; HD: Healthy donor; FACS: Fluorescence-activated cell sorting.

Supplementary Information

The online version contains supplementary material available at https://doi.org/10.1186/s13045-021-01163-6.

Additional file 1. Supplementary tables and figures.

Acknowledgements

The authors are grateful to Bettina Brauchle for help with the AML patient material and to Manuel Albanese, Marcel Stern and Oliver Keppler for help with the leukoreduction chamber material. We thank Maike Fritschle and Fabian Klein for technical assistance in the in vivo experiment, Daniel Bergér for help with the assay setup and Vindi Jurinovic for advice on statistical analysis. We acknowledge the iFlow Core Facility of the university hospital Munich (INST 409/225-1 FUGG) for assistance with the generation of flow cytometry data.

Authors' contributions

BV, BH, SS contributed equally to this work. ST, NCF and KPH designed the experiments and interpreted the data. ST generated and characterized the molecules and performed functional assays with cell lines and patient materials and data analysis. SS contributed to ADCP and SPR analysis and helped with interpreting the data. BV and IJ provided PDX cells, designed the in vivo engraftment assay and performed the experiments after ex vivo ADCC. BV

analysed the results of the in vivo engraftment experiment. BH performed experiments with PBMCs and platelets and contributed to autologous ADCP results. AM performed the AML long-term ADCC experiments. EP generated molecules. AR, CA, BT and MS provided AML patient material. AL performed PBMC binding studies. AH provided the leukoreduction chamber material. MS interpreted the data and provided critical feedback and support. ST and NCF wrote the manuscript with input from BV, MS and KPH. KPH supervised the project. All authors approved the final version of the manuscript. All authors read and approved the final manuscript

Funding
Open Access funding enabled and organized by Projekt DEAL. This study was supported by the Marie-Sklodowska-Curie Training Network "Immutrain" funded by the H2020 Program of the European Union (Grant 641549, KPH), the International Doctoral Program "i-Target" funded by the Elite Network of Bavaria (MS and KPH), the Collaborative Research Center 1243 "Cancer Evolution" of the Deutsche Forschungsgemeinschaft (IJ, MS and KPH), the Deutsche Forschungsgemeinschaft grants HO2489/10-1 and SU197/3-1 (KPH and MS), and the Exist Transfer of Research I grant (NCF).

Availability of data and materials
All data generated or analysed during this study are included in this published article [and its supplementary information files].

Declarations

Ethics approval and consent to participate
After obtaining written informed consent in accordance with the Declaration of Helsinki and approval by the Institutional Review Board of the Ludwig-Maximilians-Universität, peripheral blood, bone marrow or leukoreduction material was collected from AML patients and healthy donors. All animal studies were performed in accordance with the current ethical standards of the official committee on animal experimentation (written approval by Regierung von Oberbayern, ROB-55.2Vet-2532. Vet_02-16–7 and ROB-55.2Vet-2532. Vet_03-16–56).

Consent for publication
Not applicable.

Competing interests
KPH, MS and NCF are inventors of a patent application regarding the SIRPα-antibody fusion proteins.

Author details
[1]Gene Center and Department of Biochemistry, Ludwig-Maximilians-Universität München, Feodor-Lynen-Straße 25, 81377 Munich, Germany. [2]Research Unit Apoptosis in Hematopoietic Stem Cells, Helmholtz Zentrum München, German Research Center for Environmental Health (HMGU), Neuherberg, Germany. [3]German Cancer Consortium (DKTK), Partner Site Munich, Munich, Germany. [4]Laboratory for Translational Cancer Immunology, Gene Center, LMU Munich, Munich, Germany. [5]Department of Hematology and Oncology, Department of Medicine III, University Hospital, LMU Munich, Munich, Germany. [6]Department of Transfusion Medicine, Cellular Therapeutics and Hemostaseology, University Hospital, LMU Munich, Munich, Germany. [7]Department of Pediatrics, Dr. von Hauner Children's Hospital, LMU Munich, Munich, Germany.

Received: 5 March 2021 Accepted: 7 September 2021
Published online: 27 September 2021

References

1. Shlush LI, Mitchell A, Heisler L, Abelson S, Ng SWK, Trotman-Grant A, et al. Tracing the origins of relapse in acute myeloid leukaemia to stem cells. Nature. 2017;547(7661):104–8.
2. Wulf GG, Wang RY, Kuehnle I, Weidner D, Marini F, Brenner MK, et al. A leukemic stem cell with intrinsic drug efflux capacity in acute myeloid leukemia. Blood. 2001;98(4):1166–73.
3. Dohner H, Estey E, Grimwade D, Amadori S, Appelbaum FR, Buchner T, et al. Diagnosis and management of AML in adults: 2017 ELN recommendations from an international expert panel. Blood. 2017;129(4):424–47.
4. Tsai RK, Discher DE. Inhibition of "self" engulfment through deactivation of myosin-II at the phagocytic synapse between human cells. J Cell Biol. 2008;180(5):989–1003.
5. Majeti R, Chao MP, Alizadeh AA, Pang WW, Jaiswal S, Gibbs KD Jr, et al. CD47 is an adverse prognostic factor and therapeutic antibody target on human acute myeloid leukemia stem cells. Cell. 2009;138(2):286–99.
6. Jaiswal S, Jamieson CH, Pang WW, Park CY, Chao MP, Majeti R, et al. CD47 is upregulated on circulating hematopoietic stem cells and leukemia cells to avoid phagocytosis. Cell. 2009;138(2):271–85.
7. Vyas P, Knapper S, Kelly R, Salim R, Lubowiecki M, Royston D, et al. Initial phase 1 results of the first-in-class anti-CD47 antibody Hu5F9-G4 in relapsed/refractory acute myeloid leukemia patients. European Hematology Association Annual Meeting, Stockholm. 2018: (*Abstract PF232*).
8. Chao MP, Takimoto CH, Feng DD, McKenna K, Gip P, Liu J, et al. Therapeutic targeting of the macrophage immune checkpoint CD47 in myeloid malignancies. Front Oncol. 2019;9:1380.
9. Ring NG, Herndler-Brandstetter D, Weiskopf K, Shan L, Volkmer JP, George BM, et al. Anti-SIRPalpha antibody immunotherapy enhances neutrophil and macrophage antitumor activity. Proc Natl Acad Sci U S A. 2017;114(49):E10578–85.
10. Chao MP, Alizadeh AA, Tang C, Myklebust JH, Varghese B, Gill S, et al. Anti-CD47 antibody synergizes with rituximab to promote phagocytosis and eradicate non-Hodgkin lymphoma. Cell. 2010;142(5):699–713.
11. Weiskopf K, Jahchan NS, Schnorr PJ, Cristea S, Ring AM, Maute RL, et al. CD47-blocking immunotherapies stimulate macrophage-mediated destruction of small-cell lung cancer. J Clin Investig. 2016;126(7):2610–20.
12. Jain S, Van Scoyk A, Morgan EA, Matthews A, Stevenson K, Newton G, et al. Targeted inhibition of CD47-SIRPalpha requires Fc-FcgamaR interactions to maximize activity in T-cell lymphomas. Blood. 2019;134(17):1430–40.
13. Sallman DA, Asch AS, Malki MMA, Lee DJ, Donnellan WB, Marcucci G, et al. The first-in-class anti-CD47 antibody magrolimab (SF9) in combination with azacitidine is effective in MDS and AML patients: ongoing phase 1b results. Blood. 2019;134(Supplement_1):569 (**Abstract**).
14. Reinhold MI, Lindberg FP, Plas D, Reynolds S, Peters MG, Brown EJ. In vivo expression of alternatively spliced forms of integrin-associated protein (CD47). J Cell Sci. 1995;108:3419–25.
15. Oldenborg PA, Zheleznyak A, Fang YF, Lagenaur CF, Gresham HD, Lindberg FP. Role of CD47 as a marker of self on red blood cells. Science. 2000;288(5473):2051–4.
16. Piccione EC, Juarez S, Liu J, Tseng S, Ryan CE, Narayanan C, et al. A bispecific antibody targeting CD47 and CD20 selectively binds and eliminates dual antigen expressing lymphoma cells. MAbs. 2015;7(5):946–56.
17. Piccione EC, Juarez S, Tseng S, Liu J, Stafford M, Narayanan C, et al. SIRPalpha-antibody fusion proteins selectively bind and eliminate dual antigen-expressing tumor cells. Clin Cancer Res. 2016;22(20):5109–19.
18. Ponce LP, Fenn NC, Moritz N, Krupka C, Kozik JH, Lauber K, et al. SIRPalpha-antibody fusion proteins stimulate phagocytosis and promote elimination of acute myeloid leukemia cells. Oncotarget. 2017;8(7):11284–301.
19. Jordan CT, Upchurch D, Szilvassy SJ, Guzman ML, Howard DS, Pettigrew AL, et al. The interleukin-3 receptor alpha chain is a unique marker for human acute myelogenous leukemia stem cells. Leukemia. 2000;14(10):1777–84.
20. Taussig DC, Pearce DJ, Simpson C, Rohatiner AZ, Lister TA, Kelly G, et al. Hematopoietic stem cells express multiple myeloid markers: implications for the origin and targeted therapy of acute myeloid leukemia. Blood. 2005;106(13):4086–92.
21. Haubner S, Perna F, Kohnke T, Schmidt C, Berman S, Augsberger C, et al. Coexpression profile of leukemic stem cell markers for combinatorial targeted therapy in AML. Leukemia. 2019;33(1):64–74.
22. Yan B, Chen Q, Shimada K, Tang M, Li H, Gurumurthy A, et al. Histone deacetylase inhibitor targets CD123/CD47-positive cells and reverse chemoresistance phenotype in acute myeloid leukemia. Leukemia. 2019;33(4):931–44.
23. Broughton SE, Hercus TR, Nero TL, Dhagat U, Owczarek CM, Hardy MP, et al. Crystallization and preliminary X-ray diffraction analysis of the interleukin-3 alpha receptor bound to the Fab fragment of antibody CSL362. Acta Crystallogr F Struct Biol Commun. 2014;70(Pt 3):358–61.

24. Liu J, Wang L, Zhao F, Tseng S, Narayanan C, Shura L, et al. Pre-Clinical Development of a Humanized Anti-CD47 Antibody with Anti-Cancer Therapeutic Potential. PLoS ONE. 2015;10(9):e0137345.
25. Petrova PS, Viller NN, Wong M, Pang X, Lin GH, Dodge K, et al. TTI-621 (SIRPalphaFc): A CD47-blocking innate immune checkpoint inhibitor with broad antitumor activity and minimal erythrocyte binding. Clin Cancer Res. 2017;23(4):1068–79.
26. Hatherley D, Lea SM, Johnson S, Barclay AN. Polymorphisms in the human inhibitory signal-regulatory protein alpha do not affect binding to its ligand CD47. J Biol Chem. 2014;289(14):10024–8.
27. Dufour A, Schneider F, Metzeler KH, Hoster E, Schneider S, Zellmeier E, et al. Acute myeloid leukemia with biallelic CEBPA gene mutations and normal karyotype represents a distinct genetic entity associated with a favorable clinical outcome. J Clin Oncol. 2010;28(4):570–7.
28. Benthaus T, Schneider F, Mellert G, Zellmeier E, Schneider S, Kakadia PM, et al. Rapid and sensitive screening for CEBPA mutations in acute myeloid leukaemia. Br J Haematol. 2008;143(2):230–9.
29. Büchner T, Hiddemann W, Wörmann B, Löffler H, Gassmann W, Haferlach T, et al. Double induction strategy for acute myeloid leukemia: the effect of high-dose cytarabine with mitoxantrone instead of standard-dose cytarabine with daunorubicin and 6-thioguanine: a randomized trial by the German AML Cooperative Group. Blood. 1999;93(12):4116–24.
30. Vinholt PJ, Nybo M, Nielsen CB, Hvas A-M. Light transmission aggregometry using pre-coated microtiter plates and a Victor X5 plate reader. PLoS ONE. 2017;12(10):e0185675.
31. Krupka C, Kufer P, Kischel R, Zugmaier G, Bögeholz J, Köhnke T, et al. CD33 target validation and sustained depletion of AML blasts in long-term cultures by the bispecific T-cell–engaging antibody AMG 330. Blood. 2014;123(3):356–65.
32. Krupka C, Kufer P, Kischel R, Zugmaier G, Lichtenegger FS, Kohnke T, et al. Blockade of the PD-1/PD-L1 axis augments lysis of AML cells by the CD33/CD3 BiTE antibody construct AMG 330: reversing a T-cell-induced immune escape mechanism. Leukemia. 2016;30(2):484–91.
33. Vick B, Rothenberg M, Sandhofer N, Carlet M, Finkenzeller C, Krupka C, et al. An advanced preclinical mouse model for acute myeloid leukemia using patients' cells of various genetic subgroups and in vivo bioluminescence imaging. PLoS ONE. 2015;10(3):e0120925.
34. Ebinger S, Zeller C, Carlet M, Senft D, Bagnoli JW, Liu WH, et al. Plasticity in growth behavior of patients' acute myeloid leukemia stem cells growing in mice. Haematologica. 2020;32:939.
35. Hu Y, Smyth GK. ELDA: extreme limiting dilution analysis for comparing depleted and enriched populations in stem cell and other assays. J Immunol Methods. 2009;347(1–2):70–8.
36. Kwong LS, Brown MH, Barclay AN, Hatherley D. Signal-regulatory protein alpha from the NOD mouse binds human CD47 with an exceptionally high affinity—implications for engraftment of human cells. Immunology. 2014;143(1):61–7.
37. Busfield SJ, Biondo M, Wong M, Ramshaw HS, Lee EM, Ghosh S, et al. Targeting of acute myeloid leukemia in vitro and in vivo with an anti-CD123 mAb engineered for optimal ADCC. Leukemia. 2014;28(11):2213–21.
38. Pietsch EC, Dong J, Cardoso R, Zhang X, Chin D, Hawkins R, et al. Anti-leukemic activity and tolerability of anti-human CD47 monoclonal antibodies. Blood Cancer J. 2017;7(2):e536.
39. Ansell SM, Maris M, Lesokhin AM, Chen R, Flinn IW, Sawas A, et al. Phase 1 study of the CD47 blocker TTI-621 in patients with relapsed or refractory hematologic malignancies. Clin Cancer Res. 2021;27:2190–9.
40. Bakema JE, van Egmond M. Fc receptor-dependent mechanisms of monoclonal antibody therapy of cancer. Curr Top Microbiol Immunol. 2014;382:373–92.
41. Lapidot T, Sirard C, Vormoor J, Murdoch B, Hoang T, Caceres-Cortes J, et al. A cell initiating human acute myeloid leukaemia after transplantation into SCID mice. Nature. 1994;367(6464):645–8.
42. Sarry JE, Murphy K, Perry R, Sanchez PV, Secreto A, Keefer C, et al. Human acute myelogenous leukemia stem cells are rare and heterogeneous when assayed in NOD/SCID/IL2Rgammac-deficient mice. J Clin Investig. 2011;121(1):384–95.
43. Willingham SB, Volkmer JP, Gentles AJ, Sahoo D, Dalerba P, Mitra SS, et al. The CD47-signal regulatory protein alpha (SIRPa) interaction is a therapeutic target for human solid tumors. Proc Natl Acad Sci U S A. 2012;109(17):6662–7.
44. Logtenberg MEW, Scheeren FA, Schumacher TN. The CD47-SIRPalpha immune checkpoint. Immunity. 2020;52(5):742–52.
45. Brooke G, Holbrook JD, Brown MH, Barclay AN. Human lymphocytes interact directly with CD47 through a novel member of the signal regulatory protein (SIRP) family. J Immunol. 2004;173(4):2562–70.
46. Advani R, Bartlett N, Smith S, Roschewski M, Popplewell L, Flinn I, et al. The first in class anti CD47 antibody HU5FY G4 + rituximab induces durable responses in relapsed/refractory dlbcl and indolent lymphoma: interim phase 1B/2 results. Hematol Oncol. 2019;37:89–90.
47. Sallman DA, Asch AS, Kambhampati S, Al Malki MM, Zeidner JF, Donnellan W, Lee DJ, Vyas P, Jeyakumar D, Mannis GN, Tanaka TN, Chai-Ho W, Larson RA, Whiteley AR, Marcucci G, Komrokji RS, Garcia-Manero G, Van Elk J, Lin M, Maute R, Volkmer J-P, Takimoto CH, Chao MP, Daver N. The first-in-class anti-CD47 antibody magrolimab combined with azacitidine is well-tolerated and effective in AML patients: phase 1b results. Blood. 2020;21(Supplement_1):S213.
48. Zeidan AM, DeAngelo DJ, Palmer JM, Seet CS, Tallman MS, Wei X, et al. A phase I study of CC-90002, a monoclonal antibody targeting CD47, in patients with relapsed and/or refractory (R/R) acute myeloid leukemia (AML) and high-risk myelodysplastic syndromes (MDS): final results. Blood. 2019;134(1):1320.
49. Qi J, Li J, Jiang B, Jiang B, Liu H, Cao X, et al. A phase I/IIa study of lemzoparlimab, a monoclonal antibody targeting CD47, in patients with relapsed and/or refractory acute myeloid leukemia (AML) and myelodysplastic syndrome (MDS): initial phase I results. Blood. 2020;136(Supplement 1):30–1.
50. Weiskopf K, Ring AM, Ho CC, Volkmer JP, Levin AM, Volkmer AK, et al. Engineered SIRPalpha variants as immunotherapeutic adjuvants to anticancer antibodies. Science. 2013;341(6141):88–91.
51. Zhao XW, van Beek EM, Schornagel K, Van der Maaden H, Van Houdt M, Otten MA, et al. CD47-signal regulatory protein-alpha (SIRPalpha) interactions form a barrier for antibody-mediated tumor cell destruction. Proc Natl Acad Sci U S A. 2011;108(45):18342–7.
52. Advani R, Flinn I, Popplewell L, Forero A, Bartlett NL, Ghosh N, et al. CD47 blockade by Hu5F9-G4 and rituximab in non-Hodgkin's lymphoma. N Engl J Med. 2018;379(18):1711–21.
53. Ishikawa F, Yoshida S, Saito Y, Hijikata A, Kitamura H, Tanaka S, et al. Chemotherapy-resistant human AML stem cells home to and engraft within the bone-marrow endosteal region. Nat Biotechnol. 2007;25(11):1315–21.
54. Weinstein JN, van Osdol W. The macroscopic and microscopic pharmacology of monoclonal antibodies. Int J Immunopharmacol. 1992;14(3):457–63.
55. Godwin CD, Gale RP, Walter RB. Gemtuzumab ozogamicin in acute myeloid leukemia. Leukemia. 2017;31(9):1855–68.
56. Fournier E, Duployez N, Ducourneau B, Raffoux E, Turlure P, Caillot D, et al. Mutational profile and benefit of gemtuzumab ozogamicin in acute myeloid leukemia. Blood. 2020;135(8):542–6.
57. Fenwarth L, Fournier E, Cheok M, Boyer T, Gonzales F, Castaigne S, et al. Biomarkers of gemtuzumab ozogamicin response for acute myeloid leukemia treatment. Int J Mol Sci. 2020;21(16):5626.
58. Boyd-Kirkup J, Thakkar D, Brauer P, Zhou J, Chng W-J, Ingram PJ. HMBD004, a novel anti-CD47xCD33 bispecific antibody displays potent anti-tumor effects in pre-clinical models of AML. Blood. 2017;130(Supplement 1):1378.
59. van der Velden VHJ, te Marvelde JG, Hoogeveen PG, Bernstein ID, Houtsmuller AB, Berger MS, et al. Targeting of the CD33-calicheamicin immunoconjugate Mylotarg (CMA-676) in acute myeloid leukemia: in vivo and in vitro saturation and internalization by leukemic and normal myeloid cells. Blood. 2001;97(10):3197–204.
60. van der Jagt RHC, Badger CC, Appelbaum FR, Press OW, Matthews DC, Eary JF, et al. Localization of radiolabeled antimyeloid antibodies in a human acute leukemia xenograft tumor model. Can Res. 1992;52(1):89–94.
61. Walter RB, Appelbaum FR, Estey EH, Bernstein ID. Acute myeloid leukemia stem cells and CD33-targeted immunotherapy. Blood. 2012;119(26):6198–208.
62. Vergez F, Green AS, Tamburini J, Sarry JE, Gaillard B, Cornillet-Lefebvre P, et al. High levels of CD34+CD38low/-CD123+ blasts are predictive of an adverse outcome in acute myeloid leukemia: a Groupe Ouest-Est des

Leucemies Aigues et Maladies du Sang (GOELAMS) study. Haematologica. 2011;96(12):1792–8.
63. Vergez F, Nicolau-Travers ML, Bertoli S, Rieu JB, Tavitian S, Bories P, et al. CD34(+)CD38(-)CD123(+) leukemic stem cell frequency predicts outcome in older acute myeloid leukemia patients treated by intensive chemotherapy but not hypomethylating agents. Cancers (Basel). 2020;12(5):1174.
64. Perna F, Berman SH, Soni RK, Mansilla-Soto J, Eyquem J, Hamieh M, et al. Integrating proteomics and transcriptomics for systematic combinatorial chimeric antigen receptor therapy of AML. Cancer Cell. 2017;32(4):506-19.e5.
65. Testa U, Pelosi E, Castelli G. CD123 as a therapeutic target in the treatment of hematological malignancies. Cancers (Basel). 2019;11(9):1358.
66. Jen EY, Gao X, Li L, Zhuang L, Simpson NE, Aryal B, et al. FDA approval summary: tagraxofusp-erzs for treatment of blastic plasmacytoid dendritic cell neoplasm. Clin Cancer Res. 2020;26(3):532–6.
67. Uy GL, Aldoss I, Foster MC, Sayre PH, Wieduwilt MJ, Advani AS, et al. Flotetuzumab as salvage immunotherapy for refractory acute myeloid leukemia. Blood. 2020;137:751–62.
68. Smith BD, Roboz GJ, Walter RB, Altman JK, Ferguson A, Curcio TJ, et al. First-in man, phase 1 study of CSL362 (anti-IL3Rα/anti-CD123 monoclonal antibody) in patients with CD123+ acute myeloid leukemia (AML) in CR at high risk for early relapse. Blood. 2014;124(21):120.
69. Epling-Burnette PK, Bai F, Painter JS, Rollison DE, Salih HR, Krusch M, et al. Reduced natural killer (NK) function associated with high-risk myelodysplastic syndrome (MDS) and reduced expression of activating NK receptors. Blood. 2007;109(11):4816–24.
70. Kubasch AS, Schulze F, Giagounidis A, Gotze KS, Kronke J, Sockel K, et al. Single agent talacotuzumab demonstrates limited efficacy but considerable toxicity in elderly high-risk MDS or AML patients failing hypomethylating agents. Leukemia. 2020;34(4):1182–6.
71. Montesinos P, Roboz GJ, Bulabois CE, Subklewe M, Platzbecker U, Ofran Y, et al. Safety and efficacy of talacotuzumab plus decitabine or decitabine alone in patients with acute myeloid leukemia not eligible for chemotherapy: results from a multicenter, randomized, phase 2/3 study. Leukemia. 2020;35:62–74.
72. Deuse T, Hu X, Agbor-Enoh S, Jang MK, Alawi M, Saygi C, et al. The SIRPα–CD47 immune checkpoint in NK cells. J Exp Med. 2021. https://doi.org/10.1084/jem.20200839.
73. Tseng D, Volkmer JP, Willingham SB, Contreras-Trujillo H, Fathman JW, Fernhoff NB, et al. Anti-CD47 antibody-mediated phagocytosis of cancer by macrophages primes an effective antitumor T-cell response. Proc Natl Acad Sci U S A. 2013;110(27):11103–8.
74. Li Y, Zhang M, Wang X, Liu W, Wang H, Yang YG. Vaccination with CD47 deficient tumor cells elicits an antitumor immune response in mice. Nat Commun. 2020;11(1):581.
75. Liu X, Pu Y, Cron K, Deng L, Kline J, Frazier WA, et al. CD47 blockade triggers T cell-mediated destruction of immunogenic tumors. Nat Med. 2015;21(10):1209–15.

Publisher's Note

References

1. Jokhadze, N., Das, A. & Dizon, D. S. Global cancer statistics: A healthy population relies on population health. *CA. Cancer J. Clin.* **74**, 224–226 (2024).
2. Bray, F. *et al.* Global cancer statistics 2022: GLOBOCAN estimates of incidence and mortality worldwide for 36 cancers in 185 countries. *CA. Cancer J. Clin.* **74**, 229–263 (2024).
3. Kciuk, M. *et al.* Recent Advances in Molecular Mechanisms of Cancer Immunotherapy. *Cancers* vol. 15 (2023).
4. Coventry, B. J. & Henneberg, M. The Immune System and Responses to Cancer: Coordinated Evolution. *F1000Research* **4**, 552 (2015).
5. Kuper, C. F., Ruehl-Fehlert, C., Elmore, S. A. & Parker, G. A. Immune System. in *Haschek and Rousseaux's Handbook of Toxicologic Pathology* (eds. Haschek, W. M., Rousseaux, C. G. & Wallig, M. A. B. T.-H. and R. H. of T. P. (Third E.) 1795–1862 (Academic Press, 2013). doi:https://doi.org/10.1016/B978-0-12-415759-0.00049-2.
6. Vinay, D. S. *et al.* Immune evasion in cancer: Mechanistic basis and therapeutic strategies. *Semin. Cancer Biol.* **35**, S185–S198 (2015).
7. Swann, J. B. & Smyth, M. J. Immune surveillance of tumors. *J. Clin. Invest.* **117**, 1137–1146 (2007).
8. Zhang, Y. & Zhang, Z. The history and advances in cancer immunotherapy: understanding the characteristics of tumor-infiltrating immune cells and their therapeutic implications. *Cell. Mol. Immunol.* **17**, 807–821 (2020).
9. Seyed-Khorrami, S. M. *et al.* A promising future in cancer immunotherapy: Oncolytic viruses. *Eur. J. Pharmacol.* **960**, (2023).
10. Weiner, L. M., Dhodapkar, M. V & Ferrone, S. Monoclonal antibodies for cancer immunotherapy. *Lancet* **373**, 1033–1040 (2009).
11. Lee, J. J. *et al.* Phase 1 trial of CA-170, a novel oral small molecule dual inhibitor of immune checkpoints PD-1 and VISTA, in patients (pts) with advanced solid tumor or lymphomas. *J. Clin. Oncol.* **35**, TPS3099–TPS3099 (2025).
12. Ribas, A. & Wolchok, J. D. Cancer immunotherapy using checkpoint blockade. *Science (80-.).* **359**, 1350–1355 (2018).
13. Rosenberg, S. A. *et al.* Durable complete responses in heavily pretreated patients with metastatic melanoma using T-cell transfer immunotherapy. *Clin. Cancer Res.* **17**, 4550–4557 (2011).
14. Oppermans, N., Kueberuwa, G., Hawkins, R. E. & Bridgeman, J. S. Transgenic T-cell receptor immunotherapy for cancer: building on clinical success. *Ther. Adv. vaccines Immunother.* **8**, 2515135520933509 (2020).
15. Khan, S. H., Choi, Y., Veena, M., Lee, J. K. & Shin, D. S. Advances in CAR T cell therapy: antigen selection, modifications, and current trials for solid tumors. *Front. Immunol.* **15**, 1489827 (2024).
16. Simpson, M. C. & Schaefer, E. G. Aldesleukin. *Ext. Stab. Parenter. Drugs* **7**, 44–45 (2024).
17. Adams, S. *et al.* Topical TLR7 Agonist Imiquimod Can Induce Immune-Mediated Rejection of Skin Metastases in Patients with Breast Cancer. *Clin. Cancer Res.* **18**, 6748–6757 (2012).
18. Hemminki, O. & Hemminki, A. A century of oncolysis evolves into oncolytic immunotherapy. *Oncoimmunology* **5**, e1074377 (2016).
19. Lee, K.-W., Yam, J. W. P. & Mao, X. Dendritic Cell Vaccines: A Shift from Conventional Approach to New Generations. *Cells* **12**, (2023).
20. Cheever, M. A. & Higano, C. S. PROVENGE (Sipuleucel-T) in prostate cancer: the first FDA-approved therapeutic cancer vaccine. *Clin. cancer Res. an Off. J. Am. Assoc. Cancer Res.* **17**, 3520–3526 (2011).
21. Bai, R. *et al.* Mechanisms of Cancer Resistance to Immunotherapy. *Front. Oncol.* **10**, 1–12 (2020).
22. Köhler, G., Milstein, C. Continuous cultures of fused cells secreting antibody of predefined

specificity. *Nature* **256**, 495–497 (1975).
23. Hwang, W. Y. K. & Foote, J. Immunogenicity of engineered antibodies. *Methods* **36**, 3–10 (2005).
24. Abeyakoon, C. & Gregory, G. P. New standards of care for treatment of diffuse large B-cell lymphoma. *Br. J. Haematol.* **204**, 1132–1134 (2024).
25. Carter, P. *et al.* Humanization of an anti-p185HER2 antibody for human cancer therapy. *Proc. Natl. Acad. Sci.* **89**, 4285–4289 (1992).
26. Lonberg, N. *et al.* genetic modifications. **368**, 1132–1135 (1994).
27. Mccafferty, J., Griffiths, A. D., Winter, G. & Chiswellt, D. J. Phage antibodies: filamentous variable domains. *Nature* **348**, 552–554 (1990).
28. Paul, S. *et al.* Cancer therapy with antibodies. *Nat. Rev. Cancer* **24**, 399–426 (2024).
29. Hansel, T. T., Kropshofer, H., Singer, T., Mitchell, J. A. & George, A. J. T. The safety and side effects of monoclonal antibodies. *Nat. Rev. Drug Discov.* **9**, 325–338 (2010).
30. Suntharalingam, G. *et al.* Cytokine Storm in a Phase 1 Trial of the Anti-CD28 Monoclonal Antibody TGN1412. *N. Engl. J. Med.* **355**, 1018–1028 (2006).
31. Elshiaty, M., Schindler, H. & Christopoulos, P. Principles and current clinical landscape of multispecific antibodies against cancer. *Int. J. Mol. Sci.* **22**, (2021).
32. Vidarsson, G., Dekkers, G. & Rispens, T. IgG subclasses and allotypes: From structure to effector functions. *Front. Immunol.* **5**, 1–17 (2014).
33. Nimmerjahn, F., Vidarsson, G. & Cragg, M. S. Effect of posttranslational modifications and subclass on IgG activity: from immunity to immunotherapy. *Nat. Immunol.* **24**, 1244–1255 (2023).
34. Wang, L., Hoseini, S. S., Xu, H., Ponomarev, V. & Cheung, N.-K. Silencing Fc Domains in T cell–Engaging Bispecific Antibodies Improves T-cell Trafficking and Antitumor Potency. *Cancer Immunol. Res.* **7**, 2013–2024 (2019).
35. Chu, W. *et al.* HER2/PD1 bispecific antibody in IgG4 subclass with superior anti-tumour activities. *Clinical and translational medicine* vol. 12 e791 (2022).
36. Tapia-Galisteo, A., Compte, M., Álvarez-Vallina, L. & Sanz, L. When three is not a crowd: trispecific antibodies for enhanced cancer immunotherapy. *Theranostics* **13**, 1028–1041 (2023).
37. You, G. *et al.* Bispecific antibodies: A smart arsenal for cancer immunotherapies. *Vaccines* **9**, (2021).
38. Bird, R. E. *et al.* Single-chain antigen-binding proteins. *Science (80-.).* **242**, 423–426 (1988).
39. Rosenfeld, P. J., Heier, J. S., Hantsbarger, G. & Shams, N. Tolerability and Efficacy of Multiple Escalating Doses of Ranibizumab (Lucentis) for Neovascular Age-Related Macular Degeneration. *Ophthalmology* **113**, 623-632.e1 (2006).
40. Ridgway, J. B. B., Presta, L. G. & Carter, P. 'Knobs-into-holes' engineering of antibody CH3 domains for heavy chain heterodimerization. *Protein Eng. Des. Sel.* **9**, 617–621 (1996).
41. Hutchings, M. *et al.* Epcoritamab (GEN3013; DuoBody-CD3× CD20) to induce complete response in patients with relapsed/refractory B-cell non-Hodgkin lymphoma (B-NHL): Complete dose escalation data and efficacy results from a phase I/II trial. *J. Clin. Oncol* **38**, (2020).
42. Romano, E. A Phase 1, open-label, dose finding study of NI-1801, a bispecific mesothelin x CD47 engaging antibody, in patients with mesothelin expressing solid cancers. **10**, 3808 (2022).
43. Jiang, W. *et al.* Claudin 18.2-4-1BB bispecific antibody induced potent tumor inhibition through tumor-specific 4-1BB activation. *Cancer Res.* **80**, 5644 (2020).
44. Przepiorka, D. *et al.* FDA approval: blinatumomab. *Clin. Cancer Res.* **21**, 4035–4039 (2015).
45. Rothe, A. *et al.* A phase 1 study of the bispecific anti-CD30/CD16A antibody construct AFM13 in patients with relapsed or refractory Hodgkin lymphoma. *Blood, J. Am. Soc. Hematol.* **125**, 4024–4031 (2015).
46. Patel, M. *et al.* 313 A phase 1 evaluation of tebotelimab, a bispecific PD-1 x LAG-3 DART® molecule, in combination with margetuximab in patients with advanced HER2+ neoplasms. *J.*

Immunother. Cancer **8**, A193–A193 (2020).
47. Shalaby, M. R. *et al.* Development of humanized bispecific antibodies reactive with cytotoxic lymphocytes and tumor cells overexpressing the HER2 protooncogene. *J. Exp. Med.* **175**, 217–225 (1992).
48. Bogen, J. P. *et al.* Design of a Trispecific Checkpoint Inhibitor and Natural Killer Cell Engager Based on a 2 + 1 Common Light Chain Antibody Architecture. *Front. Immunol.* **12**, 1–16 (2021).
49. Castoldi, R. *et al.* Molecular characterization of novel trispecific ErbB-cMet-IGF1R antibodies and their antigen-binding properties. *Protein Eng. Des. Sel.* **25**, 551–560 (2012).
50. Castoldi, R. *et al.* TetraMabs: simultaneous targeting of four oncogenic receptor tyrosine kinases for tumor growth inhibition in heterogeneous tumor cell populations. *Protein Eng. Des. Sel.* **29**, 467–475 (2016).
51. Austin, R. J. *et al.* Tritacs, a novel class of t-cell–engaging protein constructs designed for the treatment of solid tumors. *Mol. Cancer Ther.* **20**, 109–120 (2021).
52. Schmohl, J. U., Felices, M., Taras, E., Miller, J. S. & Vallera, D. A. Enhanced ADCC and NK cell activation of an anticarcinoma bispecific antibody by genetic insertion of a modified IL-15 cross-linker. *Mol. Ther.* **24**, 1312–1322 (2016).
53. Lou, H. & Cao, X. Antibody variable region engineering for improving cancer immunotherapy. *Cancer Commun.* **42**, 804–827 (2022).
54. Herrmann, M. *et al.* Bifunctional PD-1× αCD3× αCD33 fusion protein reverses adaptive immune escape in acute myeloid leukemia. *Blood, J. Am. Soc. Hematol.* **132**, 2484–2494 (2018).
55. Thomas, A., Teicher, B. A. & Hassan, R. Antibody–drug conjugates for cancer therapy. *Lancet Oncol.* **17**, e254–e262 (2016).
56. Deonarain, M. P. *et al.* Small-format drug conjugates: a viable alternative to ADCs for solid tumours? *Antibodies* **7**, 16 (2018).
57. Power, C. A. & Bates, A. David vs. Goliath: The structure, function, and clinical prospects of antibody fragments. *Antibodies* **8**, (2019).
58. Redman, J. M., Hill, E. M., AlDeghaither, D. & Weiner, L. M. Mechanisms of action of therapeutic antibodies for cancer. *Mol. Immunol.* **67**, 28–45 (2015).
59. Waldman, A. D., Fritz, J. M. & Lenardo, M. J. A guide to cancer immunotherapy: from T cell basic science to clinical practice. *Nat. Rev. Immunol.* **20**, 651–668 (2020).
60. Pentcheva-Hoang, T., Egen, J. G., Wojnoonski, K. & Allison, J. P. B7-1 and B7-2 selectively recruit CTLA-4 and CD28 to the immunological synapse. *Immunity* **21**, 401–413 (2004).
61. Krummel, B. M. F. & Allison, J. CD28 and CTLA-4 have opposing effects on the response of T cells to stimulation. **182**, 459–465 (1995).
62. Latchman, Y. *et al.* PD-L2 is a second ligand for PD-1 and inhibits T cell activation. *Nat. Immunol.* **2**, 261–268 (2001).
63. Chamoto, K., Yaguchi, T., Tajima, M. & Honjo, T. Insights from a 30-year journey: function, regulation and therapeutic modulation of PD1. *Nat. Rev. Immunol.* **23**, 682–695 (2023).
64. Im, S. J. *et al.* Defining CD8+ T cells that provide the proliferative burst after PD-1 therapy. *Nature* **537**, 417–421 (2016).
65. Yost, K. E. *et al.* Clonal replacement of tumor-specific T cells following PD-1 blockade. *Nat. Med.* **25**, 1251–1259 (2019).
66. Willingham, S. B. *et al.* The CD47-signal regulatory protein alpha (SIRPa) interaction is a therapeutic target for human solid tumors. *Proc. Natl. Acad. Sci.* **109**, 6662–6667 (2012).
67. Mone, A. P. *et al.* Alemtuzumab induces caspase-independent cell death in human chronic lymphocytic leukemia cells through a lipid raft-dependent mechanism. *Leukemia* **20**, 272–279 (2006).
68. Sullivan, L. A. & Brekken, R. A. The VEGF family in cancer and antibody-based strategies for their inhibition. *MAbs* **2**, 165–175 (2010).
69. Guo, X., Wu, Y., Xue, Y., Xie, N. & Shen, G. Revolutionizing cancer immunotherapy: unleashing the potential of bispecific antibodies for targeted treatment. *Front. Immunol.* **14**, 1291836 (2023).

70. Rolin, C., Zimmer, J. & Seguin-Devaux, C. Bridging the gap with multispecific immune cell engagers in cancer and infectious diseases. *Cell. Mol. Immunol.* **21**, 643–661 (2024).
71. Di Meo, F., Kale, B., Koomen, J. M. & Perna, F. Mapping the cancer surface proteome in search of target antigens for immunotherapy. *Mol. Ther.* **32**, 2892–2904 (2024).
72. Chang, K. & Pastan, I. Molecular cloning of mesothelin, a differentiation antigen present on mesothelium, mesotheliomas, and ovarian cancers. *Proc. Natl. Acad. Sci. U. S. A.* **93**, 136–140 (1996).
73. Hassan, R., Bera, T. & Pastan, I. Mesothelin: A new target for immunotherapy. *Clin. Cancer Res.* **10**, 3937–3942 (2004).
74. Weidemann, S. *et al.* Mesothelin Expression in Human Tumors: A Tissue Microarray Study on 12,679 Tumors. *Biomedicines* **9**, (2021).
75. Bera, T. K. & Pastan, I. Mesothelin Is Not Required for Normal Mouse Development or Reproduction. *Molecular and Cellular Biology* vol. 20 2902–2906 (2000).
76. Gubbels, J. A. A. *et al.* Mesothelin-MUC16 binding is a high affinity, N-glycan dependent interaction that facilitates peritoneal metastasis of ovarian tumors. *Mol. Cancer* **5**, 1–15 (2006).
77. Fujisaka, Y. *et al.* Phase I study of amatuximab, a novel monoclonal antibody to mesothelin, in Japanese patients with advanced solid tumors. *Invest. New Drugs* **33**, 380–388 (2015).
78. Hassan, R. *et al.* First-in-human, multicenter, phase i dose-escalation and expansion study of anti-mesothelin antibody-drug conjugate anetumab ravtansine in advanced or metastatic solid tumors. *J. Clin. Oncol.* **38**, 1824–1835 (2020).
79. Hassan, R. *et al.* Mesothelin-targeting T cell receptor fusion construct cell therapy in refractory solid tumors: phase 1/2 trial interim results. *Nat. Med.* **29**, 2099–2109 (2023).
80. Hassan, R. *et al.* Phase II clinical trial of amatuximab, a chimeric antimesothelin antibody with pemetrexed and cisplatin in advanced unresectable pleural mesothelioma. *Clin. Cancer Res.* **20**, 5927–5936 (2014).
81. Santin, A. D. *et al.* Safety and activity of anti-mesothelin antibody-drug conjugate anetumab ravtansine in combination with pegylated-liposomal doxorubicin in platinum-resistant ovarian cancer: multicenter, phase Ib dose escalation and expansion study. *Int. J. Gynecol. Cancer* **33**, 562–570 (2023).
82. Arnold, D. T. & Maskell, N. A. Biomarkers in mesothelioma. *Ann. Clin. Biochem.* **55**, 49–58 (2018).
83. Hassan, R. *et al.* Detection and quantitation of serum mesothelin, a tumor marker for patients with mesothelioma and ovarian cancer. *Clin. Cancer Res.* **12**, 447–453 (2006).
84. Zhang, D. *et al.* A humanized anti-MSLN × 4-1BB bispecific antibody exhibits potent antitumour activity through 4-1BB signaling activation and fc function without systemic toxicity. (2025).
85. Ye, S. *et al.* A bispecific molecule targeting CD40 and tumor antigen mesothelin enhances tumor-specific immunity. *Cancer Immunol. Res.* **7**, 1864–1875 (2019).
86. Hatterer, E. *et al.* Targeting a membrane-proximal epitope on mesothelin increases the tumoricidal activity of a bispecific antibody blocking CD47 on mesothelin-positive tumors. *MAbs* **12**, (2020).
87. Liu, X. *et al.* Highly active CAR T cells that bind to a juxtamembrane region of mesothelin and are not blocked by shed mesothelin. *Proc. Natl. Acad. Sci. U. S. A.* **119**, 1–9 (2022).
88. Sato, N. *et al.* Expression and factor-dependent modulation of the interleukin-3 receptor subunits on human hematopoietic cells. *Blood* **82**, 752–761 (1993).
89. Testa, U. *et al.* Expression of growth factor receptors in unilineage differentiation culture of purified hematopoietic progenitors. (1996).
90. Bras, A. E. *et al.* CD123 Expression Levels in 846 Acute Leukemia Patients Based on Standardized Immunophenotyping. (2018) doi:10.1002/cyto.b.21745.
91. Jordan, C. T. *et al. The interleukin-3 receptor alpha chain is a unique marker for human acute myelogenous leukemia stem cells*. *Leukemia* vol. 14 www.nature.com/leu (2000).
92. Muñoz, L. *et al.* Interleukin-3 receptor alpha chain (CD123) is widely expressed in hematologic

malignancies. *Haematologica* **86**, 1261–1269 (2001).
93. Douglas-Smith, B. *et al.* First in man, phase I study of CSL362 (anti-IL3Rα/CD123) monoclonal antibody in patients with CD123+ acute myeloid leukemia in complete remission at high risk for early relapse. *Blood* **124**, 120 (2014).
94. Daver, N. G. *et al.* Clinical profile of IMGN632, a novel CD123-targeting antibody-drug conjugate (ADC), in patients with relapsed/refractory (R/R) acute myeloid leukemia (AML) or blastic plasmacytoid dendritic cell neoplasm (BPDCN). *Blood* **134**, 734 (2019).
95. Ravandi, F. *et al.* Complete Responses in Relapsed/Refractory Acute Myeloid Leukemia (AML) Patients on a Weekly Dosing Schedule of Vibecotamab (XmAb14045), a CD123 x CD3 T Cell-Engaging Bispecific Antibody; Initial Results of a Phase 1 Study. *Blood* **136**, 4–5 (2020).
96. Sallman, D. A. *et al.* Ameli-01: a phase I trial of UCART123v1. 2, an anti-CD123 allogeneic CAR-T cell product, in adult patients with relapsed or refractory (R/R) CD123+ acute myeloid leukemia (AML). *Blood* **140**, 2371–2373 (2022).
97. Pardoll, D. M. The blockade of immune checkpoints in cancer immunotherapy. *Nat. Rev. Cancer* **12**, 252–264 (2012).
98. Ascierto, P. A. *et al.* Ipilimumab 10 mg/kg versus ipilimumab 3 mg/kg in patients with unresectable or metastatic melanoma: a randomised, double-blind, multicentre, phase 3 trial. *Lancet Oncol.* **18**, 611–622 (2017).
99. Hellmann, M. D. *et al.* Nivolumab plus Ipilimumab in Advanced Non–Small-Cell Lung Cancer. *N. Engl. J. Med.* **381**, 2020–2031 (2019).
100. Motzer, R. J. *et al.* Nivolumab plus Ipilimumab versus Sunitinib in Advanced Renal-Cell Carcinoma. *N. Engl. J. Med.* **378**, 1277–1290 (2018).
101. Larkin, J. *et al.* Five-Year Survival with Combined Nivolumab and Ipilimumab in Advanced Melanoma. *N. Engl. J. Med.* **381**, 1535–1546 (2019).
102. Wei, S. C., Duffy, C. R. & Allison, J. P. Fundamental mechanisms of immune checkpoint blockade therapy. *Cancer Discov.* **8**, 1069–1086 (2018).
103. Gaillard, S. L., Secord, A. A. & Monk, B. The role of immune checkpoint inhibition in the treatment of ovarian cancer. *Gynecol. Oncol. Res. Pract.* **3**, 1–14 (2016).
104. Balsano, R., Zanuso, V., Pirozzi, A., Rimassa, L. & Bozzarelli, S. Pancreatic Ductal Adenocarcinoma and Immune Checkpoint Inhibitors: The Gray Curtain of Immunotherapy and Spikes of Lights. *Curr. Oncol.* **30**, 3871–3885 (2023).
105. Zhang, Z. *et al.* T Cell Dysfunction and Exhaustion in Cancer. *Front. Cell Dev. Biol.* **8**, (2020).
106. Xia, A., Zhang, Y., Xu, J., Yin, T. & Lu, X. J. T Cell Dysfunction in Cancer Immunity and Immunotherapy. *Front. Immunol.* **10**, 1719 (2019).
107. Zaretsky, J. M. *et al.* Mutations associated with acquired resistance to PD-1 blockade in melanoma. *N. Engl. J. Med.* **375**, 819–829 (2016).
108. Wang, X., Teng, F., Kong, L. & Yu, J. PD-L1 expression in human cancers and its association with clinical outcomes. *Onco. Targets. Ther.* **9**, 5023–5039 (2016).
109. Weiskopf, K. Cancer immunotherapy targeting the CD47/SIRPα axis. *Eur. J. Cancer* **76**, 100–109 (2017).
110. Poels, L. G. *et al.* Monoclonal Antibody Against Human Ovarian Tumor-Associated Antigens. *JNCI J. Natl. Cancer Inst.* **76**, 781–791 (1986).
111. Campbell, I., Freemont, P. S., Foulkes, W. & Trowsdale, J. An Ovarian Tumor Marker with Homology to Vaccinia Virus Contains an IgV-like Region and Multiple Transmembrane Domains. *Cancer Res.* **52**, 5416–5420 (1992).
112. Mawby, W. J., Holmes, C. H., Anstee, D. J., Spring, F. A. & Tanner, M. J. A. Isolation and characterization of CD47 glycoprotein: a multispanning membrane protein which is the same as integrin-associated protein (IAP) and the ovarian tumour marker OA3. *Biochem. J.* **304**, 525–530 (1994).
113. Brown, E., Hooper, L., Ho, T. & Gresham, H. Integrin-associated protein: a 50-kD plasma membrane antigen physically and functionally associated with integrins. *J. Cell Biol.* **111**, 2785–2794 (1990).
114. Brown, E. J. & Frazier, W. A. Integrin-associated protein (CD47) and its ligands. *Trends Cell*

Biol. **11**, 130–135 (2001).
115. Kale, A., Rogers, N. M. & Ghimire, K. Thrombospondin-1 cd47 signalling: From mechanisms to medicine. *Int. J. Mol. Sci.* **22**, 1–14 (2021).
116. Oldenborg, P. A. *et al.* Role of CD47 as a marker of self on red blood cells. *Science* **288**, 2051–2054 (2000).
117. Majeti, R. *et al.* CD47 Is an Adverse Prognostic Factor and Therapeutic Antibody Target on Human Acute Myeloid Leukemia Stem Cells. *Cell* **138**, 286–299 (2009).
118. Jiang, Z., Sun, H., Yu, J., Tian, W. & Song, Y. Targeting CD47 for cancer immunotherapy. *J. Hematol. Oncol.* **14**, 1–18 (2021).
119. Wang, T. *et al.* Gentulizumab, a novel anti-CD47 antibody with potent antitumor activity and demonstrates a favorable safety profile. *J. Transl. Med.* **22**, 220 (2024).
120. Kauder, S. E. *et al.* ALX148 blocks CD47 and enhances innate and adaptive antitumor immunity with a favorable safety profile. *PLoS One* **13**, 1–33 (2018).
121. Liu, J. *et al.* Pre-Clinical Development of a Humanized Anti-CD47 Antibody with Anti-Cancer Therapeutic Potential. *PLoS One* **10**, e0137345 (2015).
122. Chao, M. P. *et al.* Anti-CD47 antibody synergizes with rituximab to promote phagocytosis and eradicate non-Hodgkin lymphoma. *Cell* **142**, 699–713 (2010).
123. Chao, M. P. *et al.* Therapeutic Antibody Targeting of CD47 Eliminates Human Acute Lymphoblastic Leukemia. *Cancer Res.* **71**, 1374–1384 (2011).
124. Kim, D. *et al.* Anti-CD47 antibodies promote phagocytosis and inhibit the growth of human myeloma cells. *Leukemia* **26**, 2538–2545 (2012).
125. Edris, B. *et al.* Antibody therapy targeting the CD47 protein is effective in a model of aggressive metastatic leiomyosarcoma. *Proc. Natl. Acad. Sci.* **109**, 6656–6661 (2012).
126. Weiskopf, K. *et al.* CD47-blocking immunotherapies stimulate macrophage-mediated destruction of small-cell lung cancer. *J. Clin. Invest.* **126**, 2610–2620 (2016).
127. Krampitz, G. W. *et al.* Identification of tumorigenic cells and therapeutic targets in pancreatic neuroendocrine tumors. *Proc. Natl. Acad. Sci.* **113**, 4464–4469 (2016).
128. Tseng, D. *et al.* Anti-CD47 antibody-mediated phagocytosis of cancer by macrophages primes an effective antitumor T-cell response. *Proc. Natl. Acad. Sci. U. S. A.* **110**, 11103–11108 (2013).
129. Behrens, L. M., Berg, T. K. Van Den & Egmond, M. Van. Targeting the CD47-SIRP α Innate Immune Checkpoint to Potentiate Antibody Therapy in Cancer by Neutrophils. 1–41 (2022).
130. Chao, M. P. *et al.* Therapeutic Targeting of the Macrophage Immune Checkpoint CD47 in Myeloid Malignancies. *Front. Oncol.* **9**, 1380 (2019).
131. Lakhani, N. *et al.* 295 First-in-human Phase I trial of IBI188, an anti-CD47 targeting monoclonal antibody, in patients with advanced solid tumors and lymphomas. *J. Immunother. Cancer* **8**, A180 LP-A180 (2020).
132. Narla, R. K. *et al.* Abstract 4694: The humanized anti-CD47 monclonal antibody, CC-90002, has antitumor activity in vitro and in vivo. *Cancer Res.* **77**, 4694 (2017).
133. Evans, T. R. J. *et al.* Phase 1-2 study of TI-061 alone and in combination with other anti-cancer agents in patients with advanced malignancies. *J. Clin. Oncol.* **35**, TPS3109–TPS3109 (2017).
134. Qi, J. *et al.* A Phase I/IIa Study of Lemzoparlimab, a Monoclonal Antibody Targeting CD47, in Patients with Relapsed and/or Refractory Acute Myeloid Leukemia (AML) and Myelodysplastic Syndrome (MDS): Initial Phase I Results. *Blood* **136**, 30–31 (2020).
135. Gan, H. K. *et al.* Safety of AK117, an anti-CD47 monoclonal antibody, in patients with advanced or metastatic solid tumors in a phase I study. *J. Clin. Oncol.* **39**, 2630 (2024).
136. Patnaik, A. *et al.* Results of a first-in-human phase I study of SRF231, a fully human, high-affinity anti-CD47 antibody. *J. Clin. Oncol.* **38**, 3064 (2020).
137. Lim, H. Y. *et al.* Updated safety, efficacy, pharmacokinetics, and biomarkers from the phase 1 study of IMC-002, a novel anti-CD47 monoclonal antibody, in patients with advanced solid tumors. *J. Clin. Oncol.* **42**, 2642 (2024).
138. Burris III, H. A. *et al.* A first-in-human study of AO-176, a highly differentiated anti-CD47 antibody, in patients with advanced solid tumors. *J. Clin. Oncol.* **39**, 2516 (2021).
139. Ansell, S. *et al.* A Phase 1 Study of TTI-621, a Novel Immune Checkpoint Inhibitor Targeting

CD47, in Patients with Relapsed or Refractory Hematologic Malignancies. *Blood* **128**, 1812 (2016).
140. Patel, K. *et al.* CD47-Blocker TTI-622 Shows Single-Agent Activity in Patients with Advanced Relapsed or Refractory Lymphoma: Update from the Ongoing First-in-Human Dose Escalation Study. *Blood* **138**, 3560–3560 (2021).
141. Sun, M. *et al.* Preliminary results of a first-in-human phase I dtudy of IMM01, SIRPα Fc protein in patients with relapsed or refractory lymphoma. *J. Clin. Oncol.* **39**, 2550 (2024).
142. Lakhani, N. J. *et al.* Evorpacept alone and in combination with pembrolizumab or trastuzumab in patients with advanced solid tumours (ASPEN-01): a first-in-human, open-label, multicentre, phase 1 dose-escalation and dose-expansion study. *Lancet. Oncol.* **22**, 1740–1751 (2021).
143. Zeidan, A. M. *et al.* Phase 1 study of anti-CD47 monoclonal antibody CC-90002 in patients with relapsed/refractory acute myeloid leukemia and high-risk myelodysplastic syndromes. *Ann. Hematol.* **101**, 557–569 (2022).
144. Chao, M. P. *et al.* Calreticulin Is the Dominant Pro-Phagocytic Signal on Multiple Human Cancers and Is Counterbalanced by CD47. *Sci. Transl. Med.* **2**, 63ra94-63ra94 (2010).
145. Osorio, J. C., Smith, P., Knorr, D. A. & Ravetch, J. V. The antitumor activities of anti-CD47 antibodies require Fc-FcγR interactions. *Cancer Cell* **41**, 2051-2065.e6 (2023).
146. Storti, P. *et al.* CD14+CD16+ monocytes are involved in daratumumab-mediated myeloma cells killing and in anti-CD47 therapeutic strategy. *Br. J. Haematol.* **190**, 430–436 (2020).
147. Theruvath, J. *et al.* Anti-GD2 synergizes with CD47 blockade to mediate tumor eradication. *Nat. Med.* **28**, 333–344 (2022).
148. Upton, R. *et al.* Combining CD47 blockade with trastuzumab eliminates HER2-positive breast cancer cells and overcomes trastuzumab tolerance. *Proc. Natl. Acad. Sci. U. S. A.* **118**, 1–8 (2021).
149. Advani, R. *et al.* CD47 Blockade by Hu5F9-G4 and Rituximab in Non-Hodgkin's Lymphoma. *N. Engl. J. Med.* **379**, 1711–1721 (2018).
150. Mehta, A. *et al.* Lemzoparlimab, a Differentiated Anti-CD47 Antibody in Combination with Rituximab in Relapsed and Refractory Non-Hodgkin's Lymphoma: Initial Clinical Results. *Blood* **138**, 3542–3542 (2021).
151. Obeid, M. *et al.* Calreticulin exposure dictates the immunogenicity of cancer cell death. *Nat. Med.* **13**, 54–61 (2007).
152. Lo, J. *et al.* Anti-CD47 antibody suppresses tumour growth and augments the effect of chemotherapy treatment in hepatocellular carcinoma. *Liver Int.* **36**, 737–745 (2016).
153. Kosaka, A. *et al.* CD47 blockade enhances the efficacy of intratumoral STING-targeting therapy by activating phagocytes. *J. Exp. Med.* **218**, (2021).
154. Al-Sudani, H. *et al.* Targeting CD47-SIRPa axis shows potent preclinical anti-tumor activity as monotherapy and synergizes with PARP inhibition. *npj Precis. Oncol.* **7**, 1–10 (2023).
155. Sallman, D. A. *et al.* The First-in-Class Anti-CD47 Antibody Magrolimab (5F9) in Combination with Azacitidine Is Effective in MDS and AML Patients: Ongoing Phase 1b Results. *Blood* **134**, 569 (2019).
156. Chao, M. P. *et al.* Therapeutic Targeting of the Macrophage Immune Checkpoint CD47 in Myeloid Malignancies. *Front. Oncol.* **9**, (2020).
157. Garcia-Manero, G. *et al.* Abstract CT060: Phase 1 study of azacitidine in combination with evorpacept for higher-risk myelodysplastic syndrome (MDS). *Cancer Res.* **84**, CT060–CT060 (2024).
158. Daver, N. G. *et al.* Lemzoparlimab (lemzo) with venetoclax (ven) and/or azacitidine (aza) in patients (pts) with acute myeloid leukemia (AML) or myelodysplastic syndromes (MDS): A phase 1b dose escalation study. *J. Clin. Oncol.* **40**, TPS7067–TPS7067 (2022).
159. Yang, W. *et al.* Latest results of a phase 2 study of IMM01 combined with azacitidine (AZA) as the first-line treatment in adults with higher risk myelodysplastic syndromes (MDS). *J. Clin. Oncol.* **42**, 6510 (2024).
160. Miao, M. *et al.* A Phase 1b Study to Evaluate Safety and Efficacy of IBI188 in Combination with

Azacitidine (AZA) As a First-Line Treatment in Subjects with Newly Diagnosed Higher Risk Myelodysplastic Syndrome. *Blood* **140**, 4045–4046 (2022).
161. Miao, M. *et al.* AK117 (anti-CD47 monoclonal antibody) in Combination with Azacitidine for Newly Diagnosed Higher Risk Myelodysplastic Syndrome (HR-MDS): AK117-103 Phase 1b Results. *Blood* **142**, 1865 (2023).
162. Daver, N. *et al.* Phase I/II Study of Azacitidine (AZA) with Venetoclax (VEN) and Magrolimab (Magro) in Patients (pts) with Newly Diagnosed (ND) Older/Unfit or High-Risk Acute Myeloid Leukemia (AML) and Relapsed/Refractory (R/R) AML. *Blood* **140**, 141–144 (2022).
163. Tao, H., Qian, P., Wang, F., Yu, H. & Guo, Y. Targeting CD47 enhances the efficacy of anti-PD-1 and CTLA-4 in an esophageal squamous cell cancer preclinical model. *Oncol. Res.* **25**, 1579–1587 (2017).
164. Song, Y. *et al.* Timdarpacept (IMM01) in combination with tislelizumab in prior anti-PD-1 failed classical Hodgkin lymphoma: An open label, multicenter, phase II study (IMM01-04) evaluating safety as well as preliminary anti-tumor activity. *J. Clin. Oncol.* **42**, 7017 (2024).
165. Xia, Q. *et al.* The safety and efficacy of cadonilimab in combination with AK117 (anti-CD47 antibody) plus chemotherapy as first-line treatment for advanced gastric (G) or gastroesophageal junction (GEJ) cancer. *J. Clin. Oncol.* **41**, e16050–e16050 (2023).
166. Sikic, B. I. *et al.* First-in-Human, First-in-Class Phase I Trial of the Anti-CD47 Antibody Hu5F9-G4 in Patients With Advanced Cancers. *J. Clin. Oncol.* **37**, 946–953 (2019).
167. Chen, J. Y. *et al.* RBC-Specific CD47 Pruning Confers Protection and Underlies the Transient Anemia in Patients Treated with Anti-CD47 Antibody 5F9. *Blood* **132**, 2327 (2018).
168. Daver Naval, Vyas Paresh, Huls Gerwin, et al. Magrolimab vs placebo in combination with Venetoclax and Azacitidine in previously untreated patients with acute myeloid leukemia who are ineligible for intensive chemotherapy: the ENHANCE-3 study. *EHA Libr.* **422242**, 138 (2024).
169. Zhang, H. *et al.* S216: CD47/PD-L1 bispecific antibody (IBI322) in anti-PD-1 or PD-L1 treatment-resistant classical Hodgkin lymphoma: a phase I study. *HemaSphere* **7**, e8102841 (2023).
170. Carneiro, B. A. *et al.* Phase 1 first-in-human study of PF-07257876, a novel CD47/PD-L1 bispecific checkpoint inhibitor, in patients with PD-1/PD-L1-refractory and -naïve advanced solid tumors. *J. Clin. Oncol.* **41**, 2529 (2023).
171. Lakhani, N. *et al.* 429 Phase 1 dose escalation study of the agonist redirected checkpoint, SL-172154 (SIRPα-Fc-CD40L) in subjects with platinum-resistant ovarian cancer. *J. Immunother. Cancer* **9**, A459 LP-A459 (2021).
172. Daver, N. *et al.* Safety, Pharmacodynamic, and Anti-Tumor Activity of SL-172154 As Monotherapy and in Combination with Azacitidine (AZA) in Relapsed/Refractory (R/R) Acute Myeloid Leukemia (AML) and Higher-Risk Myelodysplastic Syndromes/Neoplasms (HR-MDS) Patients (pts). *Blood* **142**, 4278 (2023).
173. Saeed, A. *et al.* 51P Phase II dose expansion study of DSP107, a first-in-class fusion protein targeting CD47 and 4-1BB, in combination with atezolizumab in patients with advanced MSS colorectal cancer. *Ann. Oncol.* **35**, S25 (2024).
174. Piccione, E. C. *et al.* A bispecific antibody targeting CD47 and CD20 selectively binds and eliminates dual antigen expressing lymphoma cells. *MAbs* **7**, 946–956 (2015).
175. Dheilly, E. *et al.* Tumor-directed blockade of CD47 with bispecific antibodies induces adaptive antitumor immunity. *Antibodies* **7**, (2018).
176. Stefano, S. *et al.* Preclinical Evaluation of ISB 1442, a First-in-Class CD38 and CD47 Bispecific Antibody Innate Cell Modulator for the Treatment of AML and T-ALL. *Blood* **140**, 6237–6238 (2022).
177. Ring, N. G. *et al.* Anti-SIRPα antibody immunotherapy enhances neutrophil and macrophage antitumor activity. *Proc. Natl. Acad. Sci.* **114**, E10578–E10585 (2017).
178. Ponce, L. P. *et al.* SIRPα-antibody fusion proteins stimulate phagocytosis and promote elimination of acute myeloid leukemia cells. *Oncotarget* **8**, 11284–11301 (2017).
179. Hawkes, E. *et al.* First-in-Human (FIH) Study of the Fully-Human Kappa-Lambda CD19/CD47

Bispecific Antibody TG-1801 in Patients (pts) with B-Cell Lymphoma. *Blood* **140**, 6599–6601 (2022).
180. Yang, J. *et al.* 839P Preliminary results from a phase II study of amulirafusp alfa (IMM0306) in patients with relapsed or refractory CD20-positive B-cell non-Hodgkin's lymphoma. *Ann. Oncol.* **35**, S610 (2024).
181. Liu, Y. *et al.* Phase I safety and preliminary efficacy of IMM0306 in combination with lenalidomide in patients with relapsed or refractory CD20-positive B-cell non-Hodgkin's lymphoma. *J. Clin. Oncol.* **42**, e19040–e19040 (2024).
182. Zhang, B. *et al.* Development and evaluation of a human CD47/HER2 bispecific antibody for Trastuzumab-resistant breast cancer immunotherapy. *Drug Resist. Updat.* **74**, 101068 (2024).
183. Du, K. *et al.* A bispecific antibody targeting GPC3 and CD47 induced enhanced antitumor efficacy against dual antigen-expressing HCC. *Mol. Ther.* **29**, 1572–1584 (2021).
184. Yang, Y. *et al.* Dual blockade of CD47 and CD24 signaling using a novel bispecific antibody fusion protein enhances macrophage immunotherapy. *Mol. Ther. Oncolytics* **31**, 1–12 (2023).
185. Grandclément, C. *et al.* Development of ISB 1442, a CD38 and CD47 bispecific biparatopic antibody innate cell modulator for the treatment of multiple myeloma. *Nature Communications* vol. 15 (2024).
186. Wong, O. K., Wang, X., Chen, X. & Post, L. Abstract 1870: VBI-003, a CD47xEpCAM bispecific antibody as a potential treatment for colorectal and small cell lung cancers. *Cancer Res.* **83**, 1870 (2023).
187. Wang, X. *et al.* 516 CD47 x B7-H3 bispecific antibody offers a new strategy for treating B7-H3+/CD47+ tumors. *J. Immunother. Cancer* **11**, A582 LP-A582 (2023).
188. Yang, Y. *et al.* A novel bispecific antibody fusion protein co-targeting EGFR and CD47 with enhanced therapeutic index. *Biotechnol. Lett.* **40**, 789–795 (2018).
189. Meng, Y. *et al.* Preliminary results of a phase I, first-in-human, dose escalation study of IMM2902 in patients with HER2-expressing advanced solid tumors. *J. Clin. Oncol.* **41**, e15185–e15185 (2023).
190. Stelmach, P. & Trumpp, A. Leukemic stem cells and therapy resistance in acute myeloid leukemia. *Haematologica* **108**, 353–366 (2023).
191. Lumish, M. A., Kohn, E. C. & Tew, W. P. Top advances of the year: Ovarian cancer. *Cancer* **130**, 837–845 (2024).
192. Torre, L. A. *et al.* Ovarian cancer statistics, 2018. *CA. Cancer J. Clin.* **68**, 284–296 (2018).
193. Peres, L. C. *et al.* Histotype classification of ovarian carcinoma: A comparison of approaches. *Gynecol. Oncol.* **151**, 53–60 (2018).
194. Siegel, R. L., Miller, K. D., Fuchs, H. E. & Jemal, A. Cancer statistics, 2022. *CA. Cancer J. Clin.* **72**, 7–33 (2022).
195. Olson, S. H. & Harlap, S. Symptoms of Ovarian Cancer. *Obstet. Gynecol.* **98**, 1150–1151 (2001).
196. Olivier, R. I., Lubsen-Brandsma, M. A. C., Verhoef, S. & Van Beurden, M. CA125 and transvaginal ultrasound monitoring in high-risk women cannot prevent the diagnosis of advanced ovarian cancer. *Gynecol. Oncol.* **100**, 20–26 (2006).
197. Bachmann, C. New Achievements from Molecular Biology and Treatment Options for Refractory/Relapsed Ovarian Cancer—A Systematic Review. *Cancers (Basel).* **15**, (2023).
198. Bell, D. *et al.* Integrated genomic analyses of ovarian carcinoma. *Nature* **474**, 609–615 (2011).
199. Baradács, I. *et al.* PARP inhibitor era in ovarian cancer treatment: a systematic review and meta-analysis of randomized controlled trials. *J. Ovarian Res.* **17**, 1–14 (2024).
200. Heo, Y. A. Mirvetuximab Soravtansine: First Approval. *Drugs* **83**, 265–273 (2023).
201. Yoon, W. H., DeFazio, A. & Kasherman, L. Immune checkpoint inhibitors in ovarian cancer: where do we go from here? *Cancer Drug Resist.* **6**, 358–377 (2023).
202. Zhang L, Conejo-Garcia JR, et al. Intratumoral T Cells, Recurrence, and Survival in Epithelial Ovarian Cancer. *N. Engl. J. Med.* **348**, 203–213 (2003).
203. Barnett, J. C. *et al.* Ovarian cancer tumor infiltrating T-regulatory (Treg) cells are associated with a metastatic phenotype. *Gynecol. Oncol.* **116**, 556–562 (2010).
204. Tassi, E. *et al.* Epithelial ovarian cancer is infiltrated by activated effector T cells co-expressing

CD39, PD-1, TIM-3, CD137 and interacting with cancer cells and myeloid cells. *Front. Immunol.* **14**, 1–14 (2023).
205. Leutbecher, A. *et al.* P12.12 The tumor microenvironment of epithelial ovarian cancer: exhausted and immunosuppressive. *J. Immunother. Cancer* **12**, A37 LP-A38 (2024).
206. Devine, S. M. & Larson, R. A. Acute leukemia in adults: recent developments in diagnosis and treatment. *CA. Cancer J. Clin.* **44**, 326–352 (1994).
207. Dinardo, C. D. & Cortes, J. E. Mutations in AML: prognostic and therapeutic implications. *Am. Soc. Hematol.* **30**, 348–355 (2016).
208. Deschler, B. & Lübbert, M. Acute myeloid leukemia: Epidemiology and etiology. *Cancer* **107**, 2099–2107 (2006).
209. Wierzbowska, A. & Czemerska, M. Clinical Manifestation and Diagnostic Workup BT - Acute Myeloid Leukemia. in (eds. Röllig, C. & Ossenkoppele, G. J.) 119–126 (Springer International Publishing, 2021). doi:10.1007/978-3-030-72676-8_6.
210. Kabel, A. M., Zamzami, F., Al-Talhi, M., Al-Dwila, K. & Hamza, R. Acute Myeloid Leukemia: A focus on Risk Factors, Clinical Presentation, Diagnosis and Possible Lines of Management. *J. Cancer Res. Treat.* **5**, 62–67 (2017).
211. Schwede, M. *et al.* Mutation order in acute myeloid leukemia identifies uncommon patterns of evolution and illuminates phenotypic heterogeneity. *Leukemia* **38**, 1501–1510 (2024).
212. Senapati, J., Kadia, T. M. & Ravandi, F. Maintenance therapy in acute myeloid leukemia: advances and controversies. *Haematologica* **108**, 2289–2304 (2023).
213. Cornelissen, J. J. *et al.* The European LeukemiaNet AML Working Party consensus statement on allogeneic HSCT for patients with AML in remission: an integrated-risk adapted approach. *Nat. Rev. Clin. Oncol.* **9**, 579–590 (2012).
214. Dianne Pulte, E. *et al.* FDA approval summary: Gilteritinib for relapsed or refractory acute myeloid leukemia with a FLT3 mutation. *Clin. Cancer Res.* **27**, 3515–3521 (2021).
215. Levis, M. Midostaurin approved for FLT3-mutated AML. *Blood* **129**, 3403–3406 (2017).
216. Jen, E. Y. *et al.* Fda approval: Gemtuzumab ozogamicin for the treatment of adults with newly diagnosed cd33-positive acute myeloid leukemia. *Clin. Cancer Res.* **24**, 3242–3246 (2018).
217. DiNardo, C. D. *et al.* Venetoclax combined with decitabine or azacitidine in treatment-naive, elderly patients with acute myeloid leukemia. *Blood* **133**, 7–17 (2019).
218. Ravandi, F. *et al.* Safety and tolerability of AMG 330 in adults with relapsed/refractory AML: a phase 1a dose-escalation study. *Leuk. Lymphoma* **65**, 1281–1291 (2024).
219. Sekiguchi, N. *et al.* Phase I dose-escalation study of milademetan in patients with relapsed or refractory acute myeloid leukemia. *Int. J. Hematol.* **117**, 68–77 (2023).
220. Reischer, A. *et al.* Targeted CD47 checkpoint blockade using a mesothelin-directed antibody construct for enhanced solid tumor-specific immunotherapy Authors. *Cancer Immunol. Immunother.* accepted (2025).
221. Tahk, S. *et al.* SIRPα-αCD123 fusion antibodies targeting CD123 in conjunction with CD47 blockade enhance the clearance of AML-initiating cells. *J. Hematol. Oncol.* **14**, 1–17 (2021).

Acknowledgments

First and foremost, I would like to thank Marion Subklewe for the opportunity and trust to pursue my PhD in her lab. Thank you for the great working environment, the freedom to operate, the durable support, honesty, and, of course, the scientific exchange, even though ovarian cancer is not your field, and I know it never will be. It allowed me to learn so much – both scientifically and personally – helping me grow beyond myself. For that, I am deeply grateful.

A huge thank you also goes to the entire Subklewe group for the great discussions, always having fun, and, most importantly, the emotional as well as scientific support. Furthermore, the second floor of the Gene Center, especially our "Theuklewe group", where we grew very close, always had a great time, and always helped each other. All the lunch breaks, barbecues, beers, or Pfeffi shots from Falcon tubes, dinners, beer gardens, hiking in the mountains, and so much more. It was a true pleasure, and I am incredibly grateful for this special time – above all, for the genuine friendships I have made.

Special thanks to our technicians – Sabine Sandner, Simone Pentz, Marina Leeping, and Gudrun Prangenberg – who always had our backs, allowing us to focus on our projects.

Particularly, my two very talented master's students, Sophia Geweniger and Marvin Petry, were a great help and significantly contributed to my projects. I truly enjoyed supervising them, and I'm very fortunate to have been part of their educational journey.

Deep gratitude is extended to the cancer patients who generously donated their samples for research. Their courage provides hope for the future, helping to advance understanding and improve treatments for others. This invaluable contribution is making a lasting impact in the fight against cancer.

A crucial part of my dissertation was the incredible collaborations. Working with the gynecologists was always straightforward, generous, supportive, and scientifically very exciting – especially Fabian Trillsch and Bastian Czogalla. Also, a huge thank you to Mirjana Kessler for the great experience with the organoids.

Additionally, I am grateful to the Hopfner group for giving me fascinating insights into the world of antibody engineering and allowing me to understand the full chain of translational antibody therapy. The atmosphere was always very pleasant, and I am especially happy that we were able to capture our joint work in a publication. A special mention goes to Nadja Fenn – one of the most talented scientists I have ever met –who always supported me, had an open ear, and worked with me late into the night, finalizing the paper draft over pizza.

Another big thank you to Roche and, in particular, Christian Klein. Experiencing the industry and non-academic exchange was incredibly interesting, and I met some brilliant minds who always asked insightful questions, provided helpful input, and were highly supportive.

Also, a big thank you to the i-Target graduate school for the fantastic scientific exchange, numerous workshops, conferences, and inspiring speakers. Furthermore, thank you for the financial support for national and international conferences.

Of course, my biggest gratitude goes to my whole family, without whom I would not be where I am today. My parents, Maria and Roland Leutbecher, supported me unconditionally – not just financially but always with open arms, encouragement, love, and trust, which constantly gave me strength. My little brother (even though he's taller), Michi – one of the most important people in my life—who I could always rely on, laugh with, and share everything with. And my grandparents, especially my grandpa, whose pride always gave me the courage to keep going and believe in myself. And to my grandma—now I can ultimately answer that I'm finally done with "all this studying"! I couldn't imagine a better family and am infinitely grateful.

Life is better with friends by your side, and I am incredibly lucky to have so many wonderful people around me. Especially my girls – Angi, Tina, Ani, and Sophia – who were always there for me, standing by my side through thick and thin, always ready to listen – no matter if things were going well or not – and who always made time for me. And there are so many more friends, who I can't even list here, but to whom I want to express my deepest gratitude – for everything.

And most importantly, my great love, Janis. He has been there for me through all these years. He believed in me when I couldn't believe in myself and always made me laugh, no matter what. He celebrated even the smallest successes with me and supported me with endless conversations, patience, drying my tears, holding me in his arms, and, most of all, giving me the time and space to find my path. I cannot put into words how grateful I am to him. I look forward to the next, hopefully less stressful, chapter. Thank you!